TABLE OF CONTENTS

Page

INTRODUCTION 1

CHAPTER 1 LITERATURE REVIEW 5
1.1 Subarctic Area 5
1.1.1 St. Elias Mountain Range 5
1.1.2 The Duke River Valley 8
1.2 Water Sources in Subarctic Glacierized Watersheds 8
1.2.1 Glaciers 10
1.2.2 Ice-Cored Moraines 12
1.2.3 Rock Glaciers 13
1.2.4 Groundwater 13
1.2.5 Icing 14
1.3 End-Members' Contribution to Catchment Outflows 14
1.3.1 Natural Tracers 15
1.3.1.1 Major Ions 16
1.3.1.2 Isotopes 17
1.3.1.3 Dissolved Organic Carbon 19
1.4 Mixing Models 19

CHAPTER 2 STUDY SITE AND DATA COLLECTION 23

CHAPTER 3 METHODOLOGY 27
3.1 Sample Collection and on Site Measurements 27
3.2 Chemical Analyses 28
3.2.1 Laboratory Analyses and Tracer Value Calculation 28
3.2.1.1 Total Organic Carbon 28
3.2.1.2 Stable Heavy Isotopes of Water 29
3.2.1.3 Solutes: Anions 29
3.2.1.4 Solutes: Cations 29
3.2.1.5 Tracer Value Calculation 30
3.3 Qualitative Analysis 31
3.3.1 Tracer Selection 31
3.3.2 Hierarchical Cluster Analysis 31
3.4 Quantitative Analysis 32
3.4.1 Hydrochemical Basin Characterization Method 32
3.4.2 HBCM on 24 hr Sampling Cycle 37

CHAPTER 4 RESULTS 39
4.1 B Valley Water Characteristics 39
4.2 Qualitative Analysis 42
4.2.1 Bivariate Graphs and Tracer Selection 42

4.2.2 Hierarchical Cluster Analysis (HCA) 45
4.2.2.1 B1 Glacier 46
4.2.2.2 B1 Spatial Analysis 47
4.2.2.3 B1 Temporal Analysis 50
4.2.2.4 B2 Glacier 55
4.2.2.5 B3 Glacier 58
4.2.2.6 24 hr Sampling Cycle 61
4.3 Quantitative Analysis 64
4.3.1 Hydrochemical Basin Characterization Method 64
4.3.1.1 B1 Subwatershed 03/07/2015 – Set A 64
4.3.1.2 B1 Subwatershed 05/07/2015 – Set B 66
4.3.1.3 B Watershed 07/07/2015 – Set C 68
4.3.1.4 24 hr Sampling Cycle 70

CHAPTER 5 DISCUSSION 75
5.1 Qualitative Analysis 75
5.1.1 Bivariate Plots 75
5.1.2 Hierarchical Cluster Analysis 76
5.2 Quantitative Analysis 77
5.2.1 Hydrochemical Basin Characterization Method 77
5.2.2 24 hr Sampling Cycle 78

CONCLUSION 81

APPENDIX I FIELD MEASUREMENT OF B WATERSHED SAMPLES 83

APPENDIX II CHEMICAL RESULTS FOR B WATERSHED SAMPLES 87

APPENDIX III PHYSICAL PROPERTIES AND DOC RESULTS OF B WATERSHED SAMPLES 91

APPENDIX IV BIVARIATE GRAPHS 95

APPENDIX V SOLUBITY DATA OF B WATERSHED SAMPLES 101

LIST OF REFERENCES 105

LIST OF TABLES

Page

Table 2.1	Glaciers of the B Watershed	24
Table 3.1	HBCM Colour Code for Origins	37
Table 4.1	Analytical Results for End-Members in the B Watershed	40
Table 4.2	HBCM Results for the 24-Hours Sampling	71

LIST OF FIGURES

Page

Figure 1.1	St. Elias Mountain Range, Study Site Location	6
Figure 1.2	Yukon River Basin	7
Figure 1.3	Duke Upper Watershed	8
Figure 1.4	Conceptual model of the subarctic glacierized watershed for two seasons: (a)snowmelt and (b) summer	9
Figure 2.1	Duke B Watershed (2015)	24
Figure 2.2	B Watershed Sampling Map	26
Figure 3.1	Simplified HBCM	34
Figure 4.1	Electrical Conductivity as a Function of pH in End-Member Samples	43
Figure 4.2	Potassium Concentrations as a Function of Sulfate Concentrations in End-Member Samples	44
Figure 4.3	B1 Glacier Conceptual Sampling Map	46
Figure 4.4	HCA Results for B1 Glacier for Absolute Concentration, 05/07/2015	48
Figure 4.5	HCA Results for B1 Glacier for Relative Concentration, 05/07/2015	49
Figure 4.6	HCA Results for B1 Glacier by Absolute Concentration, Temporal Analysis 03/07/2015	50
Figure 4.7	HCA Results for B1 Glacier by Relative Concentration, Temporal Analysis 03/07/2015	52
Figure 4.8	B1 Repeated Samples HCA Results for the Absolute Concentrations	53
Figure 4.9	B1 Repeated Samples HCA Results for the Relative Concentrations	54
Figure 4.10	B2 Glacier Conceptual Sampling Map	55
Figure 4.11	B2 End-Members' HCA Results for Absolute Concentration, 07/07/2015	56
Figure 4.12	B2 End-Members' HCA Results for Relative Concentration, 07/07/2015	57
Figure 4.13	B3 Glacier Conceptual Sampling Map	58
Figure 4.14	B3 End-Members' HCA Results for Absolute Concentration, 07/07/2015	59
Figure 4.15	B3 End-Members' HCA Results for Relative Concentration, 07/07/2015	60

Figure 4.16 Stable Heavy Water Isotope Variations of the 24-hour Sampling..... 61
Figure 4.17 Ionic Variations over the 24-Hour Sampling..... 62
Figure 4.18 Precipitation Height Recorded during the 24-hour Sampling..... 63
Figure 4.19 HBCM Results for B1 Glacier on 03/07/2015..... 65
Figure 4.20 HBCM Results of B1 Glacier on 05/07/2015..... 67
Figure 4.21 HBCM Results for the B Watershed on 07/07/2015..... 69
Figure 4.22 Glacial vs Non-Glacial and Precipitation Relative Volumes over 24-hour Sampling Cycle..... 72

LIST OF ABREVIATIONS

AWS	Automatic Weather Station
Ca^{2+}	Calcium ion
$CaCO_3$	Calcite
Cl^-	Chloride ion
DOC	Dissolved Organic Carbon
EMMA	End-Member Mixing Analysis
eq	Equation
F^-	Fluoride ion
GW	Groundwater
H_2SO_4	Sulphuric Acid
HDPE	High Density Polyethylene
HCA	Hierarchical Cluster Analysis
HBCM	Hydrochemical Basin Characterization Method
HNO_3	Nitric Acid
IC	Ionic Chromatography
ICP-OES	Inductively Coupled Plasma Optical Emission Spectrometry
K^+	Potassium ion
KNPR	Kluane National Park and Reserve
K_{sp}	Solubility Product Constant
Na^+	Sodium ion
Mg^{2+}	Magnesium ion
Q	Ion Activation Product
SO_4^{2-}	Sulfate ion
SWE	Snow Water Equivalent
TDS	Total Dissolved Solids
V-SMOW	Vienna Mean Ocean Water

LIST OF SYMBOLS AND UNITS OF MEASUREMENTS

mg/L	Milligram per liter, concentration unit
µS/cm	Microsiemens per centimeter, electrical conductivity unit
mL	Milliliter, volume unit
$mmol \cdot L^{-1}$	Milli-moles per liter, concentration unit
$m \cdot y^{-1}$ w.e.	Meters per year water equivalent
N	Normality
ppm	Parts per million, concentration unit

INTRODUCTION

Climate change is affecting regions in the world in different ways varying on the area and their respective environments; it has led to major changes in the annual hydrological cycle of arctic and subarctic territories, affecting the livelihoods and well-being of their respective ecosystems (Deb, Butcher et Srinivasan, 2015). In these regions, the effect of increasing temperatures is particularly pronounced due to the presence of climate sensitive features such as snowpack, glaciers and permafrost. Some of the visible hydrological changes in response to climate warming have been earlier spring melt periods (Manabe et al., 2004; Nijssen et al., 2001); glacier recession and related hydrological responses (Kaser et al., 2006); shorter periods of snow cover and related shift in peak flow timing (Brown et Braaten, 1998; Whitfield, 2001) and permafrost thawing that could result in an increased runoff (Walvoord et Striegl, 2007).

Hydrological changes in northern regions have numerous consequences for both populations and ecosystems. Hydrological changes have already resulted in marked regime shifts in the biological communities of many lakes and ponds (Schindler et Smol, 2006). Partly due to increased water temperatures, fish populations, like Salmonid species, have considerably decreased over the last centuries (Grah et Beaulieu, 2013). Changes in flood regimes associated to snow cover alteration will affect ecosystems and sediment transports (Lotsari et al., 2010). Changes in river ice regimes affect access to resources and population movements (Wilson, Walter et Waterhouse, 2015). Other effects of hydrological changes include increased risks to infrastructures and water resources planning as well as a rise in nutrients and carbon outflows to the ocean (Bring et al., 2016).

The St. Elias Mountains, situated in the Canadian and American subarctic, are the headwaters of the Yukon River Basin and therefore plays a huge role in the hydrology of its watershed. Because these mountains host the largest icefields outside of the polar icecaps, the St. Elias Mountains' hydrology is highly influenced by glaciers (Fleming et Clarke, 2003). Thinning rates in the Yukon glaciers alone are estimated between 0.45 ± 0.15 $m \cdot y^{-1}$ water equivalents

(w.e.) and 0.78 ± 0.34 $m \cdot y^{-1}$ w.e (Barrand et Sharp, 2010; Flowers, Copland et Schoof, 2014) resulting in ubiquitous mass loss of 22% glacier loss in the last 50 years (Barrand et Sharp, 2010). Rapid mass loss from the glaciers of this range was shown having a direct measurable impact on the global sea levels (Flowers, Copland et Schoof, 2014). The long term influence of glaciers' retreat on hydrological regimes is known as the Peak water (Baraer et al., 2012): glaciers produce an initial increase in runoff as they lose mass. The discharge then reaches a plateau called "peak water" and subsequently declines as the volume of glacial ice continues to decrease. Other known impacts of glacier retreat on hydrology are changes in diurnal oscillation of stream discharge (Singh et al., 2005), timing of the maximum and minimum annual discharge (Janowicz, 2011), water temperature (Blaen et al., 2014) and sediment transport (Lotsari et al., 2010).

However, glaciers are not the only water source in subarctic glacierized catchments. Groundwater, whose contribution is highly related to permafrost conditions in those environments (Janowicz, 2011), plays a huge role in subarctic glacierized catchments' hydrology (Levy et al., 2015; Walvoord et Striegl, 2007). Other water sources such as buried ice bodies (Schomacker et Kjær, 2008), ice-cored moraines (Moorman, 2005) or icing (Moorman et Michel, 2000), even if by far less studied, also make potential water sources in such environments.

Facing challenges of climate change adaptation in this region of the world will require informing policy makers on how to manage water security (Bring, Jarsjö et Destouni, 2015) and therefore anticipating evolution of the different water sources that make river discharges. Thus, few studies have considered the role of extra-glacial water sources in glaciers fed catchment hydrology (Milner, Brown et Hannah, 2009). As stated by Rouse et al. (1997) "There is a clear need to improve our current knowledge of temperature and precipitation patterns…to understand better the interrelationships of cold region rivers with their basins". In this context, glaciers hydrological role has captured most of the scientific attention over the last decades, while hydrological processes of proglacial areas remain under studied (Heckmann, McColl et Morche, 2016).

The overall objective of the present study is to improve the understanding of hydrological processes in proglacial areas of glacierized headwater catchments in the St. Elias range by identifying sources and quantifying their contribution to the runoff of a small watershed (named B Valley) of the Duke River watershed in the Kluane National Park and Reserve (KNPR) during summer 2015. This overall objective can be divided into three sub-objectives:

1. Identification of the main water sources by the mean of their physico-chemical particularities at different dates of the study period.
2. Estimation of the said sources' contribution to total discharge by using a mixing model again at different dates of the study period.
3. Differentiation between glacial and non-glacial contributions to the outflows of the B Valley during a 24-hour period.

To meet these objectives, a synoptic series of sampling conducted in the B Valley between July 3rd and 10th 2015 were undertaken. Samples were then analyzed for major ions, organic carbon and heavy stable water isotopes, which were used as natural tracers to identify water sources and estimate their contribution to outflows. Quantification of sources' contribution was achieved using the hydrochemical basin characterization method (HBCM), a method developed to answer such question in the context of tropical glacierized watersheds (Baraer et al., 2015).

CHAPITRE 1

LITERATURE REVIEW

This chapter will present the knowledge already accumulated on the characterization of hydrological processes using natural tracers. Starting with a general introduction of the studied environment and its hydrological processes; the concerned sources will then be dissected and tracers previously used to differentiate them will be revealed. Finally, a broad introduction to mixing models will be narrowed down to the hydrochemical basin characterization method (HBCM), the model used in this study.

1.1 Subarctic Area

Subarctic environments are the regions in the northern hemisphere south of the Arctic generally falling between 50ºN and 70ºN parallels. With increased temperatures, subarctic hydrological sources will be affected and in turn will affect runoff volumes, a temporary increase in volumes is anticipated, which will increase erosion and habitat loss to local wildlife (Nuttall, 2007). This study focuses on the environmental changes due to global warming in the subarctic region of Canada and more precisely the St. Elias Mountain Range area.

1.1.1 St. Elias Mountain Range

The St. Elias Mountains are a segment of the Pacific Coast Ranges in northwestern North America. They are situated on the Canadian/Alaskan border, each building a protected area surrounding it: the Wrangell-St. Elias National Park and Preserve in the USA and the Kluane National Park and Reserve in Canada as seen in figure 1.1. With close to 46 000 km^2 of ice cover (Berthier et al., 2010), the St. Elias Mountains host the largest icefields outside the polar icecaps.

Figure 1.1 St. Elias Mountain Range, Study Site Location
Modified from Ricketts (1999)

The St-Elias mountain range is the headwater of the Yukon River Basin. The Yukon River empties out into the Bering Sea at the Yukon-Kuskokwim Delta as pictured in Figure 1.2. The Yukon River Basin is the fourth largest watershed in North America (831 390 km^2), its runoff occurring mainly during summer months from snowmelt, rainfall and glacial melt (Hay et McCabe, 2010).

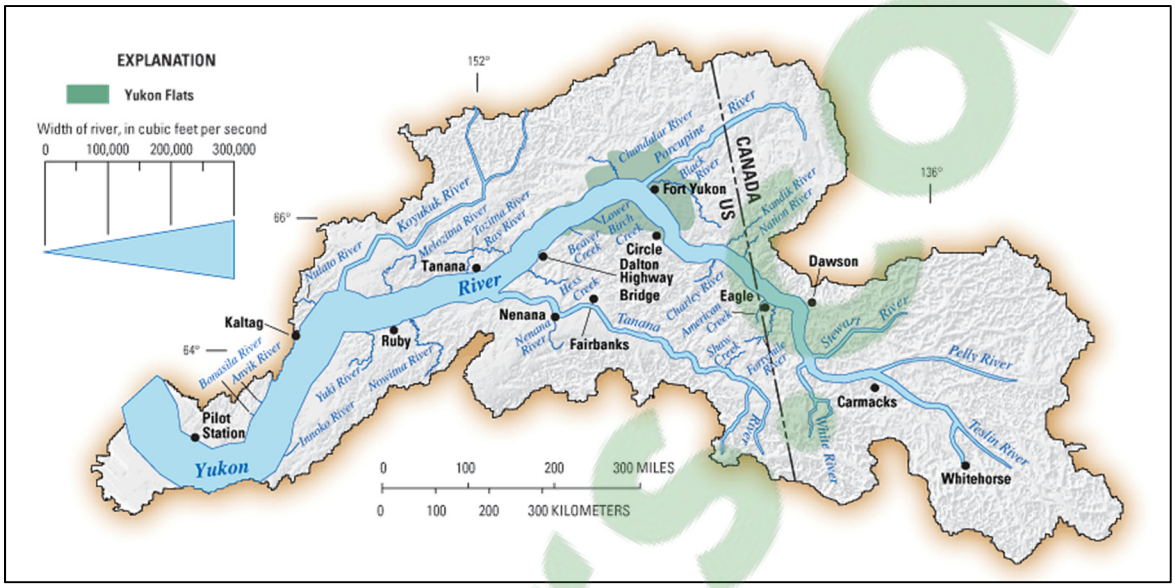

Figure 1.2 Yukon River Basin
Taken from Brabets et Schuster (2008)

The high rate of mass loss of glaciers in the St. Elias region shows significant contribution to global sea level rise (Arendt et al., 2002; Luthcke et al., 2008). An increasing number of studies are conducted in an effort to understand the response and corresponding impact these rapid changes will have (Berthier et al., 2010; Deb, Butcher et Srinivasan, 2015; Flowers, Copland et Schoof, 2014; Johnson, 1992).

Anticipated hydrological changes in this region of North America are predicted to particularly affect aboriginal populations. For instance, aboriginal peoples located along the Yukon River in both the United States and Canada depend on fish populations for livelihood (Nuttall, 2007), local people have described the environment as *of risk* and *at risk*, meaning that climate variability has changed movement and behavior of animals making everyday traditions and activities unpredictable, and *at risk* because of pollution, industrial development and global warming induced changes (Ørbæk et al., 2007).

1.1.2 The Duke River Valley

The present study takes place in the upper part of the Duke River valley. The Duke River empties into the Kluane River just below Burwash Landing, which in turn feeds the White River and consequently spills into the Yukon River in the watershed holding the same name. The study site is a small watershed (631 km^2) found in the southeast part of the range home to the Duke River (Figure 1.3 - red outline), the glacier feeding the river holding the same name is 20.1 km^2 (see Chapter 2 - Study Site).

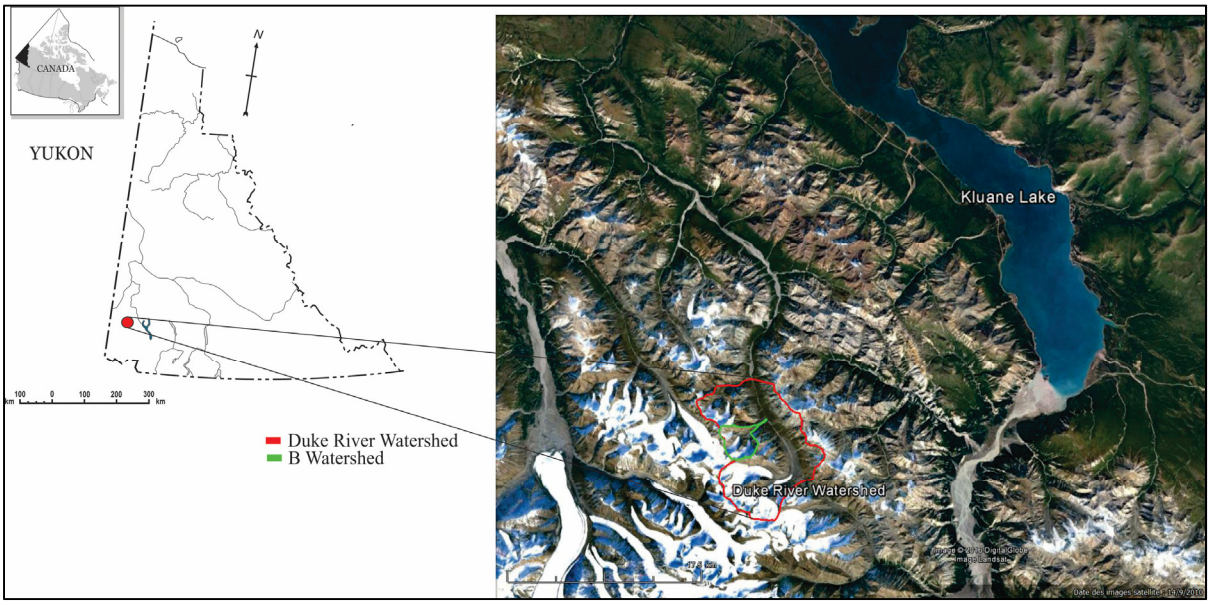

Figure 1.3 Duke Upper Watershed

1.2 Water Sources in Subarctic Glacierized Watersheds

As discussed in the introduction chapter, glacierized watersheds of the subarctic host a large number of potential water sources. Glaciers, the most studied water source, play a dominant role in the watershed they belong to (Kang et al., 2009). However, other water sources, most of them being climate sensitive, shall also be considered as potential important contributors to glacierized watershed outflows. Figure 1.4 shows, in a conceptual way, the different features that play a role in the subglacial environment. In addition to the glacier related

processes, groundwater (Walvoord et Striegl, 2007) is highly dependent on the permafrost conditions (Janowicz, 2011) in those environments, ice cored moraines (Moorman, 2005) or icing (Moorman et Michel, 2000) and rock glaciers appear to also be important factors.

Main hydrological characteristics of glacierized watersheds and proglacial fields are glaciers, ice-cored moraines, rock-glaciers, permafrost and snow cover as presented in figure 1.4. These features are affected by the energy balance with radiation as the largest flux input, hydraulic processes acting within and hydrological effects acting on them.

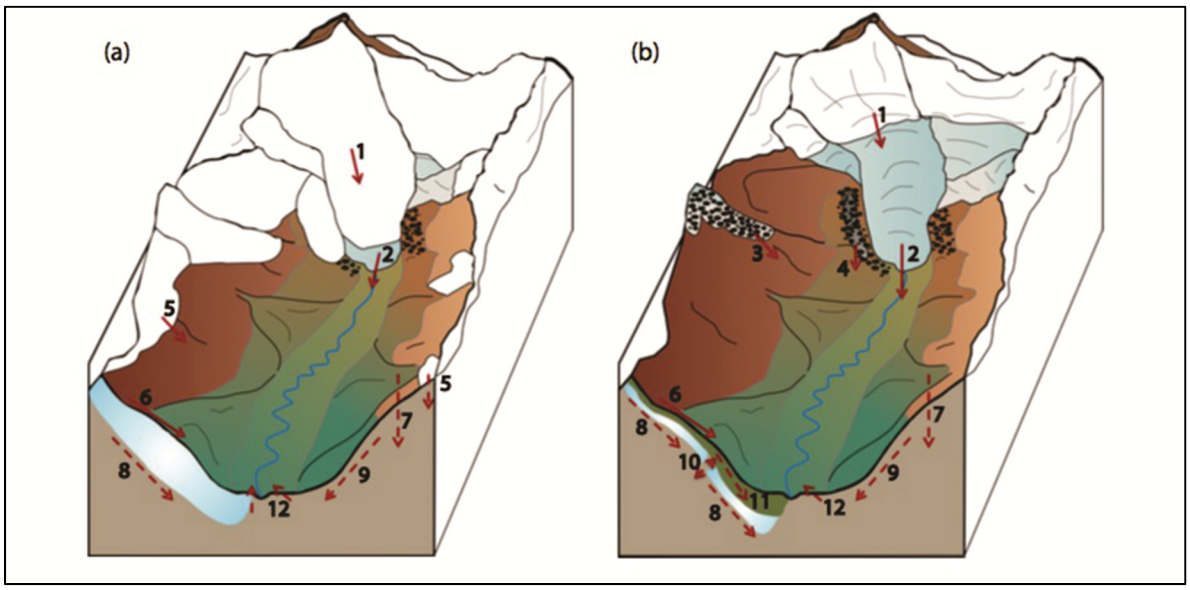

Figure 1.4 Conceptual model of the subarctic glacierized watershed for two seasons: (a)snowmelt and (b) summer; red arrows show water fluxes (solid - above the ground, dashed - under the ground): 1 - snowmelt on the glacier, 2 - glacier melt, 3 - ice melt from rock glacier, 4 - ice melt from ice-cored moraine, 5 - snowmelt of the glacier, 6 – surface runoff, 7 – precipitation infiltration, 8 – sub-permafrost groundwater, 9 – groundwater, 10 – intra-permafrost groundwater, 11 – supra-permafrost groundwater, 12 – springs

Taken from Chesnokova (2015)

Runoff from the glacier is composed of snowmelt on the glacier (1) and glacier melt (2). Gradually, the snowmelt will occur at higher elevation as summer progresses leaving the glacier uncovered and therefore melting at a faster rate. When snow melts on the edges of the glacier, ice-cored moraines (4) and buried-ice (3) are also exposed to melt during summer

season; due to their insulating debris cover, buried ice melt volumes are dependent on size and energy inputs. As snow melts, it creates a surface runoff (6) that progressively infiltrates the soil and finds its way into the hydrological processes within permafrost. Surface runoff and precipitation (7) are the major hydrological actors in seasonal growth of the permafrost active layer, they supply supra-permafrost groundwater sources (11) but will also contribute to hydraulic processes acting upon sub- (8) and intra-permafrost (10) groundwater. Due to North-facing slopes receiving less solar radiation, they usually have more permafrost (Carey et Woo, 1998; 2001) and higher snow water equivalent (SWE) prior to melt. Groundwater is also commonly found lower in the valley where it may find soils to infiltrate or in phases of permafrost to permeate through.

In this study site, only glaciers, icings, ice-cored moraines and groundwater sources were present. In the following section, we describe the main sources expected in this subarctic watershed in more details.

1.2.1 Glaciers

Glaciers present a substantial freshwater source which globally supply water to one sixth of the world's population (Barnett, Adam et Lettenmaier, 2005). Despite growing concerns for the health of glaciers and their implications in water supplies (Cruz R. V. et al., 2007), their global contribution is not yet well understood (Schaner et al., 2012). Glaciers store water in the solid form in the accumulation area during accumulation months and release most of their contribution during the ablation season.

Glaciers are complex entities, although their contribution is confined to meltwater for the ablation zone, there are multiple pathways it can follow; surface (supraglacial), internal (englacial), and basal (subglacial) all contribute to runoff composition (Boon, Flowers et Munro, 2009). The role and activity of those pathways in the hydrological systems are variable in time and space (Irvine-Fynn et al., 2011) and can be difficult to isolate.

Runoff volumes from glaciers follow the diurnal cycle. They are affected by melting season variability as well as accumulation volumes, consequently making accurate response projections difficult. Their runoff volumes are controlled by i) melt water production at the glacier-atmosphere interface, ii) volume of water it stored during the accumulation period and iii) the pathways melt water employ within the glacier surface whether it is supra-, en- or subglacial (Chesnokova, 2015). Supraglacial melt is the dominant source of meltwater for most glacierized area (Hock, 2005), as most of the melt occurs at the glacier surface. On the surface of the glacier, supraglacial channels are eroded onto the surface and meltwater finds its way into the englacial and subglacial systems via crevasses and moulins. Either through ice percolation (slow system) or englacial channels (fast system) the water will drain into the glacier's hydrological pathways (Benn et Evans, 1998). With increasing volumes during the ablation season, the pressure created within the glacier will lead to wider channels, faster snowline retreat and enhanced hydrofracturing, hence the ever changing drainage system course during melting season.

Daily, meltwater reaches its peak volume shortly after the shortwave radiation and temperature maxima (Chesnokova, 2015). Seasonally, the annual runoff reaches its peak during the ablation season, when average radiation and temperature are at their peak.

There are multiple types of glaciers based on location, form and temperature regimes. Glaciers from the Northern St. Elias slopes are classified as mainly polythermal (Benn et Evans, 1998). Polythermal glaciers are defined as "ice masses displaying a perennial concurrence of temperate (temperature at melting point) and cold ice (temperature below melting point)" (Irvine-Fynn et al., 2011). Their particular thermal regime makes the supraglacial pathway dominant compared to englacial and subglacial channels, this being at least true in the cold ice section of the glacier.

1.2.2 Ice-Cored Moraines

Moraines are glacially accumulated piles made up of glacial debris, which range from small flour-like soil to large boulders (Menzies, 2002). There are two main types of moraines: lateral moraines form at the edges of the glacier pushed by ice flow over time, and terminal moraines, as their name suggests, are at the foot of the glacier marking the maximum advance of the glacier (Barr et Lovell, 2014).

Ice-cored moraines are ice bodies that comprise a discrete body of glacier ice covered with morainic materials (Singh, Singh et Haritashya, 2011). The formation of moraines is based on a combination of supra-, en-, and subglacial debris being pushed to the edges. Proglacial debris are forced outward during glacier advance, subglacial debris can be squeezed from upward pressure as well as surrounding ridges contributing to the amount of sediment (Lukas et al., 2005).

For an ice-cored moraine to emerge, ice must be isolated from the glacier during advances but covered by enough debris to shield it from melting, thus creating a differential ablation rate than that of the glacier's (Lukas, 2011). Lukas (2011) proposed three buried-ice formations; active ice near the glacier's boundaries covered in sediment and debris are cut-off during negative mass balance, steady delivery of debris at the same location (depocenters) can lead to thickened supraglacial material cover changing the ablation rate, and finally existing dead ice can be engulfed by advancing glaciers. The debris cover affects the thermal conductivity and therefore the insulation provided by the debris above and below the ice affects the melting rate and by consequence the volume of water contributed. The thicker the debris cover, the slower the ablation rate (Brook et Paine, 2012), exposing bare ice can increase ablation rate up to 30 cm in a 1.5 month period (Johnson, 1992).

1.2.3 Rock Glaciers

Rock glaciers, behave differently than glaciers, because they consist of an ice-core covered in debris or an ice-cemented matrix (Singh, Singh et Haritashya, 2011). The insulating properties of the debris cover (Humlum, 1997) reduce and can even eliminate the characteristic glacier dynamics. Thus, rock glaciers contribute water to total discharge by snowmelt and precipitation infiltration, permafrost melt and ice-core melt (Williams et al., 2006) and can stay frozen even with the absence of snowpack cover. The interior of a rock glacier can act as an aquifer and the hydrological characteristics of the rock glacier can be viewed as its own system (Singh, Singh et Haritashya, 2011).

1.2.4 Groundwater

Groundwater is a very broad term to describe water that occupies empty spaces in soils and geographic strata (Groundwater, 2016). It englobes a mixture of sources and as it sits underground in soil layers, it absorbs its organic properties.

Groundwater drawn from periglacial sources, such as moraines and rock glaciers have been shown to affect the timing and volume of alpine discharge (Langston, Hayashi et Roy, 2013). In high latitude soils that reach temperatures below freezing point (0°C), permafrost can also contribute to groundwater source volume; glacial drainage can also promote the formation of permafrost or buried ice features (Irvine-Fynn et al., 2011). The active layer is defined as the stratum that melts and refreezes with temperature changes (Osterkamp et Burn, 2003). As active layers are becoming thicker due to climate change, water faults are growing and water melting through these faults reaching groundwater networks only contributes to the growth of the layer (Osterkamp et Burn, 2003; Shur et Jorgenson, 2007). Permafrost zones are affected by multiple local factors such as topographic location, slope, vegetative cover, snow cover and soil texture. The permafrost cover in the St. Elias range is measured to be sporadic discontinuous, meaning permafrost can be found in 10-50% of the soil, with temperatures close to 0ºC (Burn, 1994). Multiple researches have been conducted on permafrost in the

Kluane lake region since the 80s, notably on the topic of active layer evolution (Harris, 1987) and permafrost probability modelling (Bonnaventure et Lewkowicz, 2008; Kinnard et Lewkowicz, 2005), but little is known on its possible contribution to total runoff. Groundwater has been found to be an important recharge source and possibly a potential buffer on the impact of predicted lower glacial discharge (Baraer et al., 2012; Langston, Hayashi et Roy, 2013).

1.2.5 Icing

Icings are the results of refreezing at the surface of emergent discharge from sub-surface sources such as groundwater sources (Hodgkins, Tranter et Dowdeswell, 2004; Williams et Smith., 1989). They are commonly found in the proglacial field, but not limited to permafrost regions. They can also be fed by subglacial meltwater during accumulation season and go through annual cycle of growth and decay. Glacier fed icings have a fragile dependence on glacier and can easily be overthrown by change in hydrological conditions (Wainstein, Moorman et Whitehead, 2014). Their contribution to overall discharge is dependent on their size and melting rates.

1.3 End-Members' Contribution to Catchment Outflows

There are multiple techniques to quantify relative contributions of end-members: Direct discharge measurements, glaciological approaches, hydrological balance equations, hydrological modelling and finally use of hydrochemical tracers. Direct discharge measures are done at end-member's outlets, which can be difficult and hard to access given the changing landscape in glacial environments (Gascoin et al., 2011; Thayyen et Gergan, 2010). Glaciological approaches are based on the estimate of glacial mass changes (Liu et al., 2009); they are potentially the most accurate method but are limited to one end member only and existing datasets (La Frenierre et Mark, 2014). The hydrological balance equation method deduces glacier meltwater discharge (Baraer et al., 2012) where other component contribution can be estimated and using hydrological modelling, as the name suggests, relies

on models specific to watersheds (Comeau et al., 2009), but again both depend heavily on the common understanding of involved processes. Hydrochemical tracers based methods solve the hydrological balance equation by assuming conservative behaviour of the tracers (Baraer et al., 2009). Geochemical techniques and end-member mixing models have been used increasingly to characterize contributions in watershed under varying environmental conditions (Baraer et al., 2015; La Frenierre et Mark, 2014). Based on its chemistry, it is possible to "quantify the proportion" of end-members to discharge (La Frenierre et Mark, 2014). This method will be explained further in more detail.

1.3.1 Natural Tracers

Water from different end-members tends to have a distinct hydrochemical signature; its unique path is subject to specific geological, and hydrochemical processes (Drever, 1988). The individual end-member signature is then used for understanding the hydrological, geological and biological processes an end-member may be subject to and to quantify their contribution to total runoff discharge (Baraer et al., 2015).

Commonly used natural tracers dab in both chemical and physical properties. Chemically, ionic concentrations are the most prevalent source of information; anions frequently used are SO_4^{2-}, Cl^-, F^-, HCO_3^-, NO_3^- and cations used are Na^+, K^+, Mg^{2+} and Ca^{2+} (Lafreniere et Sharp, 2005; Mitchell et Brown, 2007). Organic contents have also recently emerged as efficient tracers for groundwater and permafrost sources (MacLean et al., 1999). Known signatures include organic nitrogen and carbon concentrations. In this study, organic carbon was utilized in efforts to identify permafrost contributions. Physical properties of water sources include isotopic ratios and electrical conductivity. Isotopes frequently used are the heavy stable water isotopes ^{18}O and ^{2}H, which were used in this study but other isotopes are sporadically used depending on environment and specific features.

Usually, natural tracers based methods imply the use of different kind of tracers in order to benefit from their different characteristics. For instance, major ions are most effective in the

differentiation of groundwater sources from other end-members while stable isotopes are more efficient in the distinction between glacial meltwater from precipitation and snowmelt, so they are usually used in combinations with one another (Baraer et al., 2012; Mark et Seltzer, 2003).

1.3.1.1 Major Ions

Solute tracers are very convenient because they tend to be specific to an origin affected by its own environmental, biological and geological pressures (La Frenierre et Mark, 2014) and so sources will have a unique ionic signature based on their origins. The various components of the hydrological cycle are dominated by different solutes, for example, precipitation would contain higher concentrations of chloride (Cl^-) because of its presence in oceanic water and the evaporation cycle (Ladouche et al., 2001). Mg^{2+} and Ca^{2+} ions on the other hand are usually a by-product of bedrock geology and chemical weathering (Bagard et al., 2011; Brown et al., 2006; Tranter et al., 1996). The use of solutes as tracers is only limited by the reactivity of the tracers, whether it is in its natural state, the transportation process, or in the analytical procedure.

The ions recognized as majors are NO_3^-, SO_4^{2-}, F^-, Cl^-, HCO_3^-, Na^+, K^+, Mg^{2+} and Ca^{2+} (Baraer et al., 2009; Brown et al., 2006; Mitchell et Brown, 2007). Other ionic compounds such as Br^-, Al^-, $Fe^{2+,3+}$, $Mn^{2+,3+,4+}$, PO_4^{3-} and NO_3^- (Barthold et al., 2010; Crompton et al., 2015) have already been used as tracers in several studies but their use is limited by their chemical instability in natural conditions. Silicate is also a stable solute for reconstruction of hydrological pathways; it has been used in ratio with other solutes as a tracer for multiple end-members (Klaus, 2013; Laudon et Laudon, 1997).

Solutes have proven particularly efficient in subarctic environments. For example, studies show that icings layers can be used as a solute record of highly concentrated early spring runoff, which is released in the early ablation stages (Wadham, Tranter et Dowdeswell, 2000). Yde et al. (2012) show high concentrations of Ca^{2+} and HCO_3^- as well as cryogenic

calcite ($CaCO_3$) precipitate especially at the extremities, while isotopic data shows a normal trend with the local meteoric water line. Ionic concentrations are powerful tracers best used in unison with isotopic ratios.

1.3.1.2 Isotopes

The most used isotopes for hydrological sciences are the $\delta^{18}O$ for oxygen and $\delta^{2}H$ for hydrogen; they hold the same position in the table of elements as their most abundant counterparts, ^{16}O and ^{1}H respectively (Gat, 2010). They are referred to as the heavy stable water isotopes.

Other isotopes such as the radioactive tritium ^{3}H (Maloszewski et al., 2002; Turnadge et Smerdon, 2014) and ^{222}Rn (Dugan et al., 2012; Elliot, 2014), as well as stable strontium isotopes ^{86}Sr and ^{87}Sr (Bagard et al., 2011; Keller, Blum et Kling, 2010) and sulfur isotope ^{34}S (Elliot, 2014) have been used in different studies as tracers for permafrost and groundwater end-members and even moraine tracing (Stotler, Frape et Labelle, 2014). However sampling and analyses for those isotopes are impractical in standard conditions: ^{3}H has to be collected in glass bottles (100 mL), ^{222}Rn is highly volatile gas (Freyer et al., 1997), strontium and sulfur isotopic ratios are determined by costly and labour intensive methods (Martins et al., 2008; Mason, Kaspers. et van Bergen, 1999). For a large number of samples, stable heavy isotopes of water are the most practical and cost effective analytical method.

Measurements leading to a more intuitive measure are expressed as ratios relative to the Vienna Standard Mean Ocean Water (V-SMOW) as shown in eq 1.1 and 1.2. *R* is the isotopic ratio, expressed in permil, calculated as a ratio of concentration between the rare and abundant isotope.

$$18\mathrm{R} = \frac{\text{rare isotope abundance}}{\text{abundant isotope abundance}} = \frac{/\mathrm{H}_2^{18}\mathrm{O}}{/\mathrm{H}_2^{16}\mathrm{O}} \tag{1.1}$$

$$\delta^{18}\mathrm{O} = \left(\frac{{}^{18}R_{Sample} - {}^{18}R_{std}}{{}^{18}R_{std}}\right) \text{ x } 1000 = \left(\frac{{}^{18}R_{Sample}}{{}^{18}R_{std}} - 1\right) \text{ x } 1000 \tag{1.2}$$

By definition, the standard mean has a composition of 0‰ for both heavy isotopes, representative of the average sea concentration. It is also well known that $\frac{\mathrm{H}_2^{18}\mathrm{O}}{\mathrm{H}_2^{16}\mathrm{O}}$ ratios change based on altitude, being increasingly depleted at higher elevation (Gat, 2010) due to the progressive condensation and precipitation processes in high mountainous areas (Gonfiantini et al., 2001). Due to their heavier weight and larger mass (Gat, 2010), they can induce measurable physical and chemical effects; during phase changes in the hydrological cycle, heavy isotopes will become enriched in one phase and depleted in the other, this separation is known as isotopic fractionation (Gat, 2010). For example, in warm temperatures, evaporation will occur and the phase change of a lighter molecule requires less energy, hence the gas phase would contain $\mathrm{H}_2^{16}\mathrm{O}$ while the liquid phase would be left with the heavier molecules being enriched in $\mathrm{H}_2^{18}\mathrm{O}$.

Because isotopes are affected by evaporation and transpiration, they can induce a specific signature in recharge water, which will be significantly different from isotopic ratios in precipitation samples (Hopmans, 2000; Stumpp et al., 2009).

1.3.1.3 Dissolved Organic Carbon

Dissolved organic carbon (DOC), is a good indicator of biological processes. DOC is defined as organic matter that passes through a filter, usually 0.22-0.7 μm (Brukner, 2016). As a tracer, DOC is usually used for permafrost or groundwater end-member tracing (MacLean et al., 1999), because of extended exposure to organic soil leaching, permafrost has been associated with high organic content (Carey et Quinton, 2005; Kokelj, Smith et Burn, 2002). Permafrost-dominated catchments showed higher concentrations of DOC, but lower solute contents than their neighbouring nearly permafrost-free watersheds (Carey et Pomeroy, 2009). DOC has been used with $\delta^{18}O$, (Carey et Quinton, 2005), and with HNO_3^- (Petrone et al., 2006) as tracers in important organic layer environments.

1.4 Mixing Models

The unique hydrochemical signatures of end-members are the basis of hydrochemical mixing models. By using conservative tracers, it is possible to identify sources and quantify their contribution to runoff (Baraer et al., 2009; Christophersen et Hooper, 1992; Mark, McKenzie et Gomez, 2005). The simplest mixing models are two end-member models, (e.g. glacial and non-glacial) (Mark, McKenzie et Gomez, 2005). Models distinguishing more end-members (glacier melt, surface runoff, groundwater discharge) require the use of statistical methods (e.g. Bayesian) (Baraer et al., 2009; Cable, Ogle et Williams, 2011).

There are two techniques dominating hydrological tracer studies: hydrograph separation and end-member mixing analysis (EMMA) (Barthold et al., 2011). The first relies on solving mass balance sets of equations while the latter is based on the eigenvalues approach. The use of a mixing model is to identify and quantify the major contributors of total discharge. EMMA is unrestrictive in the amounts of tracers needed (Barthold et al., 2011); two to six seems to be the majority, but the more end-members the more tracers are required. Its restrictive factor is the repetitive sampling required, which can be problematic in remote locations and difficult to access terrain (Christophersen et Hooper, 1992; Sinclair, 2014).

For the hydrochemical tracer technique to be employed there are key assumptions to take into account. Firstly, the hydrochemical signature associated to each end-member must be sufficiently distinct. Followed by the notion of conservation of the tracer between the sources and mixing points, meaning there are no further changes occurring, such as isotopic fractionation or chemical reaction which would affect solute concentrations (Baraer et al., 2009; Mark, McKenzie et Gomez, 2005). This ensures that the mass of the solutes found in the mix describes an accurate portrait of the relative inputs of the end-members involved (Baraer et al., 2009; Christophersen et Hooper, 1992). The hydrochemical tracer approach also assumes the chemical characteristics defining end-members take into account the range of hydrochemical variation each source might experience (La Frenierre et Mark, 2014) in a way, minimizing the variability of end-members. For instance, glacial meltwater would combine a mixture of different ablation processes and varying flows that would be conditioned to varying isotopic fractionation and chemical reactions (Nolin et al., 2010; Sharp et al., 1995). Glacial derived meltwater in a single watershed can originate from multiple chemically-distinct glaciers that have their own unique bedrock geology, ice flow rates and subglacial drainage patterns (Yuanqing et al., 2001).

These assumptions limit the hydrochemical tracer approach, but there are notable advantages over certain techniques. For example, chemical tracer analysis does not require long term detailed meteorological and glaciological data; a sampling period is usually sufficient to establish a logical snapshot of base flow conditions and pathways. La Frenierre et Mark (2014) also argues that the hydrochemical tracers approach doesn't require explicit calculation of hydrological parameters that can be challenging to accurately measure in the field such as evapotranspiration and groundwater exchange (Kong et Pang, 2012; Mark, McKenzie et Gomez, 2005). Hydrochemical data is rather easy and inexpensive to obtain despite a watershed's seclusion (Mark et Seltzer, 2003; Nolin et al., 2010).

The hydrochemical basin characterization method (HBCM) used in the present study, is one of the methods used to assess end-members' contribution to outflows at various points of a watershed. Based on hydrograph separation techniques, HBCM was developed to

characterise contribution of end-members in remote glacierized watersheds, where EMMA cannot be adopted due to logistical reasons.

HBCM has been used previously for quantifying groundwater contributions in the tropical glaciers of the Cordillera Blanca in Peru, more precisely the Callejon de Huaylas watershed (Baraer et al., 2009; Baraer et al., 2012). It was successful in producing reliable results in ungauged and remote areas (Baraer et al., 2009). It has also showed positive results in two sites of the Central Andes, the Tuni watershed in the Cordillera Real in Bolivia and the Pastoruri watershed in the Cordillera Blanca in Peru (Sinclair, 2014).

HBCM requires samples to be collected in a limited time-frame, following a synoptic approach, in order to generate a geospatial snapshot of the hydrological systems inner-workings within a watershed. Some of the downfalls of this method are that it is difficult to be certain, with high confidence, that the assumptions previously mentioned, which are the core components of the method, are being met. In a dynamic, geologically heterogeneous, mountain watershed, it proves to be challenging to verify the conservation of a tracer and the true unique hydrochemical signature of an end-member, even more so when only a small number of samples are collected (Nolin et al., 2010). Despite those limits, trace methods based techniques have proven very efficient for hydrograph separation in alpine environments (Baraer et al., 2009; Baraer et al., 2015; Fujita, Ohta et Ageta, 2007; Mark et Seltzer, 2003).

Although the technique has proven itself, it has yet to be tested in subarctic glacierized catchments.

CHAPITRE 2

STUDY SITE AND DATA COLLECTION

The Duke valley is located in the St. Elias mountain range in the Yukon; it has a total area of 631 km^2 and its elevation ranges from 817 to 2824m. The valley was chosen partly due to its location and relative accessibility, but also because a gauging station situated at the lower part of the Duke River, near the mouth where it intersects the Alaska Highway (61° 20′ 45″ N, 139° 10′ 04″ W) monitors stream discharge since 1981. The Duke River watershed provides an ideal sized watershed for field work periods and distances.

As of 2015, the upper Duke River watershed is being equipped with hydro-meteorological equipment with the objective of studying hydrological impacts of climate change in the St. Elias Mountains. The research program, led by École de Technologie Supérieure (ETS), aims to improve the understanding of unique hydrological processes by focusing on glacier fed watersheds at the regional scale and their specific features scale. The uppermost part of the watershed, where most of the research activities took place was subdivided into smaller watersheds; the main study area, watershed B, is highlighted in green in the previously presented figure 1.3. We used the watershed B to evaluate and provide a primary understanding of the hydrological processes of this alpine environment.

The watershed B was chosen for both scientific (i.e. the presence of multiple glaciers and an important proglacial field) and logistical reasons (i.e. its relatively small size and accessibility). Valley B hosts three small glaciers we named B1, B2 and B3 (Figure 2.1). In total, the watershed B has a surface of 8.75 km^2 and is 36.6% glacierized.

B1 is the largest of those glaciers with 1.7 km^2 area and the one with the lowest terminus (Table 2.1). B2 is second in size with an area of 0.9 km^2 and altitude terminus elevation of 2129 m, B3 is the smallest and highest glacier in the watershed with 0.6 km^2 of glacierized area and a terminus at 2272 m.

A survey was conducted by the Yukon Geological Survey in 1992 to identify bedrock geology and lithology in the Kluane National Park and Reserve. The B valley is composed of two regional terranes with slight variation in bedrock composition. The higher in altitude covers most of the icefields area. It is made of principally sedimentary rocks containing mainly siltstone, sandstone, quartzite and schist and in minor quantities argillite, phyllite, limestone, volcanic, gypsum and anhydrite (Dodds et Campbell, 1992). The lower altitude bedrock content is a mixed of volcanic and sedimentary rock, the principal lithology includes sandstone, conglomerate, breccia, greenstone and amphibolite while minor lithologies includes argillite and phyllite (Dodds et Campbell, 1992).

Table 2.1 Glaciers of the B Watershed

Name	Total Glacierized Area	Altitude of the terminus
B1	1.7 km^2	2038 m
B2	0.9 km^2	2129 m
B3	0.6 km^2	2272 m

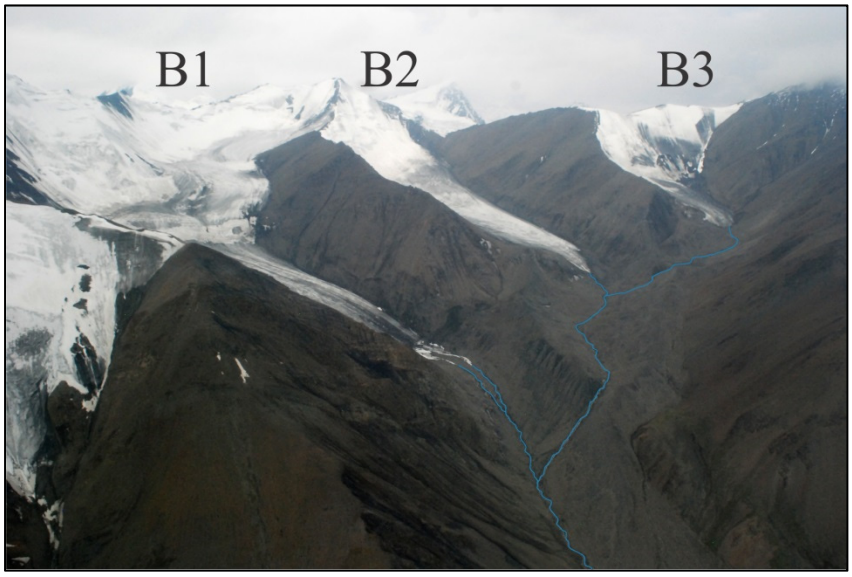

Figure 2.1 Duke B Watershed (2015)

During the field campaign of 2015, many unexpected hydrological features and water sources were observed such as icings, buried ice and ice-cored moraines scattered throughout proglacial fields. Slopes neighboring glaciers were producing small streams, possibly due to buried ice. Groundwater wells were dug in various areas of the watershed, but no permafrost was found, partially due to geological features, wells could not be built deeper than 1.5 m.

As seen in figure 2.2, 67 samples were collected in total for the sampling of the B watershed. At sampling locations, site measurements were taken such as pH, electrical conductivity, and temperature (appendix I). Sampling for ionic content, organic carbon concentration, isotopic ratios and alkalinity testing were conducted. B1 glacier was sampled on four occasions during the sampling period, twice on July 3rd, and once 5th and 7th 2015. The July 3rd sampling was exceptional due to a snow precipitation on July 2nd. Therefore, the B1 system was studied in two parts, first a spatial analysis with the established system on July 5th and secondly a temporal analysis was done on the entirety of the sampling. B2 and B3 glaciers were sampled once during the sampling period in one day, July 7th, 2015.

The B outlet was also sampled over a 27-hour period at 2-hour interval from 9h to 21h and at a 4-hour interval from 21h to 9h, for a total of 10 samples, from 09/07/2015 at 5h09 to 10/07/2015 at 8h15. This was done to capture the fast changes during the day while we expected the night variations to be much smaller.

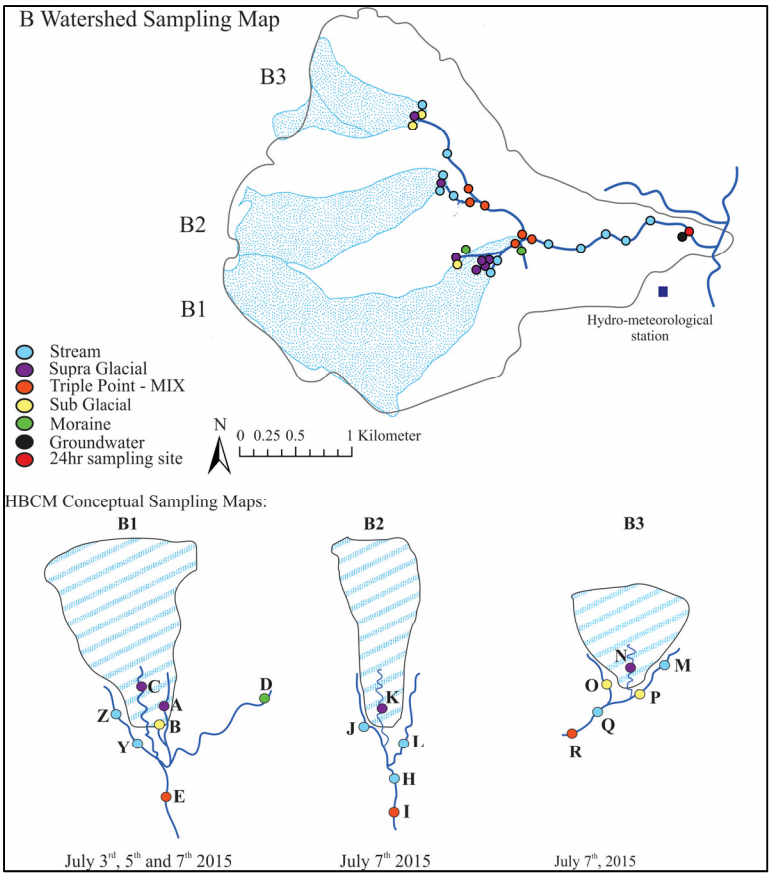

Figure 2.2 B Watershed Sampling Map

In addition to sampling, over the course of the campaign, long term hydro-meteorological equipment was installed at the outlet of the B valley, pressure gauge stations were placed in strategic outlets to measure water discharge and time-lapse cameras were placed to visually assess the evolution of subarctic proglacial field. The hydro-meteorological equipment set on an automatic weather station (AWS) (60°59'44.0"N, 138°57'45.4"W) recording air temperature, liquid precipitation, radiation and relative humidity at 15 minute intervals. This dataset provides information on the micro-climate of the valley and will eventually be used in a numerical model (Chesnokova, 2015). Stream gauging stations equipped with pressure transducers were installed in the B valley outlet and the Duke River outlet.

The following section will present the methodology used in this research.

CHAPITRE 3

METHODOLOGY

On the field, all collected samples had site measurements taken as outlined in the previous chapter, those were then analysed for isotopic ratios, DOC and major's ions following the outlined methodology. Raw data was manipulated to produce a set of calculated tracers such as relative concentrations and total dissolved solids (TDS). A bivariate analysis was then conducted on the measured and calculated tracer concentrations in order to identify tracer signatures unique to end-members. This was then followed with a hierarchical cluster analysis (HCA) to identify end-members' origins and pathways employed. Using HCA also offered the opportunity to establish any relationship with groundwater sources. HCA results were utilized to select tracers needed for the quantitative analysis in the hydrochemical model. A quantitative study was done using the hydrochemical basin characterization method (HBCM) for the B watershed and for the 24-hour sampling period. The following sections will go into greater depth and detail into the methods used for each component of this study.

3.1 Sample Collection and on Site Measurements

On site, the GPS coordinates were measured using a Magellan™ Triton® 300 while pH, conductivity (µS/cm) and temperature (ºC) were measured using a PCE-PHD-1 pH meter.

Samples for stable isotope analysis were collected in 30 mL high density polyethylene (HDPE) bottles. The bottles were rinsed three times with water at the source, and then filled to the brim with the sample. The bottles were then sealed with insulating tape to avoid evaporation.

Samples for dissolved organic carbon (DOC) and major ion samples analysis were filtered with hydrophilic polypropylene 30mm syringe filters (0.45 µm) with 50 mL syringes. HDPE

60 mL bottles were rinsed three times with filtered water, filled to the brim and sealed with insulating tape. Bottles were stored in the dark at 4°C whenever possible.

Samples for alkalinity analysis were collected in 125 mL HDPE bottles that were rinsed three times with unfiltered water and then filled to the brim with unfiltered source water.

3.2 Chemical Analyses

3.2.1 Laboratory Analyses and Tracer Value Calculation

Alkalinity was tested within 12 hours of sampling at the base camp. Tests were conducted by titration with 0.1600N H_2SO_4 with a HACH® Digital Titrator 16900, using bromocresol green as an indicator. An aliquot was first used to thrice rinse all the equipment, and then 25 mL of the sample was measured using a graduated cylinder and poured out into an Erlenmeyer. Two drops of bromocresol green were added to the sample. Titration ensued until the light blue tint changed to colourless. Samples which showed concentration above 2.0 mg/L of $CaCO_3$ were titrated three times and the average was obtained.

3.2.1.1 Total Organic Carbon

Measurements of dissolved organic carbon (DOC) were carried out using an Apollo 9000 Combustion Analyzer; combustion analysis determines elemental composition of pure organic compound by combusting the sample and using an infrared detector to measure total concentration. Results were obtained in ppm from a calibration curve made from five standards ranging from 2 to 10 ppm. Standards were run every 20 samples to ensure stability. A duplicate was done every three samples for precision and reproducibility. Three injections were done per sample.

3.2.1.2 Stable Heavy Isotopes of Water

Isotopic data was obtained using cavity ring-down spectroscopy (Picarro Analyzer L2130-*i*), a highly sensitive optical spectroscopy technique which uses the magnitude of light absorption of specific wavelength of gas-phase molecules to determine concentrations of a species. Non-filtered samples were transferred to 2 mL glass vials with rubber caps and further sealed with parafilm to ensure the least evaporation possible. Six lab standards (-15.44 $\delta^{18}O$, -119.85 $\delta^{2}H$) preceded each batch to warrant the analyzer's stability. Six injections of 5 µL each were run per sample. Only the last two injections were used for the final result calculation in order to minimize the memory effect. A standard was placed every three samples to assess stability and to perform results correction wherever justified.

3.2.1.3 Solutes: Anions

Anionic concentrations were measured with a Dionex ionic chromatographer apparatus (IC20, LC25, CD50, GD50). Ion chromatography (IC) is a process by which ions are separated through a column based on their affinity for the ion exchanger. Samples were analyzed for fluoride (F^-), chloride (Cl^-) and sulfate (SO_4^{2-}) ions. Calibration curves of seven standards were done every thirty sample injections, and a standard was run every three samples. Standard blanks of deionized water were run before and after each calibration to ensure no carryover memory. Samples with sulfate concentrations above the calibration standards were diluted by half to fit within the detection limits of the column. One sample every three injection was re-run for reproducibility testing.

3.2.1.4 Solutes: Cations

K^+ and Mg^{2+} concentrations were determined with the same Dionex Apparatus (IC20, LC25, CD50, GD50) while Na^+ and Ca^{2+} concentrations were determined using ICP-OES due to unstable results using ionic chromatographer. Calibration curves were built with 8 standards containing: Sodium (Na^+), potassium (K^+), magnesium (Mg^{2+}) and calcium (Ca^{2+}) diluted

in nano-pure deionized water. Blank standards of deionized water were also run before and after each calibration to ensure no carried over memory in the column. When samples exceeded the calibration range, they were diluted by factors of two to 30 depending on concentrations. As for precision of results, duplicates were done on one of every three samples. K^+ and Mg^{2+} results were extrapolated from the calibration curve by linear regression.

Inductively coupled plasma optical emission spectrometry (ICP-OES) uses the unique set of emission wavelength each element of the periodic table possesses to quantify elements by diffracting the emitted light into discrete component wavelengths. The 10 mL aliquots were diluted and consequently acidified with nitric acid (HNO_3) and passed through an argon flame to atomize components. Calibration curves were built with five standards, and blanks consisted of 5% nitric acid solution.

Silicate concentrations could have been useful tracers in this environment (Crompton et al., 2015) but due to lack of analytical equipment we could not make use of it.

3.2.1.5 Tracer Value Calculation

On top of analytical results used directly as tracer values, few tracer values were obtained by calculation: sum of cations (SC^+) visible in equation 3.1, sum of anions (SA^-) in equation 3.2, total dissolved solids (TDS) in equation 3.3, monovalent to bivalent cationic ratio in equation 3.4, as well as variations of ratios (e.g. SO_4^{2-}/SA^-, Ca^{2+}/SC^+, Mg^{2+}/SC^+) and d-excess in equation 3.5.

$$SC^+ = [Na^+] + [K^+] + [Mg^{2+}] + [Ca^{2+}] in\ mmol \quad (3.1)$$

$$SA^- = [F^-] + [Cl^-] + [SO_4^{2-}] in\ mmol \quad (3.2)$$

$$TDS = [SC^+] + [SA^-] + [CO_3^{2-}] + [HCO_3^-] + [OH^-]\ in\ ppm \quad (3.3)$$

$$\frac{Monovalent}{Bivalent} = \frac{[Na^+] + [K^+]}{[Mg^{2+}] + [Ca^{2+}]} \text{ in mmol} \quad (3.4)$$

$$d - excess = \delta 2\text{H} - 8(\delta 18\text{O}) \quad (3.5)$$

The use of absolute concentrations, such as direct concentrations of [Mg^{2+}] and [SO_4^{2-}], allows grouping waters of comparable hydrochemical signature while relative concentrations, such as [K^+]/[SC^+] and d-excess, allows identification of waters of similar origins when differences between those results is a simple dilution. In order to estimate water source contributions, stream samples were analyzed with end-members in bivariate plots to observe any relations there may be, and then using relative concentrations to see if end-members were truly independent.

3.3 Qualitative Analysis

3.3.1 Tracer Selection

Scatter plots of bivariate nature were produced in mass quantities with natural tracer concentrations to identify the best tracers to use in hierarchical cluster analysis (HCA). Absolute and relative concentrations of natural tracers that differed significantly depending on end-member in bivariate plots were selected for HCA.

3.3.2 Hierarchical Cluster Analysis

Hierarchical cluster analysis (HCA) is a statistical method that measures distance (or dissimilarity) in between columns of data matrices. In this study, it was used as a tool to identify tracers capable of separating end-members by similarity and to begin understanding hydrological processes by individual glacier. Dendrograms are the easiest visual

interpretation of HCA, leafs at the bottom represent specific samples, moving higher along the y-axis (normalized distance) leafs will fuse to one another through a node, these sets of branches are referred to as clusters. Based on the inputted dataset, clusters will form, and the higher the node the more disparate the samples, refer to figure 4.4 for better visualization. The clusters offered insights into the resemblance of chemical and physical properties of samples. Results were interpreted by visually analyzing the relationship of clusters in any given dendrogram.

Hierarchical cluster analysis (HCA) was carried out for each glacier's end-members on both absolute concentrations and relative concentrations. Absolute concentrations give information of the similarity of chemical composition of end-members; samples that formed a cluster based on absolute concentration have similar chemistry and could belong to the same type (supraglacial, subglacial, etc.). Relative concentration eliminates the simple dilution effect and when results are clustered by origins, main contributors may be identified. For example, in a supraglacial sample clusters with the downstream sample, the main contributor would be the supraglacial stream.

A primary understanding of hydrological pathways and contribution was mandatory to ensure end-members were truly independent for the hydrochemical basin characterization method (HBCM) to be launched.

3.4 Quantitative Analysis

3.4.1 Hydrochemical Basin Characterization Method

The obtained set of tracers from the HCA analysis is then used in the hydrochemical basin characterization method (HBCM) to quantify relative contributions of end-members. For HBCM to be successful, a minimum of tracers must be selected, $n-1$ tracers for n end-members at a mixing point, for a maximum of $n+5$ tracers. The relative contribution of each

end-member is estimated using an over-parameterized set of mass balance equations (equation 3.6) (Baraer et al., 2009; Sinclair, 2014).

$$C_{tot\ j} = \frac{\sum_{i=1}^{n}(C_{ij}Q_i) + \varepsilon_j}{Q_{tot}} \tag{3.6}$$

Where $C_{tot\ j}$ is the relative concentration of the tracer j at a mixing point, n is the total number of end-members, i is the end-member, C_{ij} is the relative concentration of tracer j in the end-member i, Q_i is the proportion of end-member present in the total discharge, ε_j is the accumulated error, finally Q_{tot} is the total discharge at the mixing point (Baraer et al., 2009). To obtain the best results from over-parameterization there should more tracers than end-members.

HBCM runs for each mixing point all possible combinations of tracers, based on a quasi Monte Carlo approach, and solves the eq 3.6 for the variable $\frac{Q_i}{Q_{tot}}$ by minimizing the cumulative residual error $\sum_{j=1}^{m}\varepsilon_j$, where m is the number of tracers considered (Baraer et al., 2009).

HBCM characterizes entire watersheds by subdividing them into nested cells (see figure 3.1).

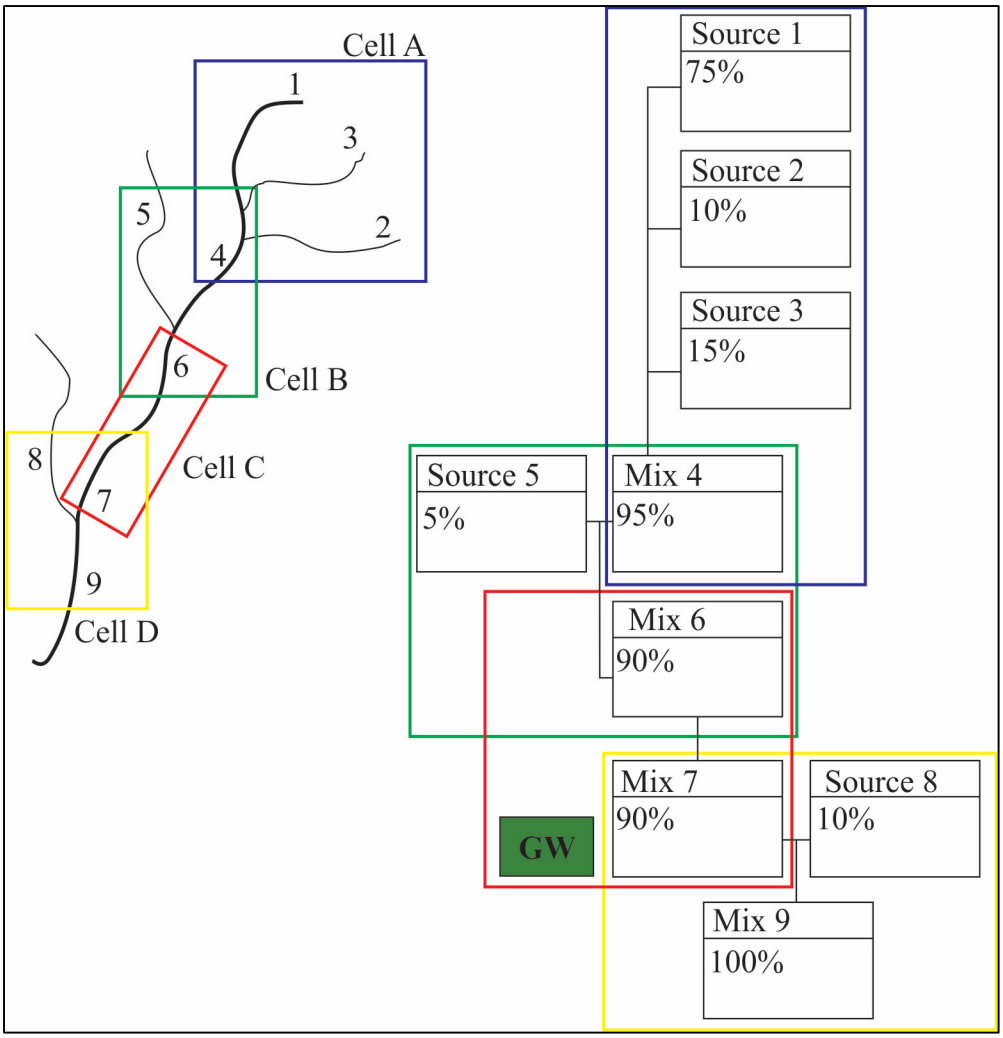

Figure 3.1 Illustration of HBCM's geographic coverage of a hypothetical watershed: on the left is the hypothetical watershed (black lines represent the main stream and its tributaries, numbers represent sampling points); on the right is the corresponding schema for HBCM where sampling points are separated into cells

In order to comprehend the visual representations of HBCM results, we must first understand the cells. Several types of cells can be distinguished. A two point cell (eg. cell C) is representative of two samples taken on a portion of the stream where there is mixing occurring with non-identified sources, referred to as groundwater sources (GW). A three point cell (eg. cell B or D), also referred to as a triple point, and represents two visibly large sources mixing into one. In this case, no other source of water contributes to the downstream sample. A third type of cell is similar to a triple point but instead of considering two

oncoming streams we consider a higher number of end-members mixing into one confluence point (Cell A). Each cell is treated individually as its own entity.

Starting at the outlet cell (cell D in figure 3.1), we make our way up the stream running HBCM for each cell. In triple points, only incoming streams are considered in the simulation, but in two point cells each possible groundwater source is tested for affinity. GW sources do not need to necessarily be from a groundwater well, it can be any source of water of varying origins. Hence, in figure 3.1 (cell C), the GW contributed 10% to total discharge at sample site 7. In this study, we tested for four types of groundwater sources separately by using specifically collected samples: Groundwater well sample, left moraine in the lower half of the B watershed sample, right moraine higher next to the glacier B1 sample and a proglacial lake sample collected in higher elevation between B1 and B2 glaciers.

Before HBCM can produce results the entered tracers are tested for dissimilarity, tracers can be rejected for being too similar or not falling within the HBCM guidelines (refer to Chapter 1 – mixing models). When the HBCM program expresses results, it gives percentages of discharge to sources by iterations with accumulated errors. The program will try all the combination of tracers possible solving for relative discharge of inputted sources while minimizing error.

When testing the groundwater sources, it can be challenging to select which sources are truly contributing. Results tend to vary slightly depending on the groundwater source entered in the HBCM program. To stay consistent in selecting the groundwater sources and general HBCM results, a set of rules was drafted (Sinclair, 2014):

1. Depending on the number of retained tracers by the program, avoid using the first and last possible numbers of tracers in the resulting predictions (i.e. 5 remaining tracers, data for 4 and 3 tracers were used).
2. The water source that reaches results with the least possible accumulated error in considered as the one that contributes for that cell.

3. For each considered number of tracers (eg. 4 and 3 from step 2), all predictions with an accumulated error, ε_i, within the range of 3 times the lowest accumulated error obtained for that number of tracer are considered as equiprobable (if the smallest error is 0.05, then the highest error tolerated would be 0.15).
4. For practical reasons, if more than 8 predictions remained after disregarding iterations that exceed the maximum tolerated error; the 8 results with the lowest cumulated error are used.
5. Finally, results were reported as the median and the extremes.

For example, if the program had been run on the cell C (figure 3.1) and we had tested the right moraine sample and the lake sample as possible groundwater sources. With 5 retained tracers, we would have considered the results for the iteration with 4 and then 3 tracers. In the right moraine simulation, the upstream sample contributes 80% while the moraine is responsible for the remaining 20% with a smallest cumulated error, ε_i, of 0.015, the lake simulation grants 90% to the upstream sample and only 10 % to the lake contribution but the cumulated error was 0.007. Therefore, we assume the lake is the groundwater source. Then, if the lowest cumulated error was 0.007, 0.0021 is the most cumulated error tolerated. If there are more than 8 iterations which fall into this range, only the 8 first iterations are considered.

The difference in extremes was used as the error, hence the range made by extremes of equiprobable prediction was the prediction's uncertainty; these ranges were accumulated by cell using equation 3.7 to present final results with their associated error.

$$A^2 + B^2 = C^2 \qquad 3.7$$

In the HBCM analysis, the results were presented as three different events corresponding each to a specific day: July 3rd, 5th and 7th. The cells and pie charts are colour coded to simplify their origins as seen in table 3.1. Percentages used were the median, while smallest and largest values are shown in parentheses below.

Table 3.1 HBCM Colour Code for Origins

Colour	Origin
	Groundwater sources
	B1 mainstream
	B2/B3 Stream
	B2 mainstream
	B3 mainstream
	Supra end-member
	Other glacial end-member
	B1 left system end-member

The final pie chart shows the total contribution of end-members at the outlet and whenever possible sub-separated into specific glacial components. All volumetric data is based on a relative discharge, assuming 100 % at the outlet of each respective set.

3.4.2 HBCM on 24 hr Sampling Cycle

Measuring diurnal variability in contribution is a difficult process in remote environments like the Duke River valley, and the B watershed. An attempt was made to assess variability in time over a 27-hour period. With less solar radiation and a decrease in temperature during the night, glaciers would be assumed to contribute less to total watershed discharge, whereas groundwater sources would contribute the same as they are not as affected by such physical factors on short time frames. Hence, ionic concentrations and electrical conductivities would increase during the night while pH would decrease. Groundwater and moraine sources generally have higher ionic content because of exposure to rocks and debris that leach solutes into the water, while glacial sources generally are not exposed to such processes for long period of time therefore limiting their ionic content. Performing HBCM with these conditions was difficult without the end-member sampling associated with the analysis.

In order to estimate end-member contribution variation during the 24-hour sampling we tested HBCM on synthetic end member signatures. Because only the B valley outlet was

sampled during the 24-hour sampling, individual end-member signatures were not available at a similar time. We tentatively compensated this lack of data by creating synthetic end-member signatures. Generated mock samples signature as typical sub- and supraglacial end-members were based on average concentrations of supraglacial and subglacial samples of each glacier (B1, B2 and B3) of the 05/07/2015 and 07/07/2915 sampling days. A moraine-type water signature was also synthetized from all 4 samples collected; a “moraine” sample instead of a groundwater sample was used due to the more positive results displayed by the moraine in the qualitative results. Finally, because precipitation occurred during the 24-hour sampling, a synthetic rain sample signature was generated using the assumption it did not contain any solutes.

HBCM was then run for each sample time using the same synthetic end-members.

CHAPITRE 4

RESULTS

This chapter starts with a presentation of the B valley water characteristics obtained with natural tracers and successive calculations. The qualitative analysis section will then present results from the tracer selection and the hierarchical cluster analysis. This section ends with a presentation of the 24-hour sampling results. The quantitative analysis section will first introduce the HBCM results for the B valley, B1 glacier being presented first, followed by B2 and B3 glaciers and ending with results for the entire valley. Finally, this chapter ends with a presentation of the HBCM analysis that was done on the 24-hour sampling cycle.

4.1 B Valley Water Characteristics

In this study, chemical analyses were done for ionic content, stable water isotopes and dissolved organic carbon. Table 4.1 shows the ionic and dissolved organic carbon concentrations, as well as the isotopic ratios for end-members and their corresponding mixing points for each subwatershed, as a snapshot of the dataset obtained the entire dataset which is presented in appendix I, II and III. In the B valley, not all water sources described in the second chapter were present. Only glacial water sources, subdivided into sub and supra end-members, groundwater and ice cored moraines were considered. Remains of an icing were found at the outlet of glacier B1 but due to their very limited sizes, those ice bodies have not been distinguished from the rest of the glacier.

Table 4.1 Analytical Results for End-Members in the B Watershed

Assigned lettering	Original Names	Type	pH	Cond. /µS·cm	Temp /°C	Date	Time	Ionic Content /mmol·L^{-1}								Isotopic ratio		DOC /ppm
								Na^+	K^+	Mg^{2+}	Ca^{2+}	F^-	Cl^-	SO_4^{2-}	Carbonate	$\delta^{18}O$	δD	
B1	**B. Main Outlet**	Sub	9,35	165,3	0,3	03/07/2015	11:46	0,024	0,032	0,174	0,550	0,001	0,002	0,471	0,656	-24,337	-186,013	0,463
A1	**B. Main Supra**	Supra	8,92	225	0,2	03/07/2015	11:49	0,039	0,036	0,256	0,970	0,001	0,001	0,784	0,913	-25,304	-193,005	0,504
Y1	**B. Sub-Main #1**	Stream	8,77	295	2,2	03/07/2015	12:07	0,038	0,019	0,362	1,446	0,001	0,001	1,108	1,031	-25,435	-193,684	0,497
Z1	**B Sub-Main Left #1**	Stream	8,82	354	1,1	03/07/2015	12:24	0,033	0,011	0,420	1,448	0,001	0,001	1,363	1,208	-24,677	-189,235	0,536
C1	**B1 Supra Center**	Supra	8,84	48,2	0,1	03/07/2015	12:35	0,009	0,006	0,020	0,427	0,000	0,002	0,063	0,769	-26,243	-199,745	0,555
D1	**B. Right side Moraine**	Moraine	8,84	544	8	03/07/2015	13:50	0,096	0,167	0,914	2,019	0,003	0,019	2,467	1,634	-24,207	-186,623	0,601
E1	**B. Mstream TP #3**	Stream	8,75	195	1,5	03/07/2015	10:52	0,036	0,042	0,239	0,793	0,001	0,002	0,619	0,806	-24,252	-185,185	0,462
	B. Right Moraine Lake	Lake	9	380	14,9	03/07/2015	15:05	0,041	0,013	0,935	1,431	0,000	0,019	1,330	1,677	-21,948	-174,751	1,161
B2	**B. Main Outlet #2**	Sub	10,19	78,5	0,8	03/07/2015	16:45	0,017	0,015	0,068	0,262	0,000	0,002	0,177	0,291	-25,937	-197,374	0,494
A2	**B. Main Supra #2**	Supra	9,58	129,4	0,2	03/07/2015	16:47	0,009	0,010	0,056	0,396	0,001	0,001	0,138	0,725	-26,716	-203,632	0,687
Y2	**B. Sub-Main #2**	Stream	9,48	92,8	1,1	03/07/2015	16:50	0,015	0,004	0,073	0,280	0,000	0,003	0,171	0,357	-24,865	-190,759	0,595
	B. Left Moraine	Moraine	8,74	1197	11,2	05/07/2015	13:24	0,058	0,143	0,910	5,554	0,005	0,016	6,597	1,588	-22,107	-171,696	0,377
Y3	**B. Sub-Main (Left) #1**	Stream	9,2	114,6	1,3	05/07/2015	15:49	0,014	0,005	0,093	0,426	0,001	0,001	0,250	0,595	-24,145	-185,693	0,366
Z3	**Sub main stream left**	Stream	9,54	70	1	05/07/2015	15:57	0,008	0,003	0,086	0,368	0,000	0,001	0,209	0,547	-24,147	-185,519	0,561
C3	**B1 Supra Center**	Supra	8,6	6,9	0,5	05/07/2015	16:23	0,008	0,001	0,014	0,037	0,000	0,001	0,002	0,102	-24,740	-189,696	0,482
B3	**B. Main Outlet**	Sub	10,23	68,3	0,6	05/07/2015	16:31	0,012	0,015	0,057	0,234	0,000	0,001	0,173	0,170	-24,423	-187,414	0,505
A3	**Main Supra**	Supra	9,58	27	0,5	05/07/2015	16:53	0,008	0,002	0,023	0,078	0,000	0,000	0,029	0,143	-24,988	-190,404	0,480
D3	**B. Right Side Moraine**	Moraine	8,84	425	8,3	05/07/2015	17:03	0,058	0,144	0,630	1,558	0,000	0,017	1,710	1,331	-24,288	-186,573	0,617
E3	**B. Mstream TP #3**	Stream	9,26	64,7	2	05/07/2015	14:14	0,011	0,010	0,056	0,290	0,001	0,002	0,129	0,463	-24,484	-187,314	0,394
	B. Moraine Left #1	Moraine	7,21	1510	1,5	07/07/2015	09:46	0,191	0,109	3,713	4,221	0,000	0,049	7,201	4,581	-23,836	-183,201	0,464
O	**B3 Glacier Main Left**	Sub	9,9	58,8	1,5	07/07/2015	14:04	0,020	0,004	0,060	0,250	0,001	0,003	0,128	0,318	-24,778	-189,550	0,322
P	**B3 Geyser**	Artesian Spring	9,66	211	1,4	07/07/2015	14:16	0,018	0,005	0,181	0,993	0,001	0,008	0,881	0,324	-24,289	-186,352	0,354
N	**B3 Supra Centre**	Supra	8,7	30,1	0,7	07/07/2015	14:26	0,021	0,002	0,055	0,127	0,000	0,001	0,159	0,133	-24,777	-189,059	0,334
M	**B3 Glacier Main Right**	Stream	8,82	128	0,4	07/07/2015	14:36	0,018	0,003	0,116	0,575	0,001	0,001	0,441	0,475	-24,405	-187,779	0,275
R	**B2 Mstream TP #2**	Stream	9,03	189,3	3,5	07/07/2015	12:53	0,012	0,007	0,172	0,747	0,000	0,003	0,662	0,598	-24,338	-186,849	0,251
Q	**B3 Mstream #1**	Stream	9,05	177,6	3,4	07/07/2015	13:29	0,017	0,006	0,145	0,734	0,001	0,002	0,586	0,559	-24,325	-186,690	0,429
L	**B2 Main Right**	Stream	9,7	49,3	2,8	07/07/2015	15:54	0,011	0,009	0,047	0,195	0,000	0,003	0,088	0,291	-24,828	-189,786	0,455
K	**B2Supra Centre**	Supra	8,9	37,3	1,3	07/07/2015	16:01	0,014	0,006	0,025	0,388	0,002	0,009	0,030	0,764	-24,907	-190,556	0,706
J	**B2 Main Left**	Stream	10,24	37,5	0,5	07/07/2015	16:06	0,010	0,007	0,031	0,127	0,000	0,002	0,061	0,134	-24,266	-186,205	0,867
I	**B2 Mstream TP #3**	Stream	9,58	47	1,4	07/07/2015	12:28	0,012	0,007	0,044	0,209	0,002	0,006	0,080	0,331	-24,495	-187,985	0,286
H	**B2 Mstream***	Stream	10,27	35,1	1,8	07/07/2015	16:33	0,011	0,010	0,031	0,167	0,000	0,001	0,100	0,132	-24,741	-189,273	0,673
B4	**B1 Mstream Outlet**	Sub	10,31	57,5	0,8	07/07/2015	17:29	0,016	0,012	0,055	0,236	0,001	0,004	0,134	0,192	-24,444	-186,363	0,600
A4	**B1 Main Supra**	Supra	9,68	17,2	0,3	07/07/2015	17:36	0,011	0,002	0,017	0,095	0,000	0,003	0,026	0,192	-24,914	-190,521	0,303
E4	**B. Mstream TP #3**	Stream	9,43	80,9	2	07/07/2015	10:47	0,013	0,014	0,114	0,287	0,001	0,002	0,200	0,494	-23,996	-183,782	0,449
	Puit Camp B	Groundwate	7,66	996	10,1	09/07/2015	12:27	0,122	0,078	1,693	4,207	0,000	0,016	3,529	5,150	-22,011	-170,990	8,031

B valley waters were substantially depleted in stable isotopes and show very high pH for natural waters that usually situates below 9 (e.g. sample B4). Many samples are highly concentrated in calcium and carbonates. Because calcium carbonate precipitate easily in basic waters (solubility product $K_{sp} = 3.3 \times 10^{-9}$ (Harris, 2007)) saturation indexes defined as the ratio between the ion activation product (Q) and the solubility product was calculated for each sample. When Q is larger than K_{sp}, meaning when the saturation index is higher than one, precipitation is likely to occur. Q was only smaller than K_{sp} for four supraglacial samples; results can be seen in appendix V. This situation raised questions about the validity of the alkalinity tests we conducted. Alkalinity measurements were made on unfiltered samples and showed very high carbonate concentrations while calcium concentrations were obtained from filtered samples. Because calcium carbonate precipitates may have been present as suspended solids in alkalinity samples, it could have been dissolved by the sulphuric acid (H_2SO_4) during the titration and therefore the test could have accounted for more carbonates in samples. Those observations showed that neither calcium nor carbonates could be considered as conservative tracers for the study. In addition, alkalinity test protocols have been modified for the 2016 field campaign.

Similarly, concentrations for fluoride (F^-), chloride (Cl^-) and sodium (Na^+) were regularly found below the detection limit of the laboratory equipment, hence they were not used in further interpretations.

By overviewing analytical results (table 4.1), it is possible to perceive different characteristics that differentiate between sample types. In general, glacial water sources were less concentrated in ions than the groundwater and moraine samples.

Dissolved organic carbon was found in great amount in the groundwater sample, but in hardly detectable amounts in the remainder of the samples and thus was not used as a tracer during further analyses.

The comparison of end-members' water characteristics was pushed further by the use of bivariate graphs presented here after.

4.2 Qualitative Analysis

A qualitative analysis is defined in the encyclopaedia Britannica to be "a systematic analysis so that all the constituents may be identified" (Qualitative chemical analysis, 2016).

4.2.1 Bivariate Graphs and Tracer Selection

Bivariate plots are visual representations of the relationship of two variables tested on the same sample. It usually allows for a glance at the degree of the relationship or pattern between the variables. In the present case, bivariate plots were used to find distinct patterns in tracers to differentiate end-members. Regardless of geographical location, end-members' characteristics were plotted by type to identify a possible common trait. In order to identify the most efficient combinations of tracers to isolate end-members, bivariate graphs were generated for all combination of tracers, excluding those involving tracers rejected at the initial review of analytical results (see previous subchapter). A selection of bivariate diagrams produced for the present research is given in Appendix IV.

Field analyses included pH, conductivity and alkalinity tests that gave an early insight into the systems' dynamics. As seen in figure 4.1, pH varied from 7.21 to 10.31; lower pH was found in groundwater and moraine water while the glacial water had a much higher averaged pH, sub-glacial sources showing the highest pH. Conductivity gave insight into ionic content of samples, in this case ranging from 17-1511 μS/cm; morainic water and groundwater had much higher conductivity than their glacial counterparts due to longer exposure to bedrock weathering.

Figures 4.1 and 4.2 represent the two combinations of tracers that show the most pronounced end-members separation.

Figure 4.1 shows conductivity as a function of pH for the four types of end-members: subglacial, supraglacial, moraines and groundwater. The combination of those two tracers allows separating groundwater and moraine samples from the glacial end-members.

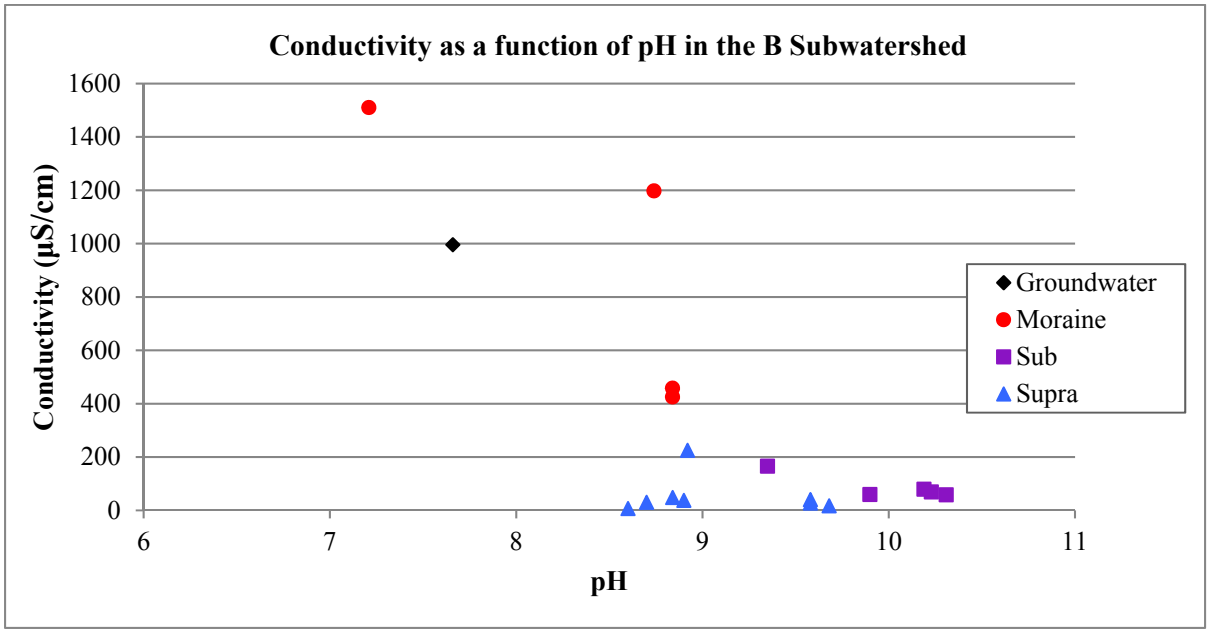

Figure 4.1 Electrical Conductivity as a Function of pH in End-Member Samples

Two moraines with two distinct hydrochemical signatures were also distinguishable. As expected, sub- and supraglacial end-members were more difficult to separate. Subglacial water that is collected at the glacier mouth is often a mixture of supraglacial water and subglacial water that remained at the glacier/bedrock interface during a longer time. Those two end-members are therefore not truly independent.

Figure 4.2 shows the relationship between potassium and sulfate ions for the same end-members.

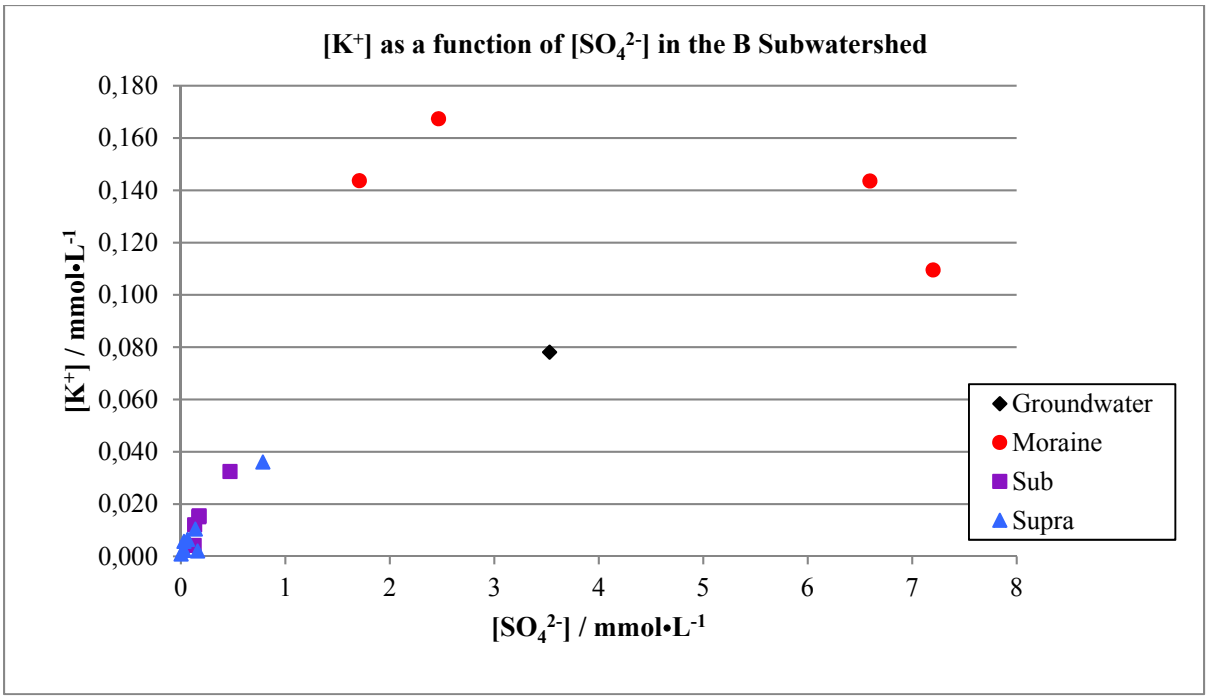

Figure 4.2 Potassium Concentrations as a Function of Sulfate Concentrations in End-Member Samples

As with figure 4.1, we can once again observe a distinction between the two moraine sources, while the sub- and supraglacial end-members are even more entangled, moraine samples showed very high ionic contents while the glacial samples had much smaller concentrations. Potassium is the only tracer we encountered being able to clearly separate between moraines and groundwater sources.

The distinct tracers for moraines were relatively lower pH and high ionic concentrations and conductivity, especially high potassium ion concentrations. Groundwater was identified with the lowest pH but with high conductivity and ionic contents falling between moraines and glacial samples. Glacial samples were high in pH, but were found on the lower end of ionic concentrations. Sub samples were more basic and more concentrated in ionic content than their supra counterparts, but their disparities were small in relation to the other end-members.

Bivariate graph results were used to determine which tracers would be most useful in the hierarchical cluster analysis (HCA). Based on our observations of the bivariate graphs, we selected potassium, magnesium and sulfate concentrations as well as pH and conductivity as tracers for the absolute concentration section of the qualitative analysis. In the relative analysis, we used the same ions over their total sums, all monovalent ions over bivalent ions and d-excess as tracers.

4.2.2 Hierarchical Cluster Analysis (HCA)

Hierarchical cluster analysis (HCA) as mentioned previously is a statistical method that separates a dataset in clusters based on dissimilarity between the data matrices. We ran the method twice, once with absolute concentrations and once with relative concentrations. Absolute concentrations are the non-manipulated concentrations chosen with the bivariate plots, K^+, Mg^{2+}, SO_4^{2-}, pH and conductivity. Relative concentrations were K^+, Mg^{2+}, SO_4^{2-} divided by the sum of cations and anions, as well as d-excess (eq 3.5) and the sum of monovalent ions over the sum of bivalent ions (eq 3.4). The use of absolute concentrations groups waters of comparable ionic content while relative concentrations identify waters of similar origins when differences between those are the result of a simple dilution.

HCA was performed on B1, B2 and B3 sub-catchments separately in order to identify relationships between end-members and estimate dominant sources of water at the sampling time. Each HCA was therefore performed on end-members found at each site (subglacial; supraglacial- moraines and/or groundwater) and immediate downstream sample(s).

As B1 was sampled several times, hydrological systems at this sub-catchment can be studied in both time and space. Here, we present first, HCA performed on the 05/07/2015 samples in what is named the “spatial analysis”. That day represented a well-established system where all fresh snow from the 02/07/15 snowfall event had melted both on the ground and on the glacier ice. Samples from the two other sampling days the 03/07/2015 and the 07/07/15 were

then compared to the samples of the 05/07/15 by performing a HCA on all end-member samples collected at B1 in what we called the “temporal analysis”.

B2 and B3 were analyzed separately.

4.2.2.1 B1 Glacier

The samples for B1 glacier end-members are labelled A to D for the right side system, E for the mixing point and Y to Z for the left system as seen in figure 4.3. In addition, they are identified by a number corresponding to their sampling day: 1 for 03/07/2015 in the morning, 2 for 03/07/2015 in the afternoon, 3 for 05/07/2015 and 4 for the 07/07/2015 as seen in table 4.1.

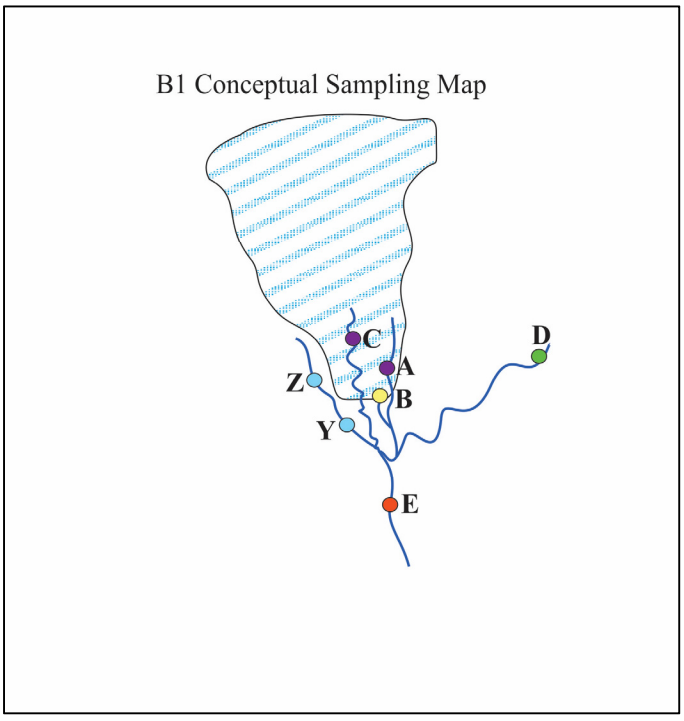

Figure 4.3 B1 Glacier Conceptual Sampling Map:
For colour code refer to Table 3.1

Sample A was collected on the top of the glacier tongue in a large stream, influence from the right slope streams was inevitable, while sample C is a purer form of supraglacial water collected in a small stream about 100m from the glacier tongue atop the glacier. Sample B was collected from a rushing stream seemingly coming out from below the tongue. Sample D was collected from a very small stream seeping out of the slopes on the right. Ice was visible in the slopes thus we assumed ice-cored moraine origins. Sample Z was collected by a stream far left on the glacier tongue, although it was collected on top of the glacier, the stream seemed to be following the left glacier boundary until flowing above the tongue. Downstream from Z, Y was collected from a braided stream where icing water would undoubtedly be leaching into. Finally, sample E was the mixing point for the B1 glacier, a large fast flowing stream.

4.2.2.2 B1 Spatial Analysis

This investigation led to a primary understanding of B1's hydrological system. A hierarchical cluster analysis was run on the 05/07/2015 samples first because the system's dynamics were established and stable. The results from the absolute concentration analysis are presented in figure 4.4.

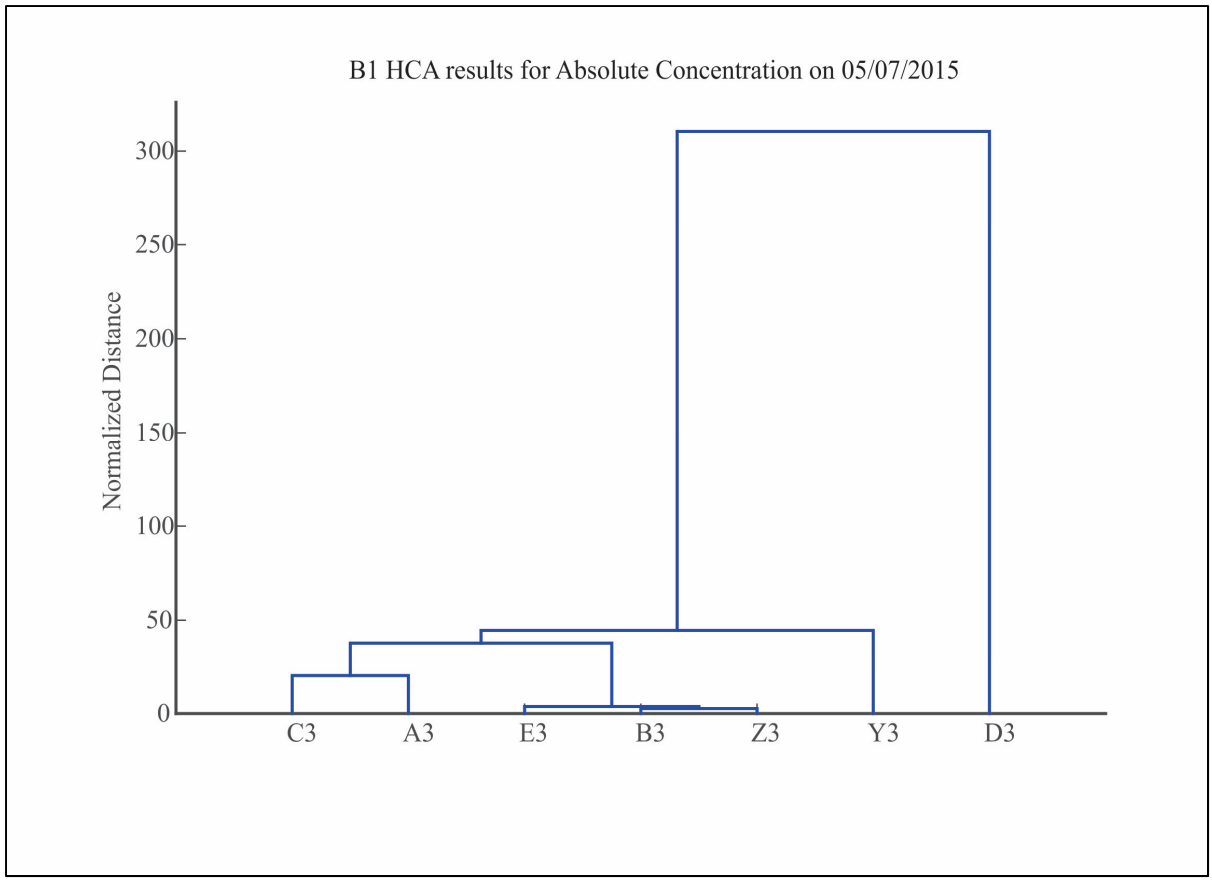

Figure 4.4 HCA Results for B1 Glacier for Absolute Concentration, 05/07/2015: the legend for letter assignment of the x-axis can be found in in Figure 4.3; number corresponds to 05/07/2015

Starting from the most prominent cluster of E3, B3 and Z3, we can deduce that the proglacial stream mixing point (E3) bears resemblance to the left outlet (Z3) and the sub stream (B3) on the right, consequently suggesting they could be important sources of water contributing to the main stream. Close to the first cluster, the next grouping, A3 and C3, confirms the two supraglacial samples have some similarities in ion concentration levels and are possible important contributor. Counterintuitively, the left system shows a disparity. Z3 and Y3 are not found in a cluster despite visibly being on the same stream, this suggests an unseen contributor was active between the two. The only moraine sample taken that day shows a considerable difference from the others' chemical signatures.

The analysis conducted on the relative concentration is presented in figure 4.5, and offers insights into the connectivity between samples by eliminating dilution effects.

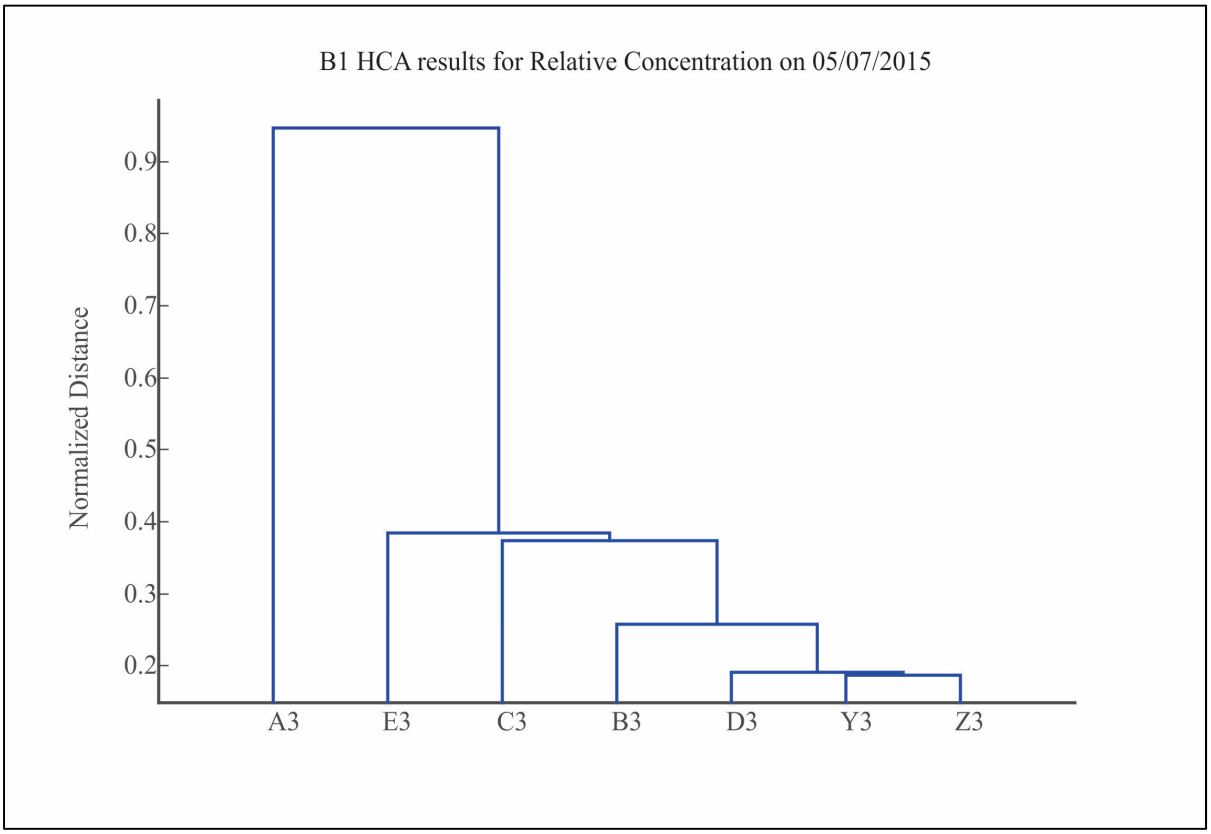

Figure 4.5 HCA Results for B1 Glacier for Relative Concentration, 05/07/2015: the legend for letter assignment of the x-axis can be found in in Figure 4.3; number corresponds to 05/07/2015

The first cluster with D3, Y3 and Z3 hints that perhaps the difference in composition of Y3 and Z3 would have been a simple dilution and that the contributor may be of moraine like composition. The other noticeable difference from the absolute concentration dendrogram is the difference between A3 and C3 supraglacial samples. The distance between them insinuates different geographical origins, thus both follow separate flow paths on the surface.

The spatial analysis allowed for a primary understanding of the pathways and contributions in B1's subwatershed dynamics.

4.2.2.3 B1 Temporal Analysis

To assess the variability in time, a comparison of samples collected at the same points at two different times of 03/07/2015 was undertaken. It is important to note the previous day's snowfall made unique conditions at that site that day. In the morning, lower temperature and snow albedo effect provided a setback in melt. Most of the fresh snow on the ground and on glacier ice melted between sampling times 1 and 2. The absolute concentration hierarchical cluster analysis results are presented in figure 4.6 below.

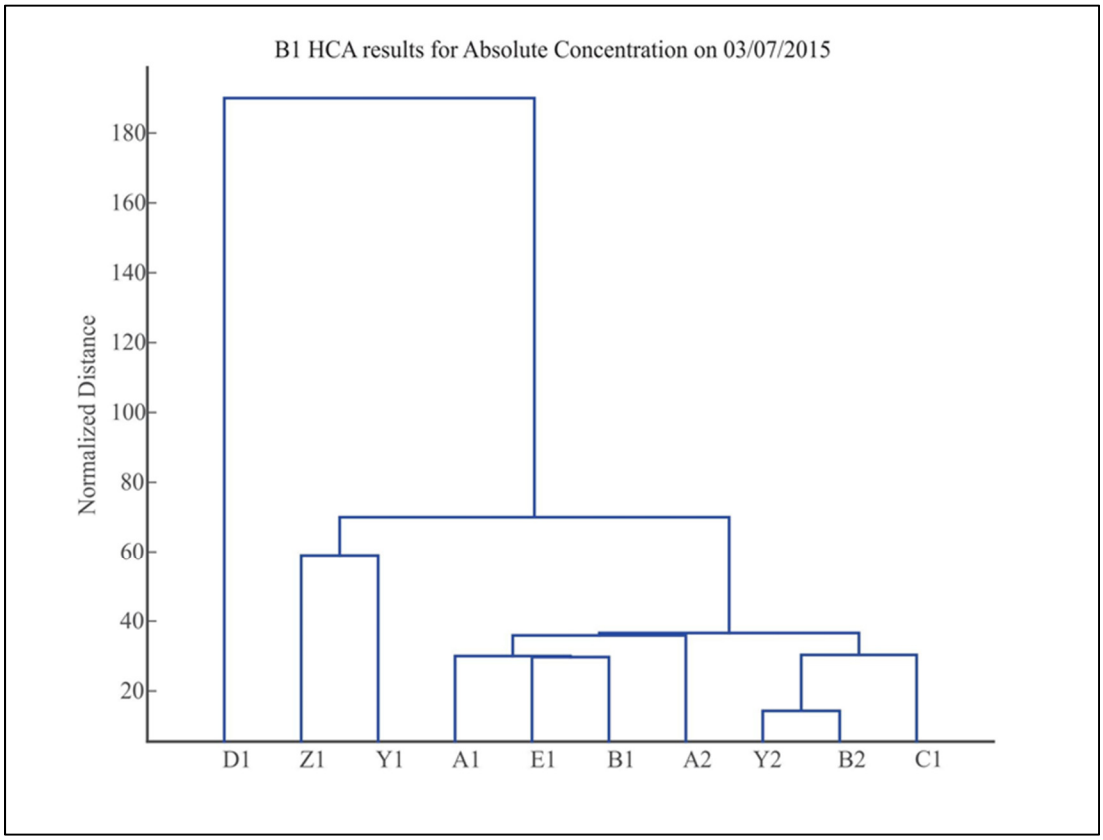

Figure 4.6 HCA Results for B1 Glacier by Absolute Concentration, Temporal Analysis 03/07/2015: the legend for letter assignment on the x-axis can be found in figure 4.4; number 1 corresponds to sampling 03/07/2015 in the morning and 2 for 03/07/2015 in the afternoon

First, we observe that the system behaves slightly differently from the one observed on 05/07/15. B1 remain clustered with E1, the system's outlet, but Y1 is clustered completely differently with Z1. Left system's Y1 and Z1 are clustered but the large normalized distance suggests that they could still have a contributor responsible for the difference in composition. The moraine sample however is confirmed as still being quite different from the glacial end-members. The most chemically similar samples were the subglacial stream B2 and the left system stream Y2; these samples were collected on opposite sides, but C1's proximity indicates that it is possibly a supraglacially dominated system in the afternoon.

The relative concentration HCA results presented in figure 4.7 offered a view of the temporal analysis without the dilution effect.

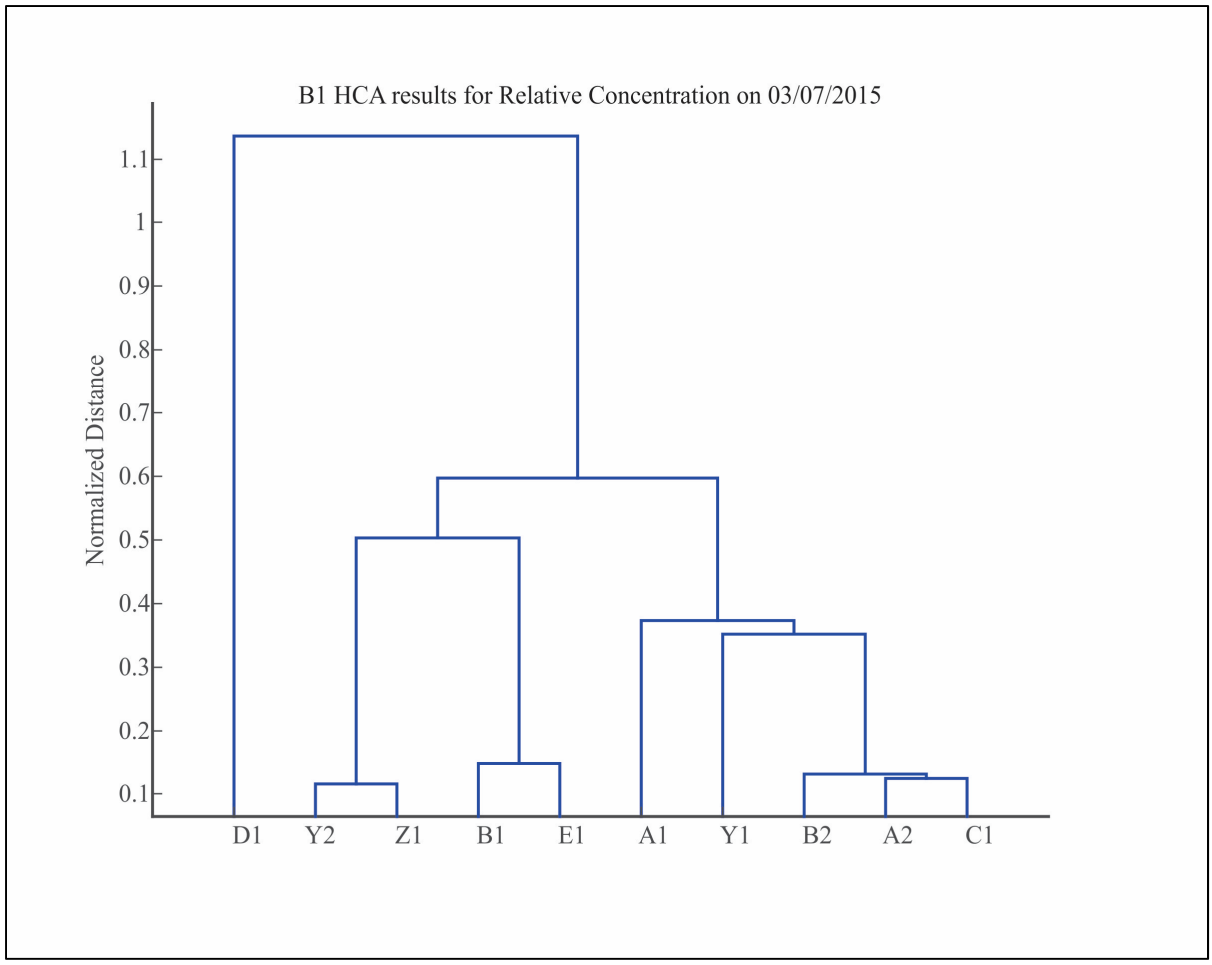

Figure 4.7 HCA Results for B1 Glacier by Relative Concentration, Temporal Analysis 03/07/2015: the legend for letter assignment on the x-axis can be found in figure 4.4; number 1 corresponds to sampling 03/07/2015 in the morning and 2 for 03/07/2015 in the afternoon

In the relative concentration, we can see a difference in origins of the morning and afternoon samples. The cluster of C1, A2 and B2 suggests supraglacial melt being more connected to subglacial water in the afternoon. The Y2 and Z1 cluster is counterintuitive, possibly hinting that the unidentified contributor has less impact in the afternoon. The B1 and E1 cluster confirms the subglacial influence on the main stream in the morning of the 03/07/15.

We furthered this process by running an HCA for all the repeats in B1: 03/07/2015, 05/07/2015 and 07/07/2015. The results for the absolute concentrations are presented in figure 4.8.

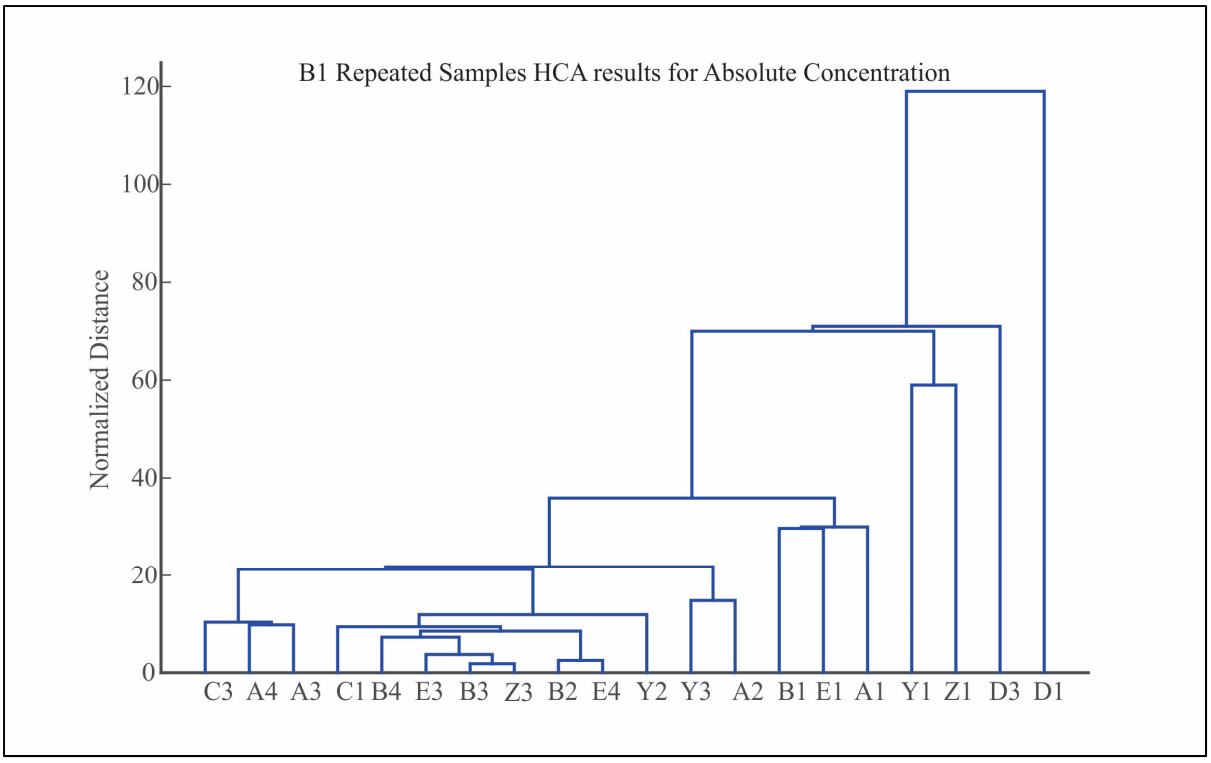

Figure 4.8 B1 Repeated Samples HCA Results for the Absolute Concentrations: the legend for letter assignment can be found in figure 4.4: numbers 1 correspond to 03/07/2015 sampling in the morning, 2 for 03/07/2015 in the afternoon, 3 for 05/07/2015 and 4 for 07/07/2015

Figure 4.8 illustrates well the evolution of the system over the studied period. The chemical signatures are separated by day rather than by end-member, bearing much dissimilarity to the morning 03/07/2015 samples which are clustered on the right (B1, E1 and A1); while on the left the cluster joins supraglacial samples for 05/07/2015 and 07/07/2015 (C3, A4, A3). In the middle of the dendrogram, samples seem to be mixed rendering it difficult to make out conclusions. With most of the 03/07/2015 morning samples plotting away from the other, we see a distinct system was established just after the snowfall and that this system evolved toward a new equilibrium as the fresh snow disappeared. The relative concentration presented in figure 4.9 offers insights into changing the subglacial and supraglacial relationship.

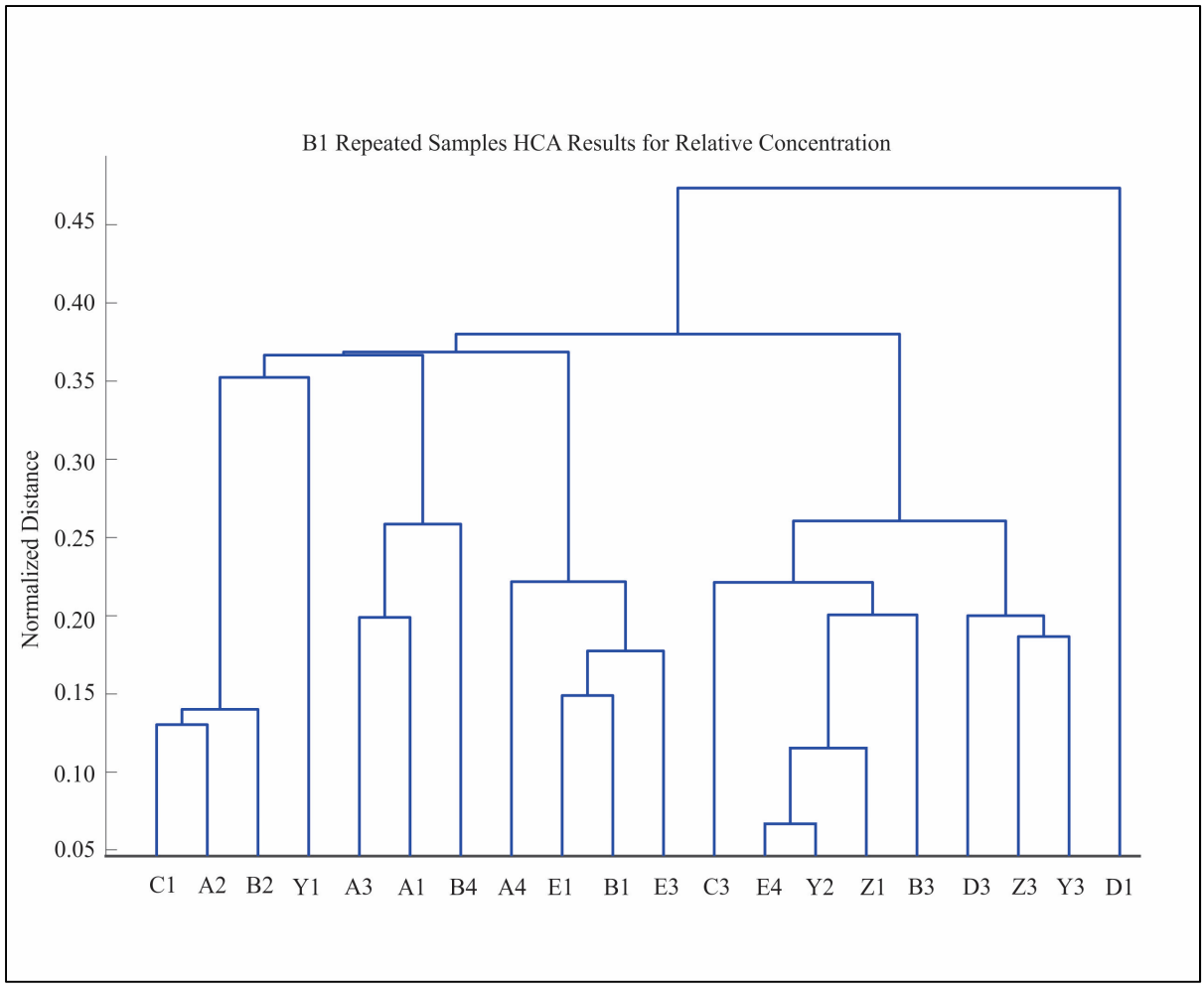

Figure 4.9 B1 Repeated Samples HCA Results for the Relative Concentrations: the legend for letter assignment can be found in figure 4.4: numbers 1 correspond to 03/07/2015 sampling in the morning, 2 for 03/07/2015 in the afternoon, 3 for 05/07/2015 and 4 for 07/07/2015

In the relative concentration analysis, we can mainly deduce the co-dependency of subglacial and supraglacial end-members. As stated earlier, subglacial water is partly composed of supraglacial water that percolates through the glacier, hence influencing subglacial water concentrations depending on supraglacial melt production.

To summarize, HCA of glacier B1 samples show an evolving system that tend to progress from subglacial water dominated system to a system where supraglacial water is more

influent. The sample taken from the ice-cored moraine seems to be playing a minor role in the studied system.

4.2.2.4 B2 Glacier

Since sampling of B2 subwatershed was only done once during the sampling period, the analysis is modestly a snapshot of the spatial hydrological pathways that specific day (07/07/2015). The conceptual map displayed on figure 4.10 shows the location of samples collected in B2 subwatershed. The five B2 samples are labelled by the letters H to L.

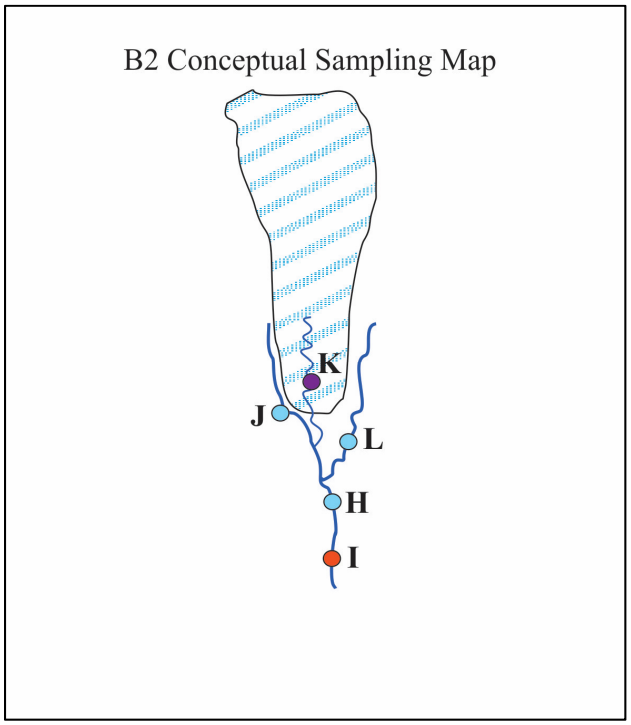

Figure 4.10 B2 Glacier Conceptual Sampling Map:
For colour code refer to Table 3.1

The J and L samples were collected on the side streams on B2 glacier but seemed to be of supraglacial origin, while the K sample was collected on the glacier making it truly supraglacial. H and I were collected in streams down from the glacier about 250m and 4

hours apart. No subglacial stream was found at B2. The dendrogram displaying the absolute concentration based analysis is presented in figure 4.11.

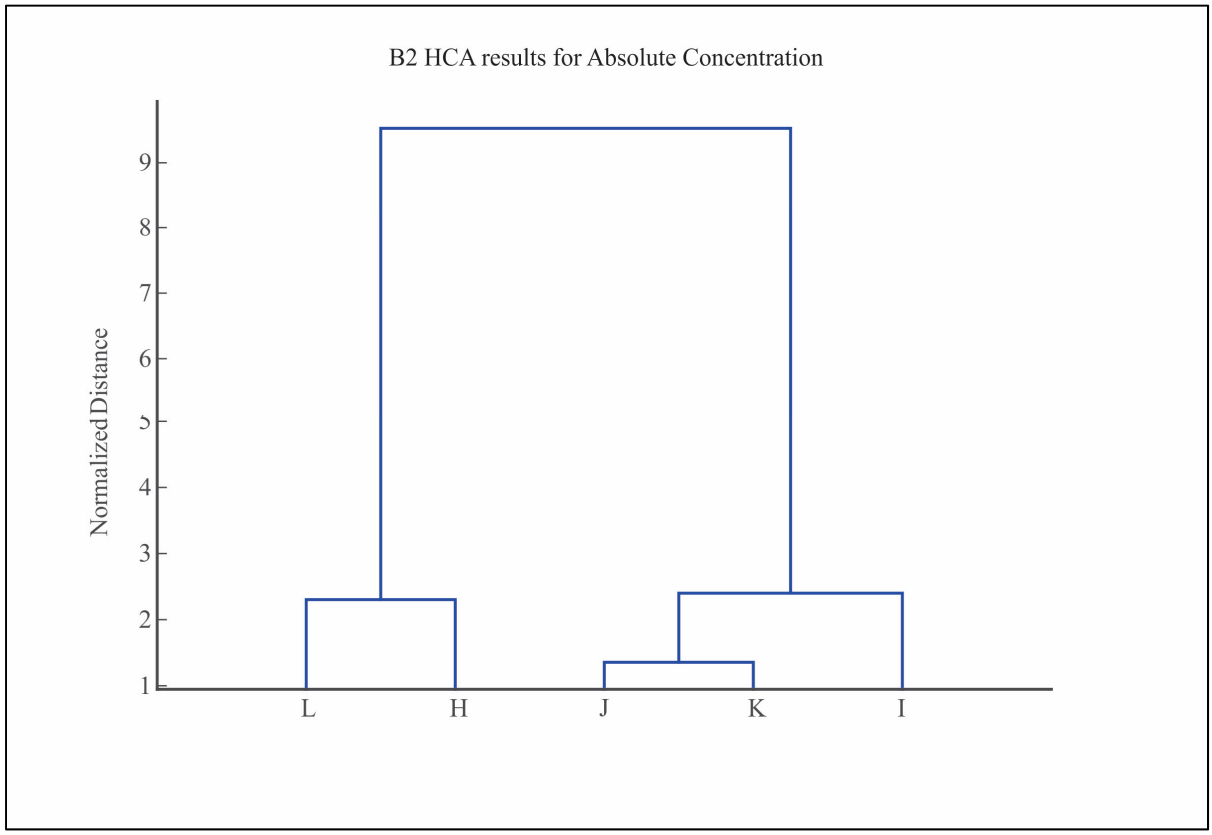

Figure 4.11 B2 End-Members' HCA Results for Absolute Concentration, 07/07/2015: the legend for the letter assignment on the x-axis can be found on figure 4.10

In the absolute concentration analysis, there are no particular cluster rising; the normalized distance is very small, therefore the dissimilarity between samples was small suggesting a homogenized system. The J and K small cluster suggests that there were minimal differences between the clean supra and the neighbouring stream. From the site, no other sources were identified, all the water origins seemed supraglacial and excessive mixing renders a conclusion difficult regarding the B2 end-members. Counterintuitively, the relative concentration HCA shows a left system dominated flow as seen in figure 4.12. This may show the limit of the HCA in depicting hydrological processes where only one type of end-member is sampled.

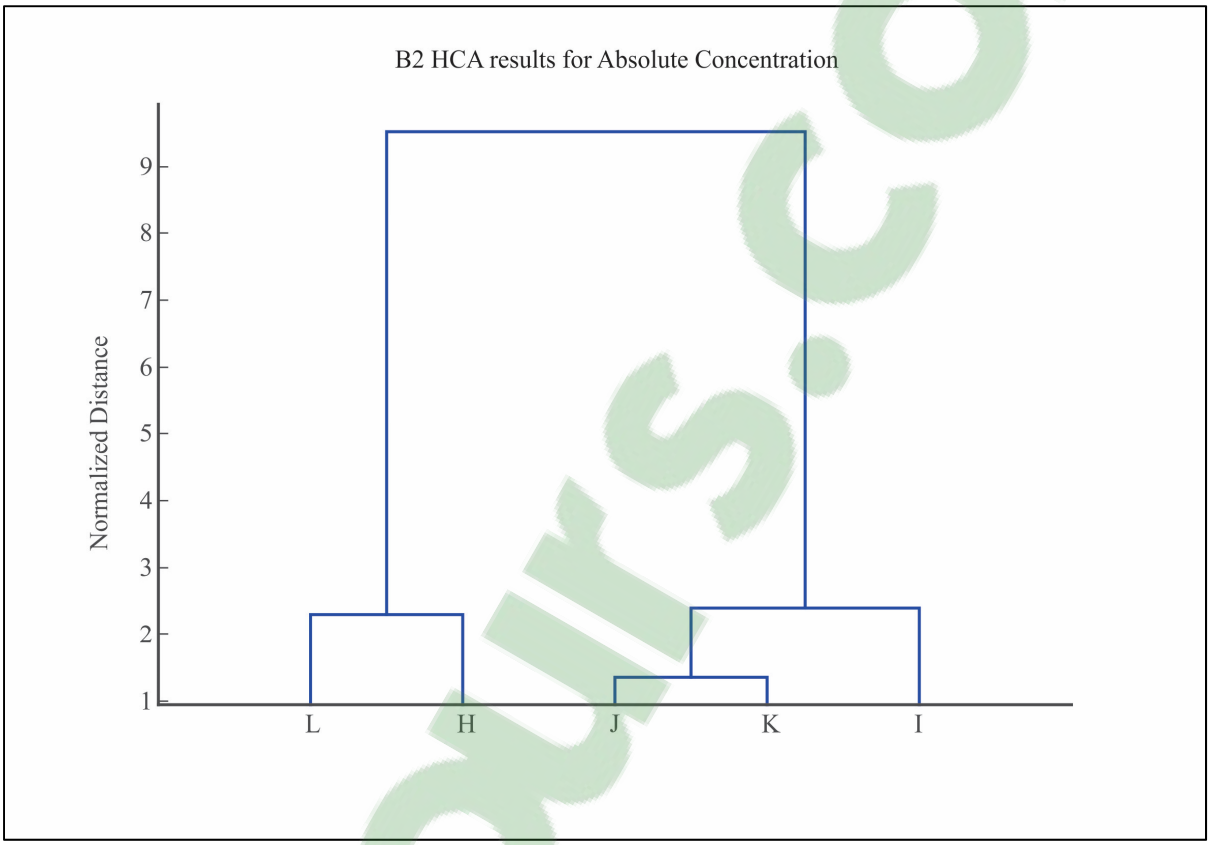

Figure 4.12 B2 End-Members' HCA Results for Relative Concentration, 07/07/2015: the legend for the letter assignment on the x-axis can be found on figure 4.10

B3 subwatershed proved to be a much more diverse system.

4.2.2.5 B3 Glacier

The smallest glacier in the B watershed was hanging quite steeply over the hills. The surrounding slopes hiding buried ice provided small visible volumes of water. B3 subwatershed was also sampled only once during the sampling period, the spatial analysis is therefore only applicable to that day. Six samples were collected in the area as shown by the conceptual map in figure 4.13.

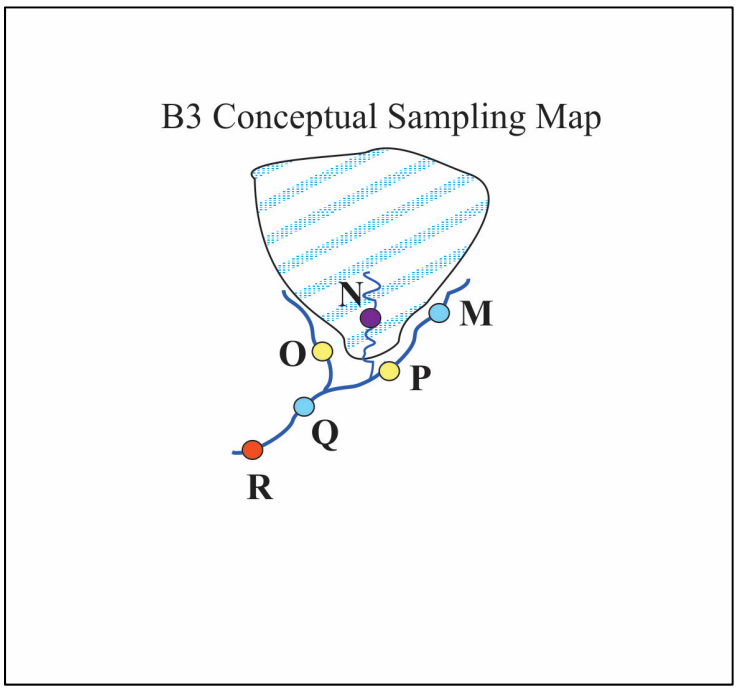

Figure 4.13 B3 Glacier Conceptual Sampling Map:
For colour code refer to Table 3.1

The type assigned to these samples was solely based on the visible conditions during the sampling. The sample O seemed to be of subglacial origin, but it could have been a left boundary stream finding its way under the glacier, while P looked like a small fountain of water escaping the stream. Visibly, P was an artesian spring. M was a stream mixed with supraglacial water and streams coming from the right hand slopes. N was a purer form of

supraglacial source collected on the surface of the glacier's tongue. Q and R are the mixing points on the stream leaving B3 subwatershed.

Hierarchical cluster analysis was conducted on the B3 samples to start interpreting the hydrological system of this watershed, the absolute concentration results are presented in figure 4.14 below.

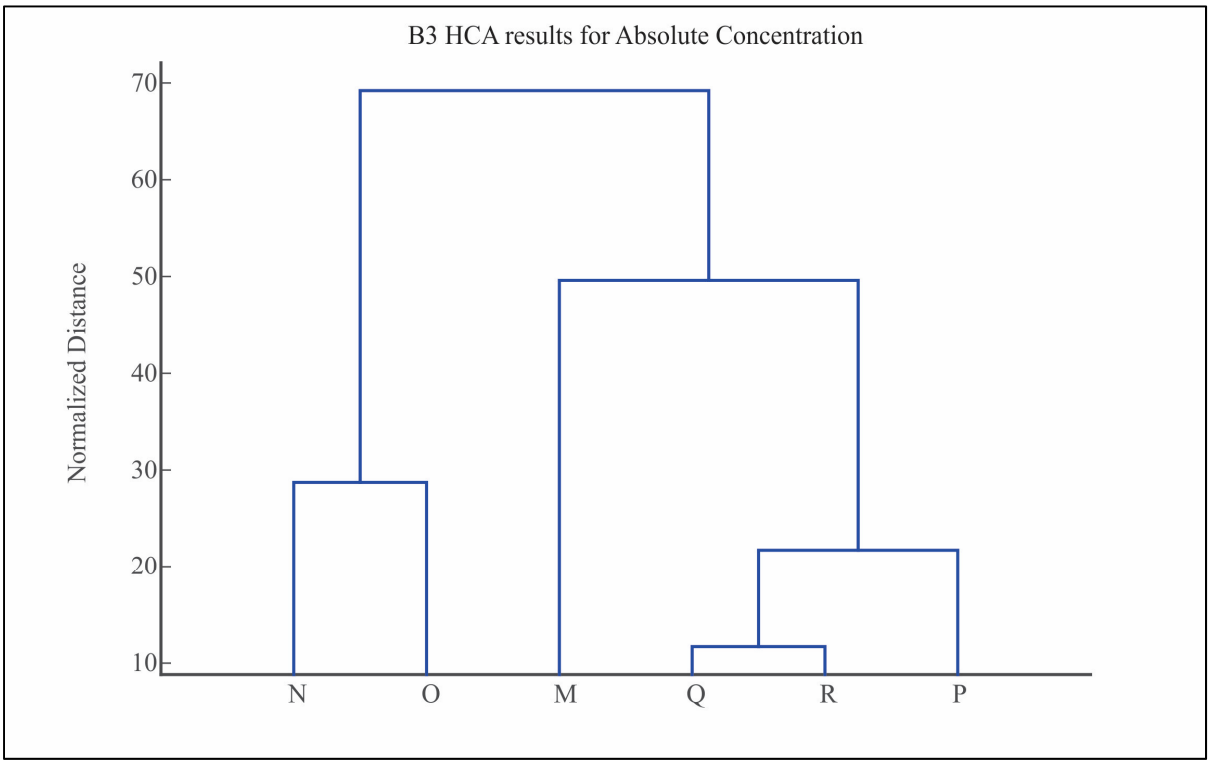

Figure 4.14 B3 End-Members' HCA Results for Absolute Concentration, 07/07/2015: the legend for the letter assignment on the x-axis can be found in figure 4.13

The absolute concentration analysis shows a strong chemical correlation between the two stream samples, Q and R, indicating very limited contribution from other end-members to that segment of the stream. The next node attaches the artesian spring, P, to the stream samples suggesting close compositions between the spring and the stream but also separating the artesian spring from the other end-members. We can hypothesize that P flows from a reservoir recharged higher in elevation (artesian), and considering B3 is a polythermal

glacier, this reservoir could be subglacial water located in the warm zone of the glacier. N and O cluster hints towards the hypothesis that O could be a supraglacial stream that found its way under the glacier through a small low tunnel in the lower part of the glacier.

The relative concentration analysis eliminating the dilution effect from the interpretations is shown on figure 4.15 below.

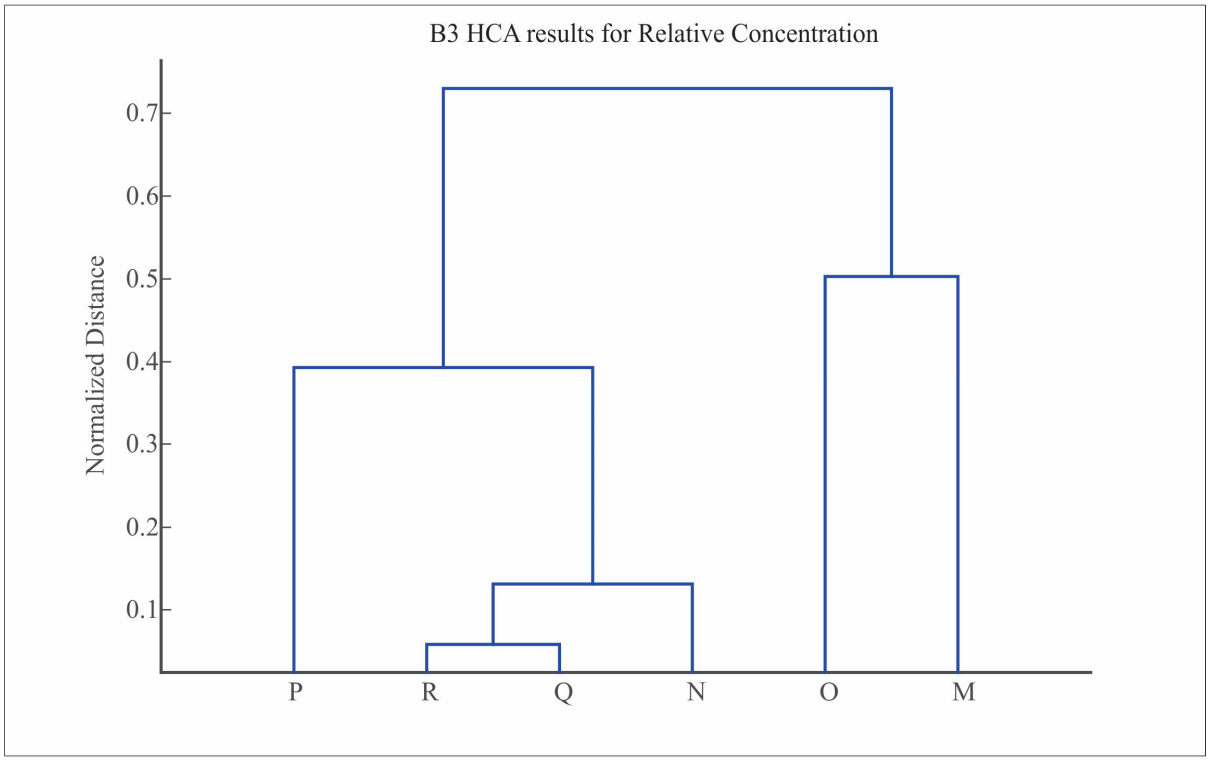

Figure 4.15 B3 End-Members' HCA Results for Relative Concentration, 07/07/2015: the legend for the letter assignment on the x-axis can be found in figure 4.13

Q and R are still clustered which supports the hypothesis that there were little to no source between the two. The proximity of N suggests that stream water would be mostly supraglacial melt. The node with artesian spring, sample P, would suggest a relation between supraglacial melt and the spring.

The qualitative analysis of end-members was pushed forward by applying the same principles to the ten samples collected during 24-hour sampling cycle in an attempt to distinguish if end-members could be recognized so far from their original point.

4.2.2.6 24 hr Sampling Cycle

As mentioned earlier, ten samples were collected over a period of 27 hours: from 5h09 on 09/07/2015 to 8h15 on 10/07/2015 to observe trends in possible contributions during the diurnal cycle. The stable isotopes and ions concentrations' diurnal variations are observable in figure 4.16 and 4.17 respectively. The complete dataset for physical characteristics are found in appendix III.

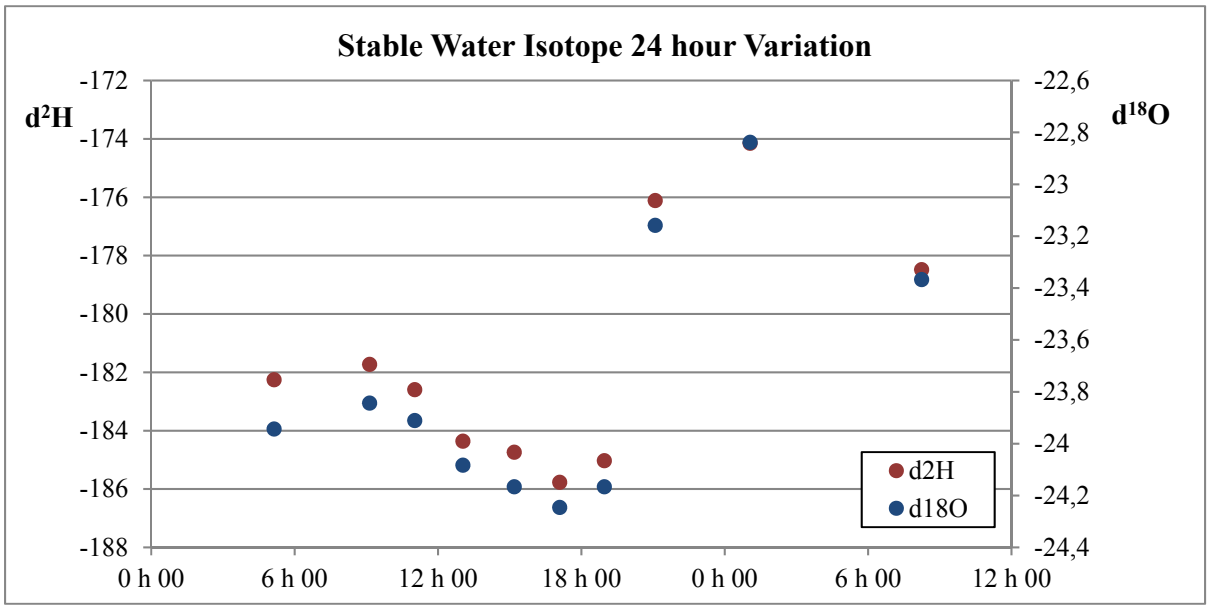

Figure 4.16 Stable Heavy Water Isotope Variations of the 24-hour Sampling

Both figures show a non-symmetrical diurnal variation of the tracers' content. Water samples were more depleted in heavy isotopes during the day than during the night. The second morning however was less depleted than the first one. Interestingly, the peak in enrichment of heavy isotopes in samples does not occur at the same time the 09/07/2015 (around 9 am) than the 10/07/2015 (around 1 am).

A similar pattern is observed with the samples' ionic signatures (figure 4.17). Magnesium, sulfate and potassium concentrations were considerably more diluted in the afternoon than during the night. For two of these tracers (magnesium and sulfate), the concentration effect during the night is more pronounced the 10/07/2015 than the day before.

These curves illustrate well the diurnal cycle commonly observed in glacierized catchment (e.g. (Mitchell et Brown, 2007)). Because melt is mainly triggered by temperatures and solar radiations, highly glacierized catchments tend to have more diluted major ions in outflows at the time of day those factors reach their peaks. Similarly, isotopes being to some extent a proxy for water sources elevation (Baraer et al., 2015), isotopic signatures in highly glacierized catchment outflows tend to be more depleted in heavy isotopes during the period of the day when melt is at its maximum.

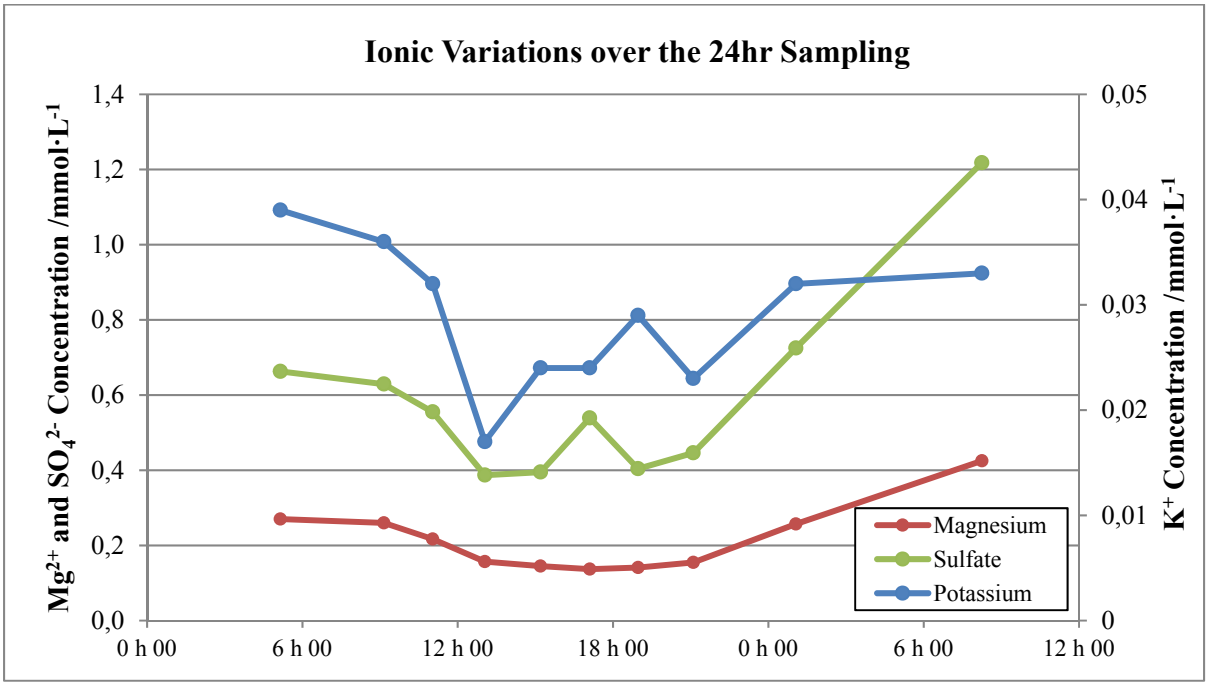

Figure 4.17 Ionic Variations over the 24-Hour Sampling

Explanation for the non-symmetric pattern in the 24-hour sampling signal variation can be found in the weather station records. Records (figure 4.18) show that it rained at the AWS

during the 24-hour sampling period. The rain started at 17h00 on the 08/07/2015 going on and off until 2h00 on the 10/07/2015 with a peak at 21h00 on the 09/07/2015. Over the 33 hours a total of 11.6 mm of precipitation was recorded.

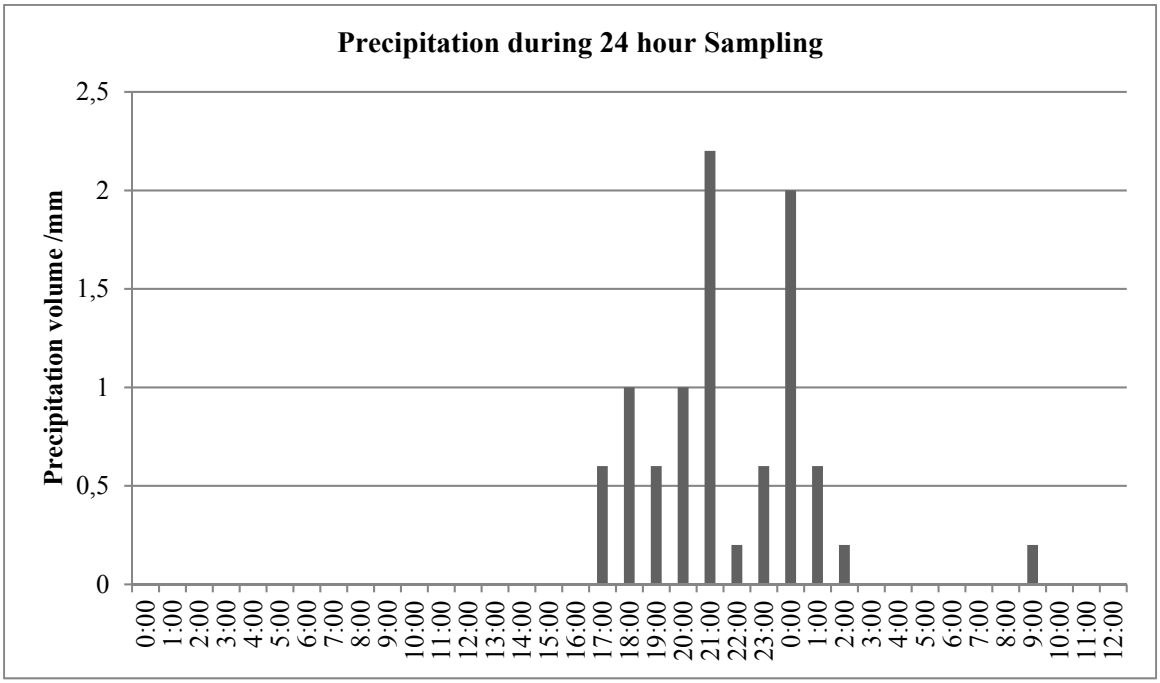

Figure 4.18 Precipitation Height Recorded during the 24-hour Sampling

The precipitation could have had different effects: a dilution effect due to the extra volume brought to the system and a melt volume reduction effect if precipitation was in a solid state on the glaciers (similar to what was observed the 03/07/2015).

4.3 Quantitative Analysis

4.3.1 Hydrochemical Basin Characterization Method

HBCM was run three times at the watershed scale, for the samples taken the 03/07/2015 (set A), the 05/07/2015 (set B) and the 07/07/2015 (set C). Because B2 and B3 were sampled only on the 07/07/2015, it is the only day for which a complete description of the system can be performed. However, because samples were taken from the stream that collects both B2 and B3 sub-catchment water during the two other sampling days, an estimation of B2+B3 contributions was possible for those days too (see figure 2.2).

4.3.1.1 B1 Subwatershed 03/07/2015 – Set A

The A set relates to the B1 subwatershed on 03/07/2015, as seen in figure 4.19. Sampling was done twice on samples A, B and Y, but because the second sampling wasn't complete, we used the first set to run the analysis.

The percentage found in the cell refers to the portion it supplies while the small pie diagram shows the percentage contributed by groundwater sources and the associated cumulated error with the associated ε_j underneath.

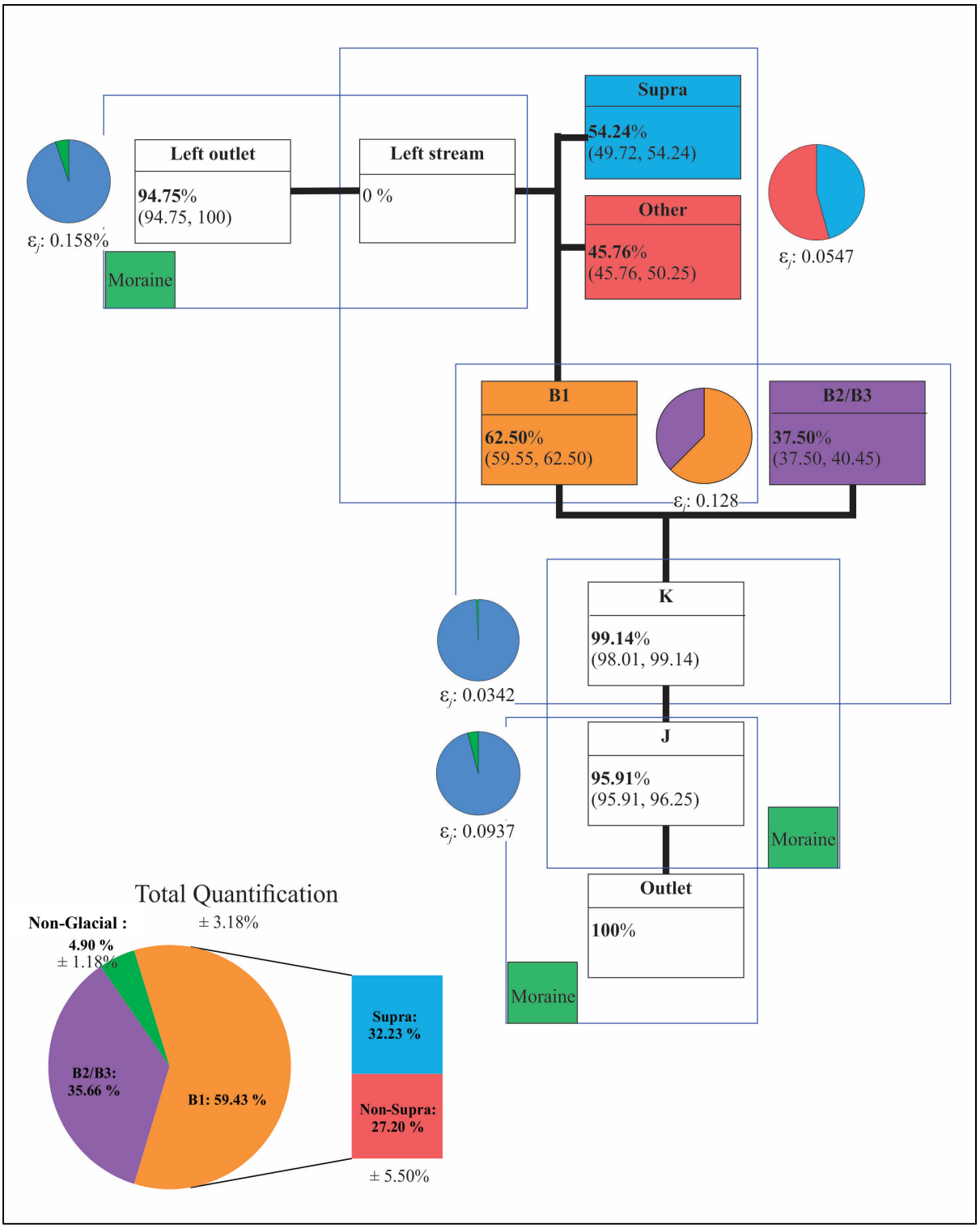

Figure 4.19 HBCM Results for B1 Glacier on 03/07/2015: individual cell results are presented in the boxes by median while extremes are in the parentheses below; the large pie chart presents total contributions made by end-members

Under the hypothesis that B2+B3 is made of melt water only, we can state that, at the outlet about 4.9% (± 1.18%) of the total discharge were non-glacial water sources and were identified as being of mainly from morainic origin. The triple point shows a majority of water coming from B1 59.43% (± 3.18%) while only 35.66% (± 3.18%) from the B2+B3. The sub and supra separation yielding a 5.50% error range.

4.3.1.2 B1 Subwatershed 05/07/2015 – Set B

Set A and B use the same set of samples just different days, 03/07/2015 and 05/07/2015 respectively. Set B samples were collected in a more established system as temperatures were higher and had been consistently over the last 3 days. The results of HBCM analysis are presented in figure 4.20.

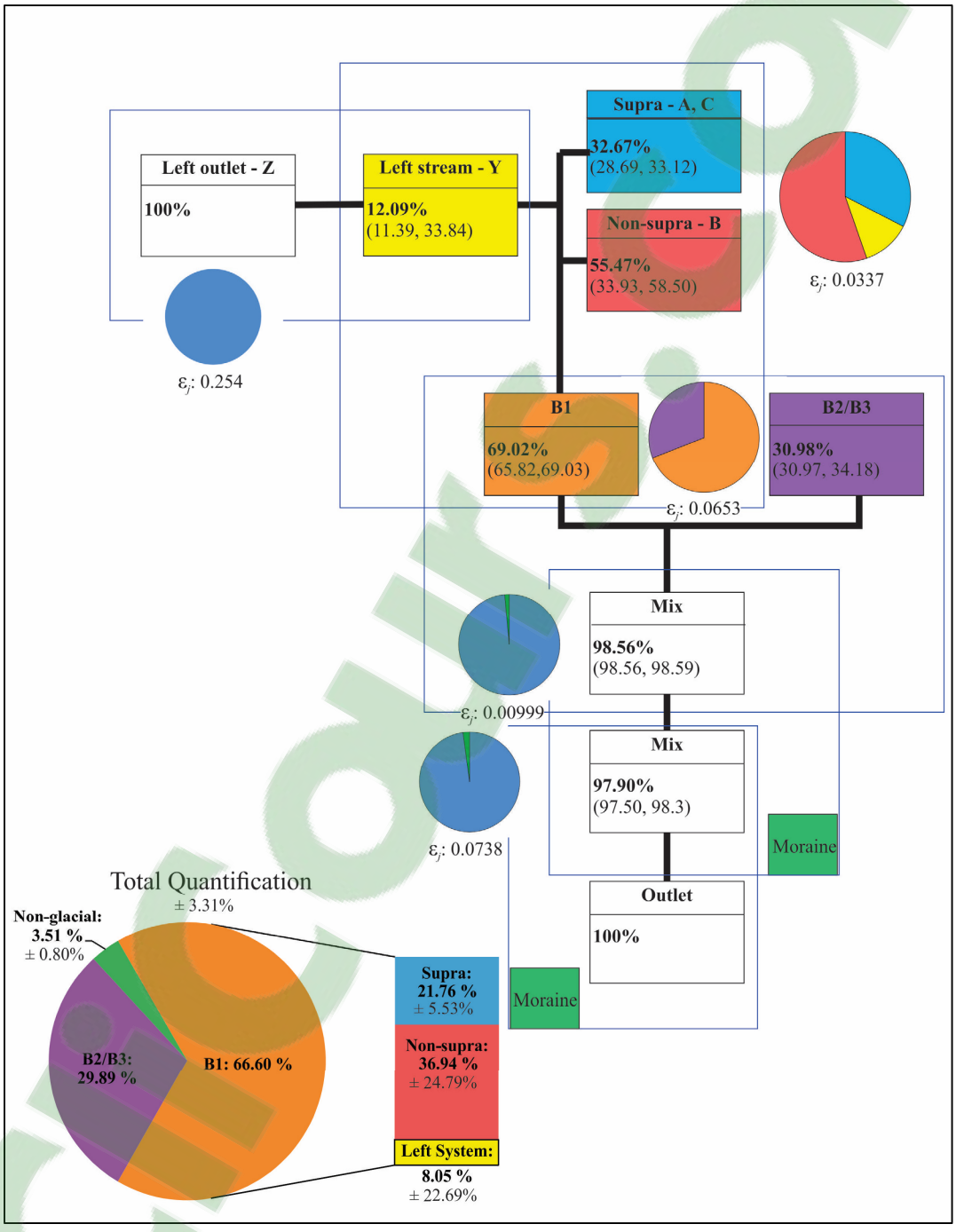

Figure 4.20 HBCM Results of B1 Glacier on 05/07/2015: individual cell results are presented in the boxes by median while extremes are in the parentheses below; the large pie chart presents total contributions made by end-members

Set B had a much more established system, hotter temperatures, as well later sampling times all contributed to a slightly smaller influence from the non-glacierized sources, a total of 3.51% ± 0.80% (2.08, 3.91) mainly from the moraine. The triple point collected had a large error (9.1%) and few retained tracers, most likely due to a non-mixed sample therefore the data used for the triple point is the set C data, chosen because the environmental conditions were most similar to set B. Accordingly, the triple point shows a slightly larger contribution from the B1 glacier 66.6% (±3.31%), with 29.89% (±3.31%) from the B2+B3 stream. The glacial separation between supra, non-supra and the left system yielded high accumulated errors of ±5.53%, ±24.79% and ±22.69% respectively.

4.3.1.3 B Watershed 07/07/2015 – Set C

The final set C was collected on 07/07/2015 between the hours of 9h46 to 17h36 on a sunny day. This hydrochemical analysis takes into consideration the entire watershed, B1, B2 and B3 glacier end-members included, but the lowest part of the valley was not sampled that day, making total non-glacierized contribution estimation not comparable to the sets A and B. The results are presented in the following figure 4.21.

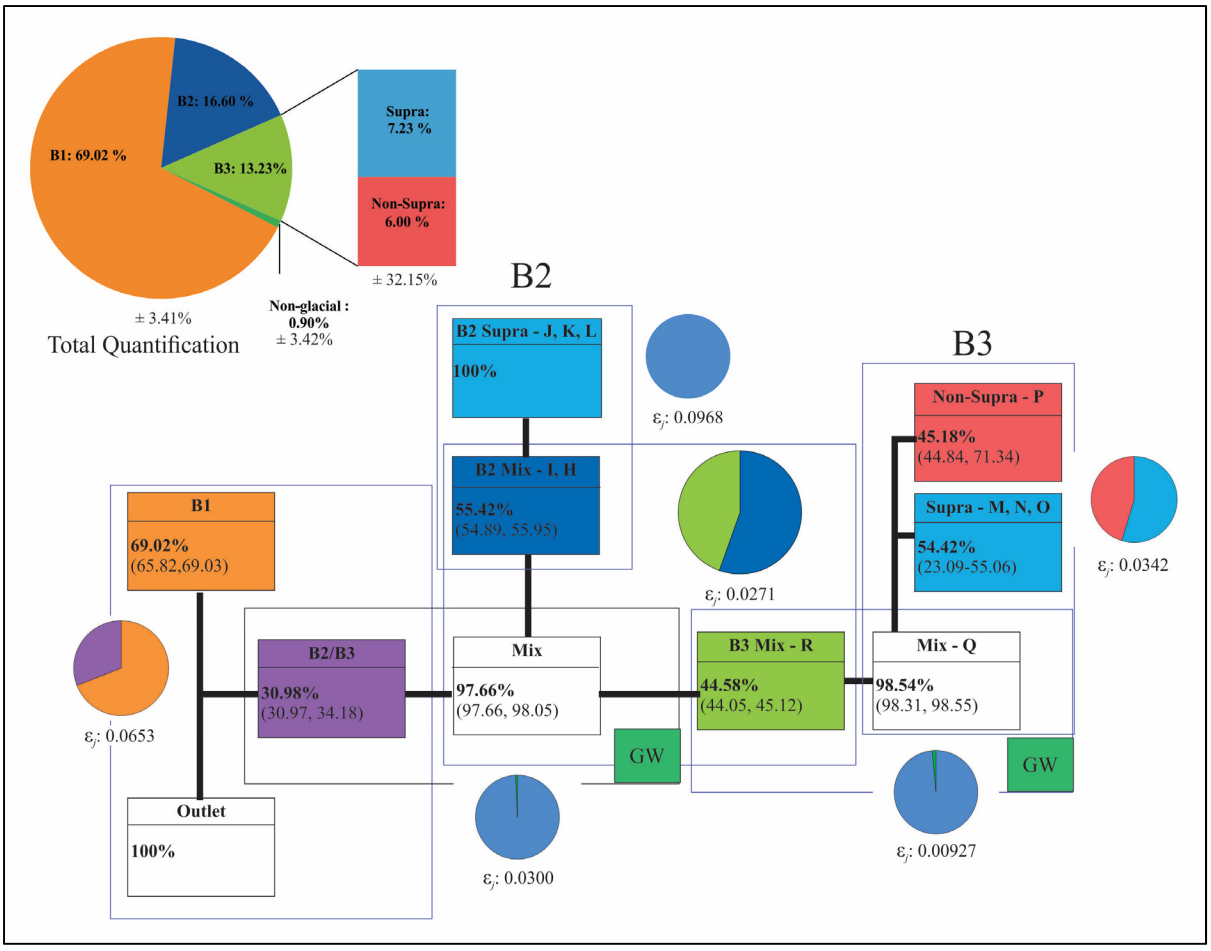

Figure 4.21 HBCM Results for the B Watershed on 07/07/2015: individual cell results are presented in the boxes by median while extremes are in the parentheses below: the large pie chart presents total contributions made by end-members

There were less traces of groundwater as no samples were collected below the first triple point. The triple point showed a larger relative contribution by the B1 glacier, 69.02% (±3.41%) and 30.98% (±3.41) by B2+B3 stream. In the B2 subwatershed, we eliminated sample H from the HBCM analysis due to high cumulated error between H and I samples. All groundwater source contributed in total 0.9% ± 3.42% (0.79, 0.99), chemical signatures indicate a resemblance to groundwater rather than moraine sample; the surrounding landscapes weren't prone to store water, suggesting there could have been a rock glacier, a covered icing or moraine that were missed in the sampling. The relative contribution of B2 being 16.77% (16.61, 18.75) while B3 was 13.49% (13.33, 15.12). B3 had a small

groundwater contribution to the total volume of about 0.2% (0.19, 0.26). The B3 glacial separation of end-members yielded a ±32.15% error range which is quite large for such small quantities of 7.23% for supra sources and 6.00% for non-supra sources of total discharge.

Altogether, HBCM sets show a consistent dominant contribution of glacier meltwater with very few contributions (estimated at around 5% ±5%) of the valley outflow being associated with other sources. B1 always showed contribution higher than 50% of total discharge volumes, and are in reality closer to 2/3 of total contribution.

4.3.1.4 24 hr Sampling Cycle

24-hour HBCM results are detailed in table 4.2. As expected, errors associated with each HBCM at the outlet are higher than the one seen previously in this study. This increase is most probably due to the use of synthetic end-member signatures where the method was designed for real end-member signatures.

Table 4.1 HBCM Results for the 24-Hours Sampling

Sample	**Moraine***	**Rain 09/07**	**Sub***	**Supra***	**Glacial**
5:09	**13.33%** (11.24, 18.60)	**6.26%** (5.92, 8.80)	80.74% (0, 82.84)	0% (0, 77.33)	**80.74%** (77.33, 82.84)
9:09	**12.12%** (10.36, 17.36)	**7.84%** (0, 10.52)	80.40% (0, 89.64)	0.01% (0, 76.35)	**80.41%** (76.35, 89.64)
11:02	**9.06%** (7.73, 16.67)	**7.16%** (0, 9.87)	84.01% (0, 92.27)	0% (0, 79.35)	**84.01%** (79.35, 92.27)
13:03	**5.15%** (4.59, 7.27)	**5.05%** (0, 8.04)	89.66% (0, 95.41)	0% (0, 84,69)	**89.66%** (84.69, 95.41)
15:12	**4.33%** (3.40, 11.93)	**4.29%** (0, 7.21)	91.83% (0, 96.60)	0.24% (0, 86.48)	**92.07%** (86.48, 96.60)
17:06	**5.79%** (4.33, 14.99)	**2.60%** (0, 4.49)	91.75% (0, 95.67)	0% (0, 82.61)	**91.75%** (82.61, 95.67)
18:58	**4.04%** (1.84, 15.00)	**4.83%** (0, 6.52)	71.23% (0, 96.84)	20.54% (0, 79.60)	**91.77%** (79.60, 96.84)
21:06	**7.09%** (5.02, 14.85)	**20.23%** (18.30, 21.03)	10.75% (0, 75.99)	61.14% (0, 66.52)	**71.89%** (66.52, 75.99)
1:04	**13.44%** (10.14, 20.19)	**22.62%** (0, 24.81)	63.15% (0, 89.86)	0% (0, 61.75)	**63.15%** (61.75, 89.86)
8:15	**20.94%** (20.49, 25.60)	**13.55%** (13.09, 16.56)	65.74% (2.18, 66.00)	0% (0, 58.66)	**65.74%** (60.84, 66.00)

*Synthetic signatures

Due to lack of contrast between subglacial and supraglacial synthetic signatures, HBCM kept jumping the majority contribution from one to the other, therefore we amalgamated the results and instead determined glacial contribution in relation to rain and non-glacial volumes (table 4.2). In order to make easier results interpretation, we reported HBCM outputs together with the stream gauge results (figure 4.22).

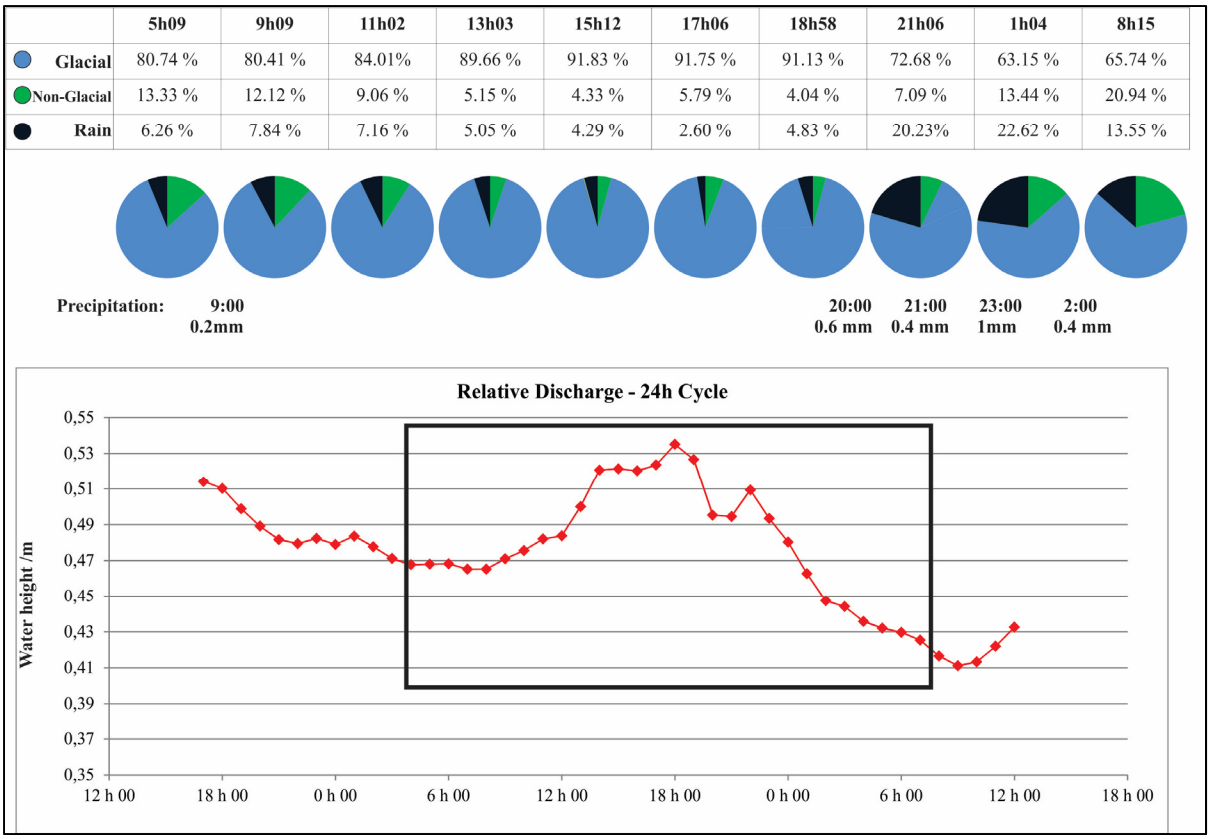

Figure 4.22 Glacial vs Non-Glacial and Precipitation Relative Volumes over 24-hour Sampling Cycle: The top table shows individual contributions for each sample which is visually represented in pie charts below; precipitation heights recorded at the AWS are written underneath and the bottom plot is the discharge height recorded at the gauging station during the 24-hour sampling period highlighted in the black box

Overall, we see that HBCM accounts well for the diurnal changes observed in the non-symmetric tracers' signature evolution presented in figure 4.16 and 4.17. HBCM results associate the decrease in mid-day ion concentration and isotopic depletion as an increase in meltwater contribution. Interestingly, towards the end of the afternoon, non-glacial water estimated around 8% of total outflow. Results from this particular application of HBCM meet those obtained previously in the study. The dissymmetry in tracer evolution observed previously is here explained by both an increase in rain and moraine water relative contribution at the end of the 24-hour sampling. This high relative contribution occurs at the same time the water level at the gauging station is at its lowest, meaning that the drop in the

glacial contribution could be due to a decline of the glacial water, following the decrease in shortwave radiation influx.

The synthetic moraine contributor shows a larger relative contribution during the lower discharge hours (5h09-9h09 and 21h06-8h15), while the rain sample is more prominent at 21h06 and 1h04, conveniently the largest precipitation volume during the cycle occurred between 20h00 to 23h00. These results reach the limits of the HBCM application in conditions where there was missing end-member samples collected at a proper time. The detection of rain water at a period when no rain was detected at the weather station makes a clear illustration of those limits.

This concludes the presentation and primary interpretation of results of the research; the next section will interpret these results further and will suggest improvements for the method.

CHAPTER 5

DISCUSSION

In this chapter, we will further our interpretations of results presented in the previous chapter and identify methodological improvements particularly important in a context where the hydrochemical basin characterization method (HBCM) was used for the first time in a non-typical environment for future studies and for the larger scale HBCM analysis of the entire Duke River upper watershed.

5.1 Qualitative Analysis

5.1.1 Bivariate Plots

The qualitative analysis conducted was extensive and produced compelling results. Preliminary analyses by bivariate plots showed that subglacial and supraglacial waters were difficult to separate in comparison to other sources but were still noticeably different from each other. Crompton et al. (2015) determined high concentration of carbonates in supraglacial water; that could potentially be used as a separating tracer. Unfortunately, in the present study, this option was not tested because carbonate was rejected from the tracers due to gaps in alkalinity test protocols. For further use, samples obtained in the Duke valley tested for alkalinity should be filtered, and if samples are collected for ionic concentration determination, samples should be acidified to avoid precipitation of calcium carbonate.

The groundwater well sample seemed to sit in the middle in terms of ionic concentrations and electrical conductivity, but did have the lower pH and distinctly had the highest isotopic ratios outside of precipitation data and, logically, high level of dissolved organic carbon. Little to no trace of dissolved carbon was found in stream samples, suggesting little to no contribution from the permafrost active layer or groundwater.

Ice-cored moraines were easily identifiable. Highest ionic concentrations and electrical conductivity with lower relative pH isolated them from the other end-members. The separation between the two ice-cored moraines was visible on bivariate graphs, but a distinction in further data manipulations, such as the dendrogram analysis and HBCM results, was unsuccessful. Other hydrochemical tracers should be taken into consideration such as silicate concentration (Ladouche et al., 2001) or calcium and carbonate concentrations (Hodson et al., 2002). However, tracers' analysis showed that B valley conditions were favorable to natural tracers based hydrological studies.

5.1.2 Hierarchical Cluster Analysis

Dendrogram clustering offered important insights into the hydrological pathways of the subwatersheds.

The temporal analysis could have been further explored and yielded more conclusive results with a more complete sampling. B1 progressed from a subglacial dominated to a supraglacial dominated system during the study period. The second sampling series of B1 collected in the afternoon hours of July 3rd was not a complete sampling making it difficult to understand completely the evolution of contributions with a solid precipitation disturbance as well as its progress as the snow melted. The clusters forming by sampling day rather than by end-member did however show a certain evolution into the hydrochemistry of contributors. This temporal analysis would have greatly benefited of a constant hourly sampling at the contributors, if the method was not so demanding to carry out.

B2 system was a challenging analysis via dendrograms. The lack of contrast between samples and absence of other sources outside of supraglacial melt, made a HCA difficult to conduct. Surrounding slopes should be examined for smaller sources of water in further sampling; if no other water sources exist it could be because the B2 glacier is a cold-base glacier, the ice-ground interface is below freezing point leaving little opportunity for sub- and englacial melt.

Discharge at the B3 subwatershed was shown to be of supraglacial origin and have a strong link with the small artesian spring present at the base of the glacier. A long term monitoring of the artesian spring would determine if it is a seasonally occurring phenomenon and a reservoir may be present in the englacial system of the glacier or if it was a unique occurrence during the sampling period.

In general, HCA analysis depicted the three glacial systems being significantly different from each other, which can be seen as a surprise taking into consideration those glaciers are of comparable size, orientation and geographic situation.

5.2 Quantitative Analysis

5.2.1 Hydrochemical Basin Characterization Method

The quantification of end-member contributions was a successful procedure in the B watershed over the various days it was conducted. For the most part, it showed B1 being a more substantial contributor than its neighbours, B2 and B3 and that glacial melt is the main source of discharge, other sources were found to contribute less than 5%.

With hotter temperatures and more solar radiation on 05/07/2015 than on 03/07/2015, supraglacial contribution was expected to have been greater in set B (05/07/2015) than in A (03/07/2015), nevertheless, set B (21.76% ± 5.53%) showed a smaller contribution from supraglacial end-members than set A (32.23% ± 5.50%). However, set B also recognized a contribution from the left system (8.05% ± 22.69%), which set A had not. The left system being mostly a supraglacial stream following the boundary of the glacier, it could be added to the total supraglacial contribution adding up to a total supraglacial contribution in set B to be 29.81% ± 23.35%. Sets A and B also differ in the total contribution percentage of B1 and B2+B3. In set A, the contribution from B1 is 59.43% ± 3.18% while in set B it is 66.60% ± 3.21%. B1 is the lowest and largest glacier of all three, it would be logical that it contributes

the most and with respect to higher temperature and radiation it would produce more meltwater than the other two. The effect of snowfall is also impacting the B1 contribution; snow albedo would have reflected solar radiation, decreasing glacial melt.

In the Set C (07/07/2015), one MIX cell was eliminated due to high error yield, the cell would have fallen between the B2/B3 cell and the MIX cell at the junction of B2 and B3 mainstreams. Poor results in the separation of B2 glacial end-members also pressed to combine all the end-members and consider them as one unique supraglacial contributor. B1 total contribution elevating to 69%, while B2+B3 was a combined 29.8%, and groundwater sources being hardly noticeable with less than 1% contribution.

HBCM proved to be successful in the B watershed suggesting it could have the same success in the larger upper Duke watershed.

5.2.2 24 hr Sampling Cycle

Despite being an interesting demonstration of diurnal variability, the results produced by HBCM for the 24-hour sampling had large cumulated errors even with glacial sources being amalgamated. An average of 12.6% range in extremes at the outlet ensured much care and precision would be needed in the interpretation of results. The precipitation data correlated well with the HBCM output for the 21h06, 1h04 and 8h15 samples and the peak temperatures and discharge hours showed a mostly glacial contribution, but oscillated between 2.60-7.16% of rain water contribution at other times (5h09 – 18h58), when no precipitation was recorded at the automatic weather station (AWS). The exception would be the 9h09 and 11h02 samples due to a small 0.2 mm of rain recorded at 9h00. Glacial contributions were dominant throughout the cycle but were variable with time. At peak temperature and solar radiation (13h03-18h58), they were contributing around 90% of total discharge while during the night (1h04-8h15), contributions were around 60%. The decline in glacial meltwater coincides with the precipitation event; at higher elevation, precipitation could have been solid and prevented contributions from glacial sources. To assess the variation in discharge from the

glacial end-members during the diurnal cycle, the sampling should have been done closer to the outlet of the glacier; at the outlet of B watershed there were too many sources mixing, thus rendering the separation difficult. Nonetheless, HBCM showed encouraging results as a mixing model for glacial vs non-glacial contributors with synthetic end-member signatures.

CONCLUSION

The first objective of the present research was to identify main water sources by the mean of their physico-chemical particularities at different dates of the study period. This objective was met by the use of hierarchical cluster analysis (HCA) at different locations and times and confirmed by use of the hydrochemical basin characterization method (HBCM). Despite being difficult to distinguish between sub- and supraglacial waters due to their connectivity in the drainage systems, this study was able to show that glaciers were by far the most dominant end-member of the B valley during the entire study period. Moraines were identified by the analysis as minor contributors compared to glaciers outputs. Groundwater from the well was hardly seen as a contributor. Even if distinction between sub and supraglacial water contribution was difficult to make at the entire watershed scale with only natural tracers, this study succeeded in showing that the B1 glacier had important subglacial and supraglacial contributions, that B2 was home to only supraglacial systems (B2 is potentially a cold ice glacier), and that B3 provided supraglacial water mixed with spring water that was possibly of subglacial origin.

The second objective was to estimate the sources contribution to total discharge by using a mixing model again at different dates of the study period. HBCM gave unambiguous indications that, whatever the sampling day or time, glacial meltwater was the dominant contributor for the B valley. The three times HBCM was used for the valley, the hydrological system was almost exclusively glacial, with non-glacial contributions estimated around 5% (+/- 5%). The system showed however an evolution in time. The effect of snowfall in particular showed impacting the meltwater production in a measurable way. Snow seemed to slow down considerably the production of supraglacial water making the subglacial water the main contributor when snow was present at the ice surface.

The third objective was to differentiate between glacial and non-glacial contributions to the outflows of the B Valley during a 24-hour period. Here again, HBCM results exhibited a dynamic hydrological system. Glacial sources contribution varied from 91.83% at 15h12 to

63.15% contribution at 1h04. The 24 hours sampling suggests that the precipitations that affected the watershed during the second half of sampling did have a double effect. It fed the stream with the rain itself and, most probably because of solidification of precipitation at higher elevations, decreased the production of meltwater, both effects led to the event having a negative net effect of the watershed outflows.

This study has successfully demonstrated that the B valley is a study area compatible with the use of natural tracer based hydrological characterization methods; leading to believe it has potential in the larger upper Duke watershed. Further sampling and monitoring of the B watershed would also benefit long term studies of the changing hydrological processes and their specific responses to climate change. The use of HBCM with synthetic end-member signatures was an interesting exercise. Despite limitations such assumption implies and their corresponding calculated errors, HBCM was practical in the identification of hydrological processes associated with the diurnal fluctuations and with the precipitation event. On the other hand, the study also shows that for HBCM to quantify accurately end-member contributions, a thorough and rigorous sampling is required.

APPENDIX I

FIELD MEASUREMENT OF B WATERSHED SAMPLES

Table A I-1 Field Measurements of B Watershed Samples 03/07/2015

Assigned Letter	Name	Type	Time	Lat	Long	pH	Cond. (µS/cm)	Temp /°C
	B. MStream #1	Stream	09:09	60,99317	138,9724	8,88	307	2.0
	B. MStream #2	Stream	09:36	60,99279	138,9762	8,81	232	2.0
	B. Mstream TP #1	Stream	10:13	60,98902	138,9837	8,79	225	1,8
	B. Mstream TP #2	Stream	10:39	60,9884	138,9863	8,83	275	2,5
E1	B. Mstream TP #3	Stream	10:52	60,98801	138,9867	8,75	195	1,5
B1	B. Main Outlet	Sub	11:46	60,98479	138,9911	9,35	165,3	0,3
A1	B. Main Supra	Supra	11:49	60,98465	138,9913	8,92	225	0,2
Y1	B. Sub-Main #1	Stream	12:07	60,98566	138,9891	8,77	295	2,2
	Glacier B Icing Right Stream #1	Icing - Supra	12:03	60,98471	138,9898			
	Glacier B Icing Right Stream #2	Icing - Supra	12:08	60,98476	138,9894			
	Glacier B Icing Right Stream #3	Icing - Supra	12:12	60,9849	138,9884			
Z1	B Sub-Main Left #1	Stream	12:24	60,98492	138,9884	8,82	354	1,1
C1	B1 Supra Center	Supra	12:35	60,98433	138,9907	8,84	48,2	0,1
D1	B. Right side Moraine	Moraine	13:50	60,98484	138,9918	8,84	458	8.0
	B. Right Moraine Lake	Lake	15:05	60,9854	138,9942	9	380	14,9
B2	B. Main Outlet #2	Sub	16:45	60,98479	138,9908	10,19	78,5	0,8
A2	B. Main Supra #2	Supra	16:47	60,98464	138,9913	9,58	40,3	0,2
Y2	B. Sub-Main #2	Stream	16:50	60,98487	138,9885	9,48	92,8	1,1

Table A I-2 Field Measurements of B Watershed Samples 05/07/2015

Assigned Letter	Name	Type	Time	Lat	Long	pH	Cond. (µS/cm)	Temp /°C
	B. Mstream #1	Stream	12:20	60,99602	138,9719	9,53	110,5	5,4
	B. Mstream #2	Stream	12:48	60,99222	138,9768	9,1	113,1	4,1
	B. Mstream TP #1	Stream	13:10	60,98716	138,9834	9,26	106,6	3,5
	B. Left Moraine	Moraine	13:24	60,98924	138,9826	8,74	1197	11,2
	B. MStream TP #2	Stream	13:57	60,98859	138,9865	9,37	105,4	5,2
E3	B. Mstream TP #3	Stream	14:14	60,98702	138,9859	9,26	64,7	2.0
Y3	B. Sub-Main (Left) #1	Stream	15:49	60,98554	138,989	9,2	114,6	1,3
Z3	Sub main stream left	Stream	15:57	60,98491	138,9884	9,54	70	1.0
	B. Glacier Icing Stream #3	Icing - Supra	16:08	60,9849	138,9884			
	B. Glacier Icing Stream #2	Icing - Supra	16:09	60,98476	138,9894			
	B. Glacier Icing Stream #1	Icing - Supra	16:15	60,98471	138,9898			
C3	B1 Supra Center	Supra	16:23	60,98433	138,9907	8,6	6,9	0,5
B3	B. Main Outlet	Sub	16:31	60,98485	138,9907	10,23	68,3	0,6
A3	Main Supra	Supra	16:53	60,9847	138,9914	9,58	27	0,5
D3	B. Right Side Moraine	Moraine	17:03	60,98488	138,9916	8,84	425	8,3

Table A I-3 Field Measurements of B Watershed Samples 07/07/2015

Assigned Letter	Name	Type	Time	Lat	Long	pH	Cond. (µS/cm)	Temp /°C
	B. Moraine Left #1	Moraine	09:46	60,99415	138,9735	7,21	1510	1,5
	B. Mstream TP #1	Stream	10:26	60,9894	138,9824	9,23	11,9	2,6
E4	B. Mstream TP #3	Stream	10:47	60,98813	138,9866	9,43	80,9	2
	B. Mstream TP #2	Stream	11:03	60,98872	138,9871	9,24	136,1	3,9
	B2 Mstream #1	Stream	11:36	60,9879	138,9955	8,85	176,2	3,3
	B2 Mstream TP #1	Stream	12:09	60,98788	138,9954	9,09	113,6	3,4
I	B2 Mstream TP #3	Stream	12:28	60,98788	139,0023	9,58	47	1,4
R	B2 Mstream TP #2	Stream	12:53	60,98821	139,0026	9,03	189,3	3,5
Q	B3 Mstream #1	Stream	13:29	60,98942	139,0058	9,05	177,6	3,4
O	B3 Glacier Main Left	Sub	14:04	60,99037	139,0143	9,9	58,8	1,5
P	B3 Geyser	Artesian Spring	14:16	60,99066	139,0146	9,66	211	1,4
N	B3 Supra Centre	Supra	14:26	60,99081	139,0151	8,7	30,1	0,7
M	B3 Glacier Main Right	Stream	14:36	60,99084	139,0159	8,82	128	0,4
L	B2 Main Right	Stream	15:54	60,98779	139,0045	9,7	49,3	2,8
K	B2Supra Centre	Supra	16:01	60,98706	139,0049	8,9	37,3	1,3
J	B2 Main Left	Stream	16:06	60,98703	139,0045	10,24	37,5	0,5
H	B2 Mstream	Stream	16:33	60,98781	139,0027	10,27	35,1	1,8
B4	B1 Mstream Outlet	Sub	17:29	60,98511	138,991	10,31	57,5	0,8
A4	B1 Main Supra	Supra	17:36	60,98462	138,9913	9,68	17,2	0,3

Table A I-4 Field Measurements of B Watershed Samples 08/07/2015 - 10/07/2015

Name	Type	Date dd/mm	Time	Lat	Long	pH	Cond. (µS/cm)	Temp /°C
Rain Sample	Rain	08/07	17:35	60,99593	138,9628			
B Mstream - 5:09	Stream	09/07	05:09	60,99909	138,9627	8,67	219	
Rain Sample	Rain	09/07	08:47	60,99593	138,9628			
B Mstream - 9:09	Stream	09/07	09:09	60,99909	138,9627	8,78	206	4
B Mstream - 11:02	Stream	09/07	11:02	60,99909	138,9627	9.00	199,2	3,8
Puit Camp B	Groundwater	09/07	12:27	60,99593	138,9628	7,66	996	10,1
B Mstream - 13:03	Stream	09/07	13:03	60,99909	138,9627	9,17	154,9	5,3
B Mstream - 15:12	Stream	09/07	15:12	60,99909	138,9627	9,35	143,5	5,7
B Mstream - 17:06	Stream	09/07	17:06	60,99909	138,9627	9,49	163,5	4,4
B Mstream - 18:58	Stream	09/07	18:58	60,99909	138,9627	9,56	160,1	4
B Mstream - 21:06	Stream	09/07	21:06	60,99909	138,9627	9,23	161,3	3
B Mstream - 1:04	Stream	10/07	01:04	60,99909	138,9627	9,05	230	2,5
B Mstream - 8:15	Stream	10/07	08:15	60,99909	138,9627	8,71	323	2,4
Rain Sample	Rain	10/07	06:59	60,99593	138,9628			

dd/mm is for day/month

APPENDIX II

CHEMICAL RESULTS FOR B WATERSHED SAMPLES

Table A II-1 Chemical Results for B Watershed 03/07/2015

Assigned Letter	Name	Time	Concentration /mmol·L^{-1}								
			[Na+]	[K^+]	[Mg^{2+}]	[Ca^{2+}]	[F^-]	[Cl^-]	[SO_4^{2-}]	SC^+	SA^-
	B. MStream #1	09:09	0,047	0,034	0,420	0,866	0,000	0,004	0,779	2,654	2,794
	B. MStream #2	09:36	0,031	0,029	0,265	0,835	0,001	0,009	0,759	2,259	2,712
	B. Mstream TP #1	10:13	0,031	0,041	0,270	0,932	0,000	0,005	0,708	2,476	2,340
	B. Mstream TP #2	10:39	0,033	0,044	0,313	1,057	0,001	0,001	0,839	2,817	3,088
E1	B. Mstream TP #3	10:52	0,036	0,042	0,239	0,793	0,001	0,002	0,619	2,141	2,065
B1	B. Main Outlet	11:46	0,024	0,032	0,174	0,550	0,001	0,002	0,471	1,505	1,657
A1	B. Main Supra	11:49	0,039	0,036	0,256	0,970	0,001	0,001	0,784	2,527	2,514
Y1	B. Sub-Main #1	12:07	0,038	0,019	0,362	1,446	0,001	0,001	1,108	3,672	3,275
	Glacier B Icing Right Stream #1	12:03									
	Glacier B Icing Right Stream #2	12:08									
	Glacier B Icing Right Stream #3	12:12									
Z1	B Sub-Main Left #1	12:24	0,033	0,011	0,420	1,448	0,001	0,001	1,363	3,779	3,969
C1	B1 Supra Center	12:35	0,009	0,006	0,020	0,427	0,000	0,002	0,063	0,908	0,721
D1	B. Right side Moraine	13:50	0,096	0,167	0,914	2,019	0,003	0,019	2,467	6,130	6,636
	B. Right Moraine Lake	15:05	0,041	0,013	0,935	1,431	0,000	0,019	1,330	4,786	4,422
B2	B. Main Outlet #2	16:45	0,017	0,015	0,068	0,262	0,000	0,002	0,177	0,691	0,760
A2	B. Main Supra #2	16:47	0,009	0,010	0,056	0,396	0,001	0,001	0,138	0,922	1,103
Y2	B. Sub-Main #2	16:50	0,015	0,004	0,073	0,280	0,000	0,003	0,171	0,726	1,089

Table A II-2 Chemical Results for B Watershed 05/07/2015

Assigned Letter	Name	Time	Concentration /mmol·L^{-1}								
			[Na+]	[K^+]	[Mg^{2+}]	[Ca^{2+}]	[F^-]	[Cl^-]	[SO_4^{2-}]	SC^+	SA^-
	B. Mstream #1	12:20	0,018	0,015	0,097	0,858	0,001	0,001	0,296	1,942	1,234
	B. Mstream #2	12:48	0,014	0,012	0,093	0,396	0,001	0,001	0,279	1,004	1,191
	B. Mstream TP #1	13:10	0,013	0,010	0,087	0,389	0,001	0,002	0,258	0,974	1,248
	B. Left Moraine	13:24	0,058	0,143	0,910	5,554	0,005	0,016	6,597	13,130	14,839
	B. MStream TP #2	13:57	0,011	0,014	0,091	0,744	0,001	0,003	0,295	1,696	1,442
E3	B. Mstream TP #3	14:14	0,011	0,010	0,056	0,290	0,001	0,002	0,129	0,712	0,758
Y3	B. Sub-Main (Left) #1	15:49	0,014	0,005	0,093	0,426	0,001	0,001	0,250	1,057	1,133
Z3	Sub main stream left	15:57	0,008	0,003	0,086	0,368	0,000	0,001	0,209	0,919	1,036
	B. Glacier Icing Stream #3	16:08									
	B. Glacier Icing Stream #2	16:09									
	B. Glacier Icing Stream #1	16:15									
C3	B1 Supra Center	16:23	0,008	0,001	0,014	0,037	0,000	0,001	0,002	0,111	0,110
B3	B. Main Outlet	16:31	0,012	0,015	0,057	0,234	0,000	0,001	0,173	0,611	1,555
A3	Main Supra	16:53	0,008	0,002	0,023	0,078	0,000	0,000	0,029	0,213	0,266
D3	B. Right Side Moraine	17:03	0,058	0,144	0,630	1,558	0,000	0,017	1,710	4,577	4,805

Table A II-3 Chemical Results for B Watershed 07/07/2015

Assigned Letter	Name	Time	Concentration /mmol·L^{-1}								
			[Na+]	[K^+]	[Mg^{2+}]	[Ca^{2+}]	[F^-]	[Cl^-]	[SO_4^{2-}]	SC^+	SA^-
	B. Moraine Left #1	09:46	0,191	0,109	3,713	4,221	0,000	0,049	7,201	16,169	19,036
	B. Mstream TP #1	10:26	0,019	0,017	0,147	0,481	0,000	0,003	0,322	1,293	1,464
E4	B. Mstream TP #3	10:47	0,013	0,014	0,114	0,287	0,001	0,002	0,200	0,828	0,948
	B. Mstream TP #2	11:03	0,014	0,015	0,126	0,494	0,000	0,001	0,385	1,268	1,445
	B2 Mstream #1	11:36	0,022	0,016	0,155	0,723	0,001	0,001	0,463	1,794	1,624
	B2 Mstream TP #1	12:09	0,024	0,009	0,095	0,415	0,001	0,002	0,343	1,051	1,168
I	B2 Mstream TP #3	12:28	0,012	0,007	0,044	0,209	0,002	0,006	0,080	0,525	0,544
R	B2 Mstream TP #2	12:53	0,012	0,007	0,172	0,747	0,000	0,003	0,662	1,855	1,951
Q	B3 Mstream #1	13:29	0,017	0,006	0,145	0,734	0,001	0,002	0,586	1,782	1,759
O	B3 Glacier Main Left	14:04	0,020	0,004	0,060	0,250	0,001	0,003	0,128	0,643	0,821
P	B3 Geyser	14:16	0,018	0,005	0,181	0,993	0,001	0,008	0,881	2,370	2,148
N	B3 Supra Centre	14:26	0,021	0,002	0,055	0,127	0,000	0,001	0,159	0,387	0,455
M	B3 Glacier Main Right	14:36	0,018	0,003	0,116	0,575	0,001	0,001	0,441	1,403	1,371
L	B2 Main Right	15:54	0,011	0,009	0,047	0,195	0,000	0,003	0,088	0,505	0,787
K	B2Supra Centre	16:01	0,014	0,006	0,025	0,388	0,002	0,009	0,030	0,846	0,183
J	B2 Main Left	16:06	0,010	0,007	0,031	0,127	0,000	0,002	0,061	0,334	0,940
H	B2 Mstream	16:33	0,011	0,010	0,031	0,167	0,000	0,001	0,100	0,418	0,666
B4	B1 Mstream Outlet	17:29	0,016	0,012	0,055	0,236	0,001	0,004	0,134	0,609	1,101
A4	B1 Main Supra	17:36	0,011	0,002	0,017	0,095	0,000	0,003	0,026	0,236	0,279

Table A II-4 Chemical Results for B Watershed 08/07/2015-10/07/2015

Name	Date dd/mm	Time	Concentration /mmol·L^{-1}								
			[Na+]	[K^+]	[Mg^{2+}]	[Ca^{2+}]	[F^-]	[Cl^-]	[SO_4^{2-}]	SC^+	SA^-
Rain Sample	08/07	17:35									
B Mstream - 5:09	09/07	05:09	0,034	0,039	0,270	1,061	0,001	0,001	0,663	2,735	2,457
Rain Sample	09/07	08:47									
B Mstream - 9:09	09/07	09:09	0,032	0,036	0,260	0,940	0,001	0,004	0,629	2,468	2,327
B Mstream - 11:02	09/07	11:02	0,033	0,032	0,217	0,769	0,001	0,001	0,555	2,036	2,081
Puit Camp B	09/07	12:27	0,122	0,078	1,693	4,207	0,000	0,016	3,529	11,999	12,234
B Mstream - 13:03	09/07	13:03	0,027	0,017	0,157	0,659	0,001	0,002	0,387	1,674	1,641
B Mstream - 15:12	09/07	15:12	0,031	0,024	0,145	0,611	0,000	0,002	0,395	1,567	1,879
B Mstream - 17:06	09/07	17:06	0,023	0,024	0,137	0,847	0,001	0,002	0,539	2,016	2,427
B Mstream - 18:58	09/07	18:58	0,032	0,029	0,141	0,698	0,002	0,003	0,404	1,740	2,333
B Mstream - 21:06	09/07	21:06	0,026	0,023	0,155	0,774	0,001	0,001	0,446	1,909	2,862
B Mstream - 1:04	10/07	01:04	0,026	0,032	0,257	1,024	0,001	0,004	0,725	2,622	2,447
B Mstream - 8:15	10/07	08:15	0,044	0,033	0,425	1,331	0,010	0,015	1,218	3,589	3,716
Rain Sample	10/07	06:59									

dd/mm is for day/month

APPENDIX III

PHYSICAL AND ORGANIC CARBON CONCENTRATION RESULTS OF B WATERSHED SAMPLES

Table A III-1 Physical Properties and DOC Results of B Watershed Samples 03/07/2015

	Name	Time	Physical Properties			DOC /ppm
			$\delta^{18}O$	$\delta^{2}H$	d-excess	
	B. MStream #1	09:09	-24,253	-185,405	8,616	1,061
	B. MStream #2	09:36	-24,211	-185,088	8,601	1,104
	B. Mstream TP #1	10:13	-24,163	-184,504	8,802	0,795
	B. Mstream TP #2	10:39	-24,236	-185,971	7,913	0,425
E1	B. Mstream TP #3	10:52	-24,252	-185,185	8,829	0,462
B1	B. Main Outlet	11:46	-24,337	-186,013	8,681	0,463
A1	B. Main Supra	11:49	-25,304	-193,005	9,426	0,504
Y1	B. Sub-Main #1	12:07	-25,435	-193,684	9,797	0,497
	Glacier B Icing Right Stream #1	12:03	-26,247	-199,150	10,828	
	Glacier B Icing Right Stream #2	12:08	-26,762	-203,152	10,946	
	Glacier B Icing Right Stream #3	12:12	-26,409	-201,303	9,972	
Z1	B Sub-Main Left #1	12:24	-24,677	-189,235	8,185	0,536
C1	B1 Supra Center	12:35	-26,243	-199,745	10,197	0,555
D1	B. Right side Moraine	13:50	-24,207	-186,623	7,036	0,601
	B. Right Moraine Lake	15:05	-21,948	-174,751	0,836	1,161
B2	B. Main Outlet #2	16:45	-25,937	-197,374	10,126	0,494
A2	B. Main Supra #2	16:47	-26,716	-203,632	10,094	0,687
Y2	B. Sub-Main #2	16:50	-24,865	-190,759	8,162	0,280

Table A III-2 Physical Properties and DOC Results of B Watershed Samples 05/07/2015

Assigned Letter	Name	Time	Physical Properties			DOC /ppm
			$\delta^{18}O$	$\delta^{2}H$	d-excess	
	B. Mstream #1	12:20	-24,429	-187,453	7,977	0,492
	B. Mstream #2	12:48	-24,579	-188,340	8,292	0,378
	B. Mstream TP #1	13:10	-24,512	-187,997	8,095	0,432
	B. Left Moraine	13:24	-22,107	-171,696	5,162	0,377
	B. MStream TP #2	13:57	-24,593	-188,620	8,123	0,471
E3	B. Mstream TP #3	14:14	-24,484	-187,314	8,558	0,394
Y3	B. Sub-Main (Left) #1	15:49	-24,145	-185,693	7,470	0,366
Z3	Sub main stream left	15:57	-24,147	-185,519	7,656	0,561
	B. Glacier Icing Stream #3	16:08	-24,057	-184,097	8,363	
	B. Glacier Icing Stream #2	16:09	-23,943	-184,076	7,465	
	B. Glacier Icing Stream #1	16:15	-24,444	-186,716	8,834	
C3	B1 Supra Center	16:23	-24,740	-189,696	8,225	0,482
B3	B. Main Outlet	16:31	-24,423	-187,414	7,972	0,505
A3	Main Supra	16:53	-24,988	-190,404	9,503	0,480
D3	B. Right Side Moraine	17:03	-24,288	-186,573	7,730	0,617

Table A III-3 Physical Properties and DOC Results of B Watershed Samples 07/07/2015

Assigned Letter	Name	Time	Physical Properties			DOC /ppm
			$\delta^{18}O$	$\delta^{2}H$	d-excess	
	B. Moraine Left #1	09:46	-23,836	-183,201	7,484	0,464
	B. Mstream TP #1	10:26	-24,016	-184,325	7,799	0,402
E4	B. Mstream TP #3	10:47	-23,996	-183,782	8,190	0,449
	B. Mstream TP #2	11:03	-24,370	-186,582	8,380	0,556
	B2 Mstream #1	11:36	-24,449	-187,404	8,189	0,261
	B2 Mstream TP #1	12:09	-24,467	-187,370	8,367	0,383
I	B2 Mstream TP #3	12:28	-24,495	-187,985	7,976	0,286
R	B2 Mstream TP #2	12:53	-24,338	-186,849	7,851	0,251
Q	B3 Mstream #1	13:29	-24,325	-186,690	7,908	0,429
O	B3 Glacier Main Left	14:04	-24,778	-189,550	8,674	0,322
P	B3 Geyser	14:16	-24,289	-186,352	7,963	0,354
N	B3 Supra Centre	14:26	-24,777	-189,059	9,160	0,334
M	B3 Glacier Main Right	14:36	-24,405	-187,779	7,465	0,275
L	B2 Main Right	15:54	-24,828	-189,786	8,837	0,455
K	B2Supra Centre	16:01	-24,907	-190,556	8,700	0,706
J	B2 Main Left	16:06	-24,266	-186,205	7,927	0,867
H	B2 Mstream	16:33	-24,741	-189,273	8,652	0,673
B4	B1 Mstream Outlet	17:29	-24,444	-186,363	9,187	0,600
A4	B1 Main Supra	17:36	-24,914	-190,521	8,792	0,303

Table A III-4 Physical Properties and DOC Results of B Watershed Samples
08/07/2015 - 10/07/2015

Name	Date dd/mm	Time	Physical Properties			DOC /ppm
			$\delta^{18}O$	$\delta^{2}H$	d-excess	
Rain Sample	08/07	17:35	-15,897	-122,064	5,110	
B Mstream - 5:09	09/07	05:09	-23,944	-182,260	9,292	0,467
Rain Sample	09/07	08:47	-17,799	-136,886	5,505	
B Mstream - 9:09	09/07	09:09	-23,844	-181,732	9,023	1,061
B Mstream - 11:02	09/07	11:02	-23,912	-182,602	8,693	0,339
Puit Camp B	09/07	12:27	-22,011	-170,990	5,101	8,031
B Mstream - 13:03	09/07	13:03	-24,084	-184,364	8,307	0,433
B Mstream - 15:12	09/07	15:12	-24,167	-184,746	8,592	0,328
B Mstream - 17:06	09/07	17:06	-24,246	-185,776	8,194	1,000
B Mstream - 18:58	09/07	18:58	-24,167	-185,034	8,302	0,438
B Mstream - 21:06	09/07	21:06	-23,159	-176,117	9,153	0,365
B Mstream - 1:04	10/07	01:04	-22,839	-174,157	8,553	0,430
B Mstream - 8:15	10/07	08:15	-23,368	-178,490	8,456	0,349
Rain Sample	10/07	06:59	-17,266	-135,032	3,095	

dd/mm is for day/month

APPENDIX IV

BIVARIATE GRAPHS

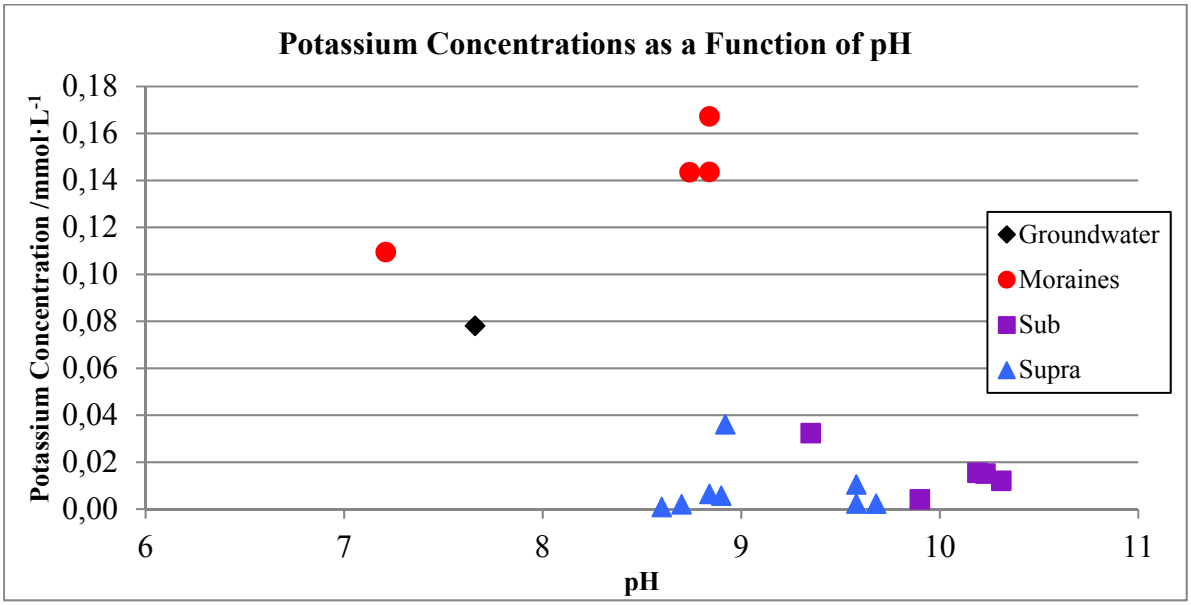

Figure A IV-1 Potassium Concentrations as a Function of pH for B watershed End-Members

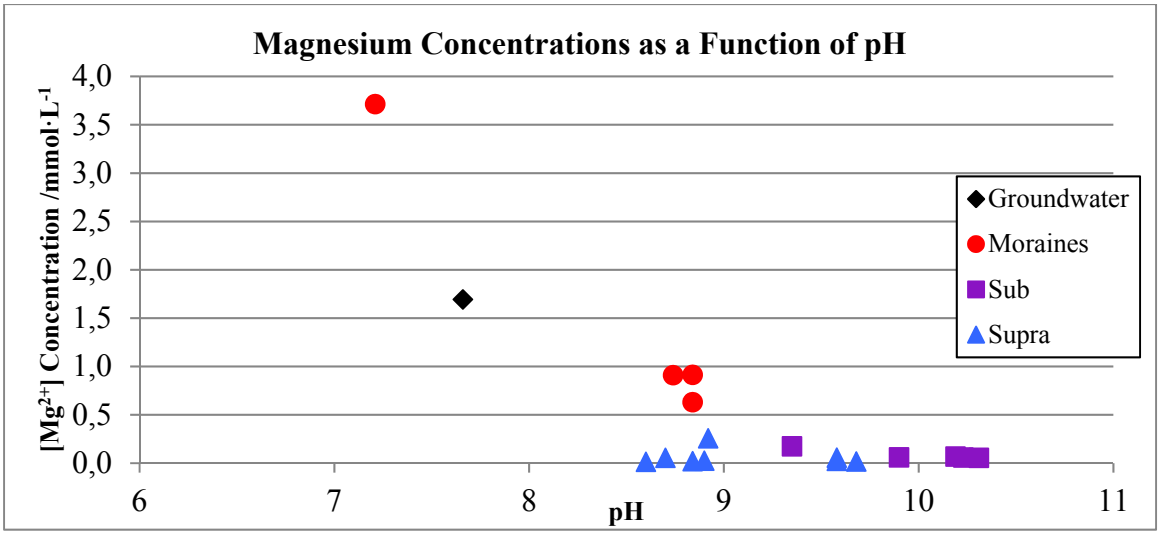

Figure A IV-0.23 Magnesium Concentration as a Function of pH for B Watershed End-Members

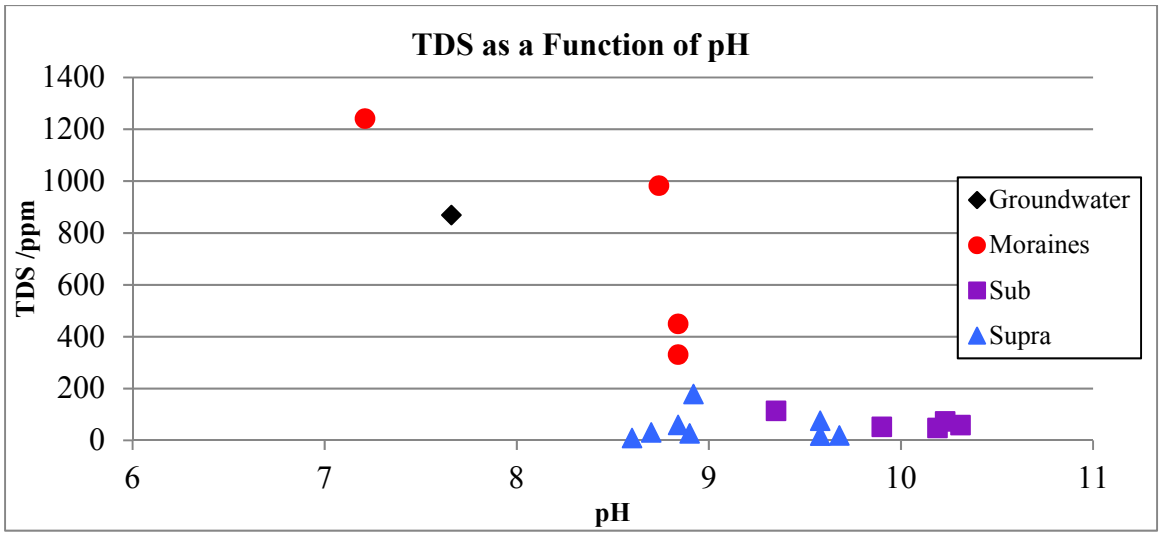

Figure A IV-3 TDS as a Function of pH for B Watershed End-Members

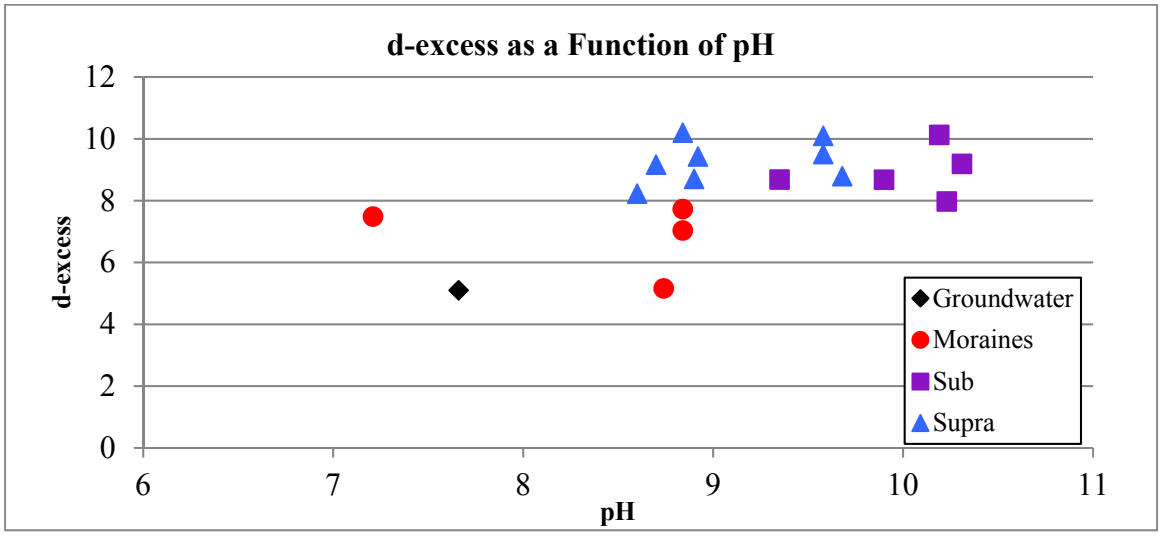

Figure A IV-4 d-excess as a Function of pH

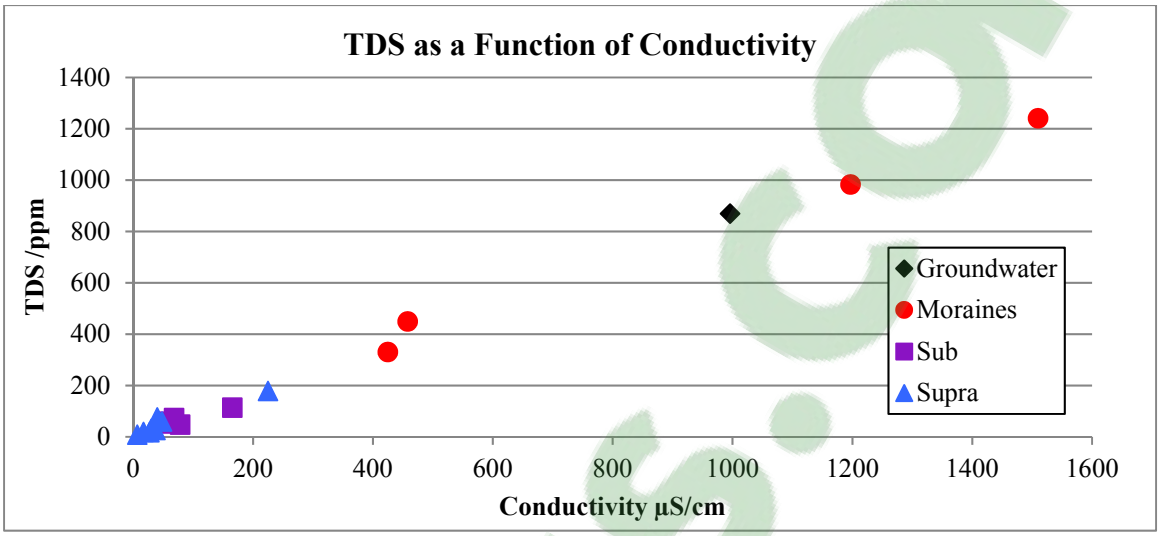

Figure A IV-5 TDS as a Function of Conductivity for B Watershed End-Members

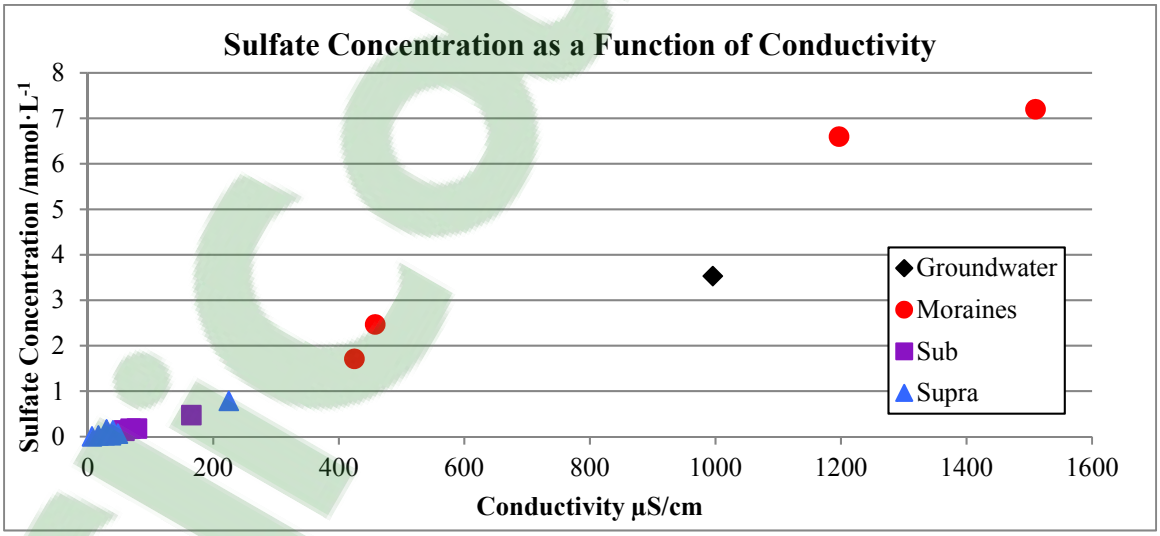

Figure A IV-6 Sulfate Concentrations as a Function of Conductivity in B Watershed End-Members

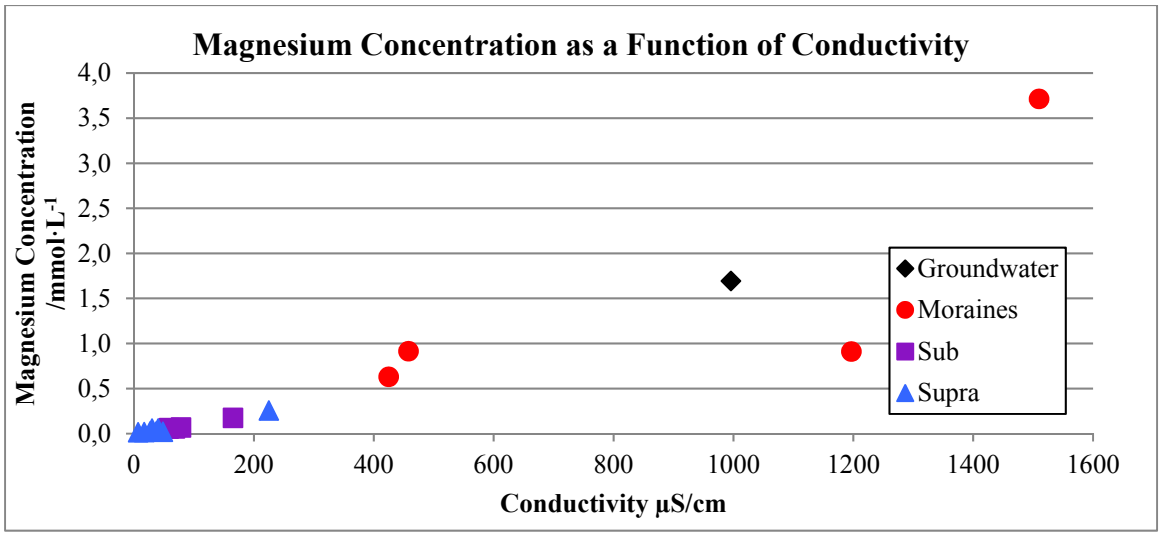

Figure A IV-7 Magnesium Concentrations as a Function of Conductivity in B Watershed End-Members

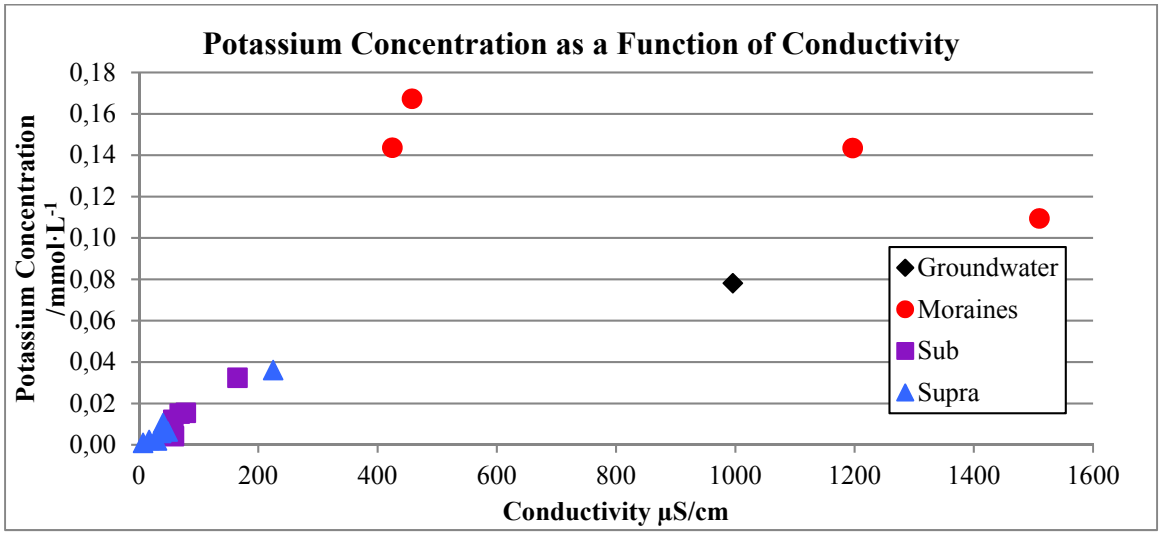

Figure A IV-8 Potassium Concentrations as a Function of Conductivity for B Watershed End-Members

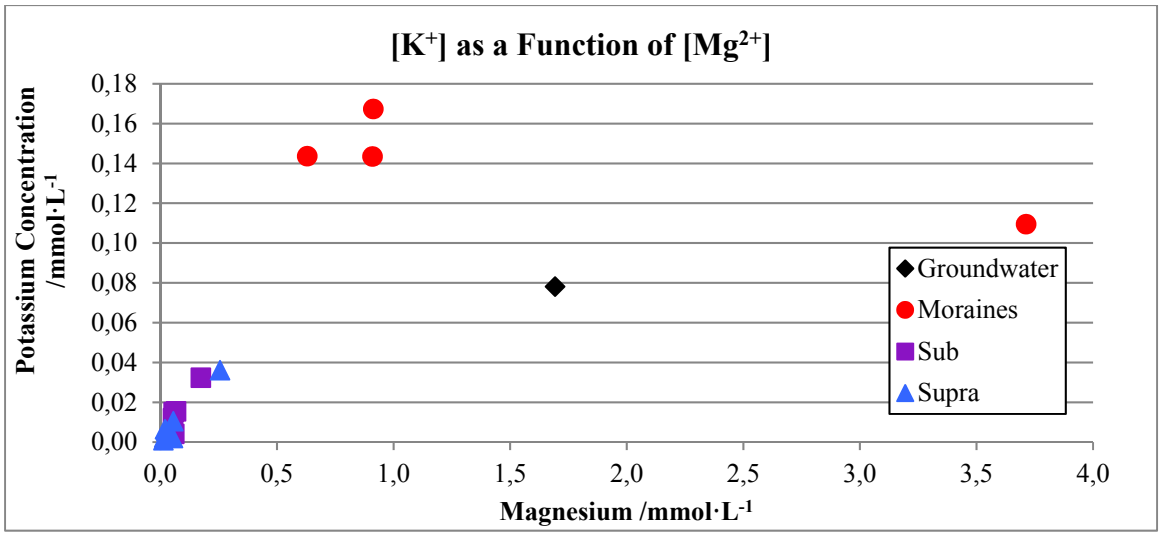

Figure A IV-9 Potassium Concentrations as a Function of Magnesium Concentrations of B Watershed End-Members

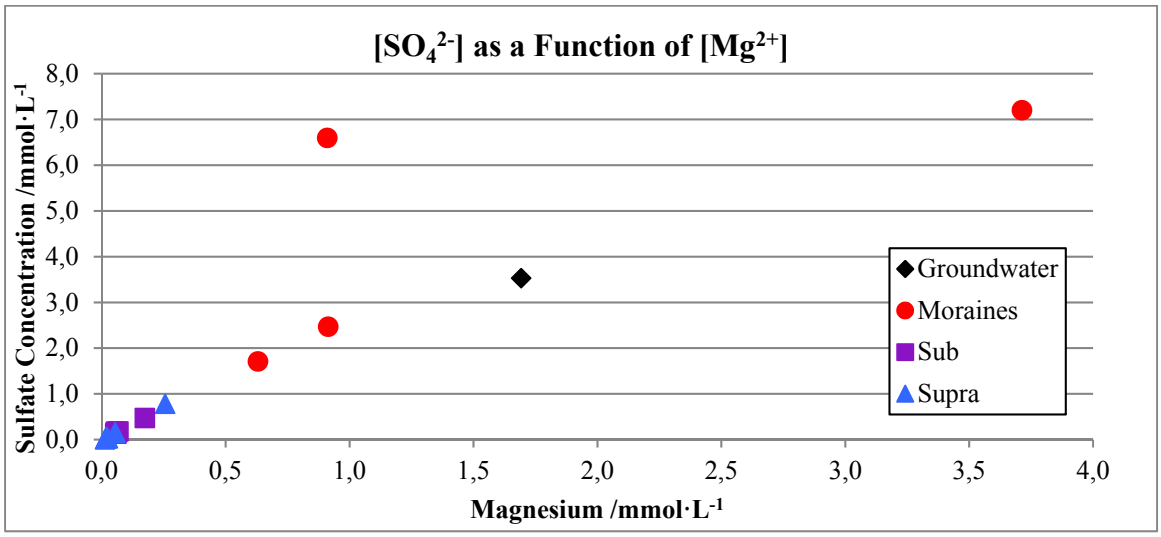

Figure A IV-10 Sulfate Concentrations as a Function of Magnesium Concentrations for B Watershed End-Members

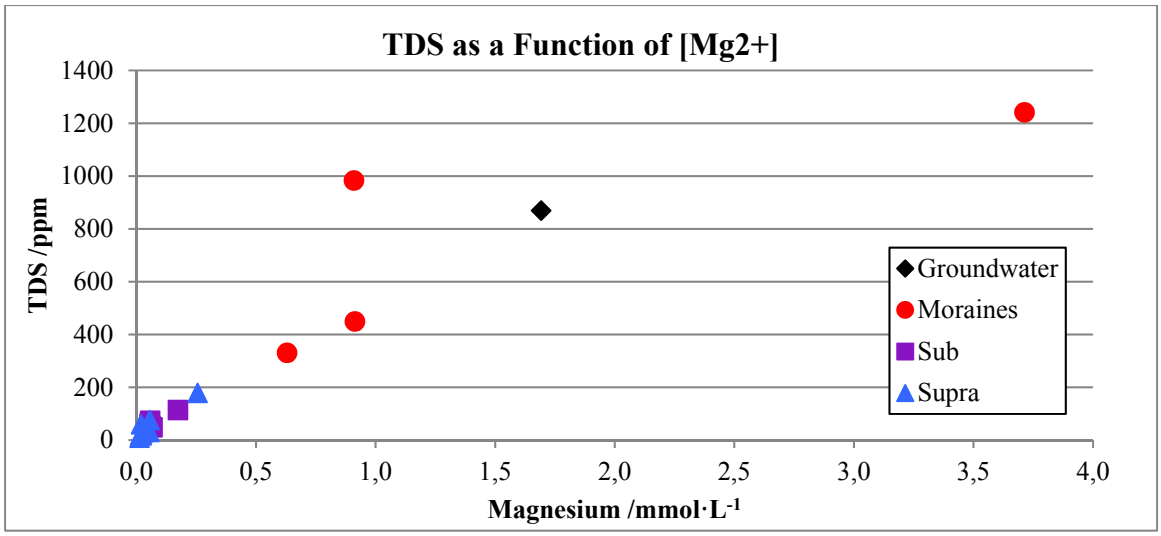

Figure A IV-11 TDS as a Function of Magnesium Concentrations in B Watershed End-Members

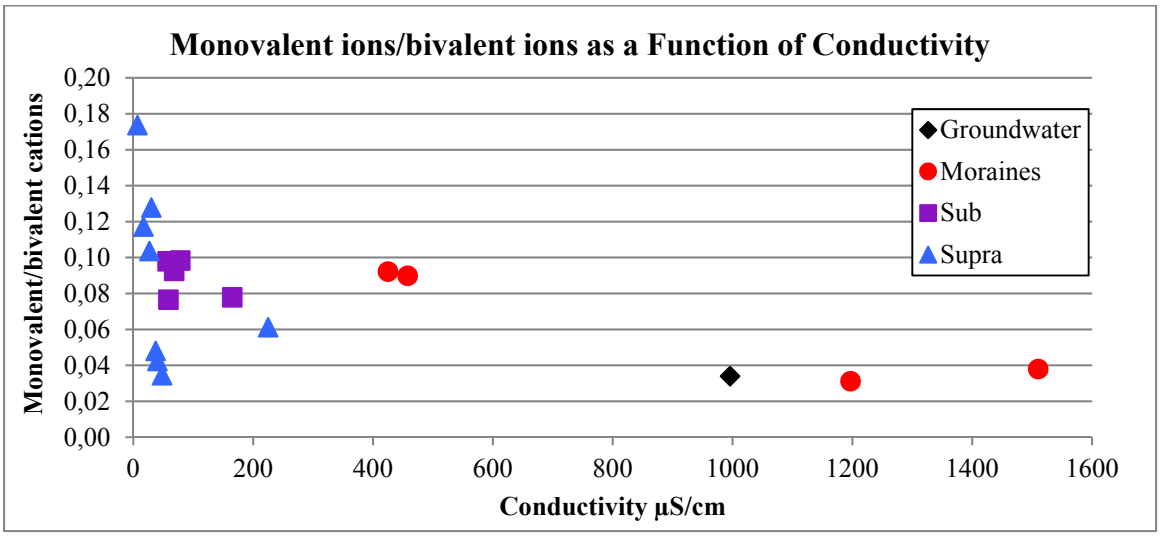

Figure A IV-12 Monovalent/Bivalent cations as a function of Conductivity for B Watershed End-Members

APPENDIX V

SOLUBITY DATA OF B WATERSHED SAMPLES

Table A V-1 Solubility Data for B Watershed Samples Collected 03/07/2015

Assigned Letter	Name	Type	Time	pH	Solutes			Solubility $CaCO_3$	
					$[Ca^{2+}]$	$[CO_3^{2-}]$	$[HCO_3^-]$	Q	Q/K_{sp}
	B. MStream #1	Stream	09:09	8.88	0.8664	0.0366	1.1587	3.174E-08	9.6197
	B. MStream #2	Stream	09:36	8.81	0.8346	0.0100	0.7110	8.346E-09	2.5291
	B. Mstream TP #1	Stream	10:13	8.79	0.9320	0.0225	0.8750	2.096E-08	6.3523
	B. Mstream TP #2	Stream	10:39	8.83	1.0572	0.0376	1.3329	3.971E-08	12.0342
E1	B. Mstream TP #3	Stream	10:52	8.75	0.7928	0.0185	0.7871	1.463E-08	4.4326
B1	B. Main Outlet	Sub	11:46	9.35	0.5502	0.0560	0.6000	3.081E-08	9.3367
A1	B. Main Supra	Supra	11:49	8.92	0.9696	0.0306	0.8828	2.968E-08	8.9931
Y1	B. Sub-Main #1	Stream	12:07	8.77	1.4456	0.0247	1.0066	3.572E-08	10.8242
	Glacier B Icing Right Stream #1	Icing - Supra	12:03						
	Glacier B Icing Right Stream #2	Icing - Supra	12:08						
	Glacier B Icing Right Stream #3	Icing - Supra	12:12						
Z1	B Sub-Main Left #1	Stream	12:24	8.82	1.4476	0.0324	1.1753	4.686E-08	14.1990
C1	B1 Supra Center	Supra	12:35	8.84	0.4266	0.0110	0.7580	4.692E-09	1.4219
D1	B. Right side Moraine	Moraine	13:50	8.84	2.0193	0.0458	1.5884	9.250E-08	28.0315
	B. Right Moraine Lake	Lake	15:05	9	1.4311	0.0671	1.6098	9.604E-08	29.1021
B2	B. Main Outlet #2	Sub	16:45	10.19	0.2618	0.1142	0.1768	2.988E-08	9.0560
A2	B. Main Supra #2	Supra	16:47	9.58	0.3956	0.0992	0.6257	3.923E-08	11.8870

Table A V-2 Solubility Data for B Watershed Samples Collected 05/07/2015

Assigned Letter	Name	Type	Time	pH	Solutes			Solubility $CaCO_3$	
					$[Ca^{2+}]$	$[CO_3^{2-}]$	$[HCO_3^-]$	Q	Q/K_{sp}
	B. Mstream #1	Stream	12:20	9.53	0.8575	0.0940	1.1600	8.061E-08	24.4271
	B. Mstream #2	Stream	12:48	9.1	0.3956	0.0300	0.5720	1.187E-08	3.5982
	B. Mstream TP #1	Stream	13:10	9.26	0.3886	0.0170	0.4190	6.606E-09	2.0017
	B. Left Moraine	Moraine	13:24	8.74	5.5543	0.0356	1.5529	1.976E-07	59.8750
	B. MStream TP #2	Stream	13:57	9.37	0.7444	0.0693	0.7094	5.160E-08	15.6365
E3	B. Mstream TP #3	Stream	14:14	9.26	0.2898	0.0327	0.4307	9.467E-09	2.8689
Y3	B. Sub-Main (Left) #1	Stream	15:49	9.2	0.4260	0.0369	0.5582	1.571E-08	4.7613
Z3	Sub main stream left	Stream	15:57	9.54	0.3683	0.0691	0.4779	2.544E-08	7.7098
	B. Glacier Icing Stream #3	Icing - Supra	16:08						
	B. Glacier Icing Stream #2	Icing - Supra	16:09						
	B. Glacier Icing Stream #1	Icing - Supra	16:15						
C3	B1 Supra Center	Supra	16:23	8.6	0.0374	0.0017	0.1007	6.254E-11	0.0190
B3	B. Main Outlet	Sub	16:31	10.23	0.2345	0.0930	0.0770	2.181E-08	6.6080
A3	Main Supra	Supra	16:53	9.58	0.0780	0.0120	0.1310	9.357E-10	0.2835
D3	B Right Side Moraine	Moraine	17:03	8.84	1,5575	0,0373	1,2934	5,810E-08	17,6055

Table A V-3 Solubility Data for B Watershed Samples Collected 07/07/2015

Assigned Letter	Name	Type	Time	pH	Solutes			Solubility $CaCO_3$	
					$[Ca^{2+}]$	$[CO_3^{2-}]$	$[HCO_3^-]$	Q	Q/K_{sp}
	B. Moraine Left #1	Moraine	09:46	7.21	4.2210	0.0031	4.5778	1.306E-08	3.9588
	B. Mstream TP #1	Stream	10:26	9.23	0.4811	0.0506	0.7148	2.435E-08	7.3775
E4	B. Mstream TP #3	Stream	10:47	9.43	0.2873	0.0499	0.4443	1.432E-08	4.3402
	B. Mstream TP #2	Stream	11:03	9.24	0.4936	0.0425	0.5870	2.099E-08	6.3600
	B2 Mstream #1	Stream	11:36	8.85	0.7235	0.0194	0.6572	1.403E-08	4.2523
	B2 Mstream TP #1	Stream	12:09	9.09	0.4146	0.0223	0.4353	9.257E-09	2.8052
I	B2 Mstream TP #3	Stream	12:28	9.58	0.2092	0.0452	0.2855	9.464E-09	2.8680
R	B2 Mstream TP #2	Stream	12:53	9.03	0.7466	0.0256	0.5728	1.910E-08	5.7888
Q	B3 Mstream #1	Stream	13:29	9.05	0.7339	0.0250	0.5340	1.833E-08	5.5555
O	B3 Glacier Main Left	Sub	14:04	9.9	0.2496	0.0630	0.2550	1.572E-08	4.7647
P	B3 Geyser	Artesian Spring	14:16	9.66	0.9925	0.0519	0.2722	5.149E-08	15.6021
N	B3 Supra Centre	Supra	14:26	8.7	0.1273	0.0027	0.1305	3.473E-10	0.1053
M	B3 Glacier Main Right	Stream	14:36	8.82	0.5746	0.0127	0.4625	7.320E-09	2.2182
L	B2 Main Right	Stream	15:54	9.7	0.1953	0.0340	0.2570	6.639E-09	2.0118
K	B2Supra Centre	Supra	16:01	8.9	0.3877	0.0110	0.7530	4.264E-09	1.2923
J	B2 Main Left	Stream	16:06	10.24	0.1275	0.0760	0.0580	9.687E-09	2.9354
H	B2 Mstream	Stream	16:33	10.27	0.1674	0.0830	0.0490	1.390E-08	4.2112
B4	B1 Mstream Outlet	Sub	17:29	10.31	0.2355	0.1430	0.0490	3.368E-08	10.2064
A4	B1 Main Supra	Supra	17:36	9.68	0.0950	0.0319	0.1601	3.034E-09	0.9195

Table A V-4 Solubility Data for B Watershed Samples Collected 09/07/2015 - 10/07/2015

Name	Type	Time	pH	Solutes			Solubility $CaCO_3$	
				$[Ca^{2+}]$	$[CO_3^{2-}]$	$[HCO_3^-]$	Q	Q/K_{sp}
B Mstream - 5:09	Stream	05:09	8.67	1.0610	0.0212	1.0857	2.246E-08	6.8062
B Mstream - 9:09	Stream	09:09	8.78	0.9399	0.0254	1.0131	2.392E-08	7.2478
B Mstream - 11:02	Stream	11:02	9.00	0.7688	0.0372	0.8935	2.864E-08	8.6781
B Mstream - 13:03	Stream	13:03	9.17	0.6586	0.0474	0.7691	3.123E-08	9.4651
B Mstream - 15:12	Stream	15:12	9.35	0.6112	0.0856	0.9169	5.230E-08	15.8484
B Mstream - 17:06	Stream	17:06	9.49	0.8469	0.0600	0.8130	5.081E-08	15.3977
B Mstream - 18:58	Stream	18:58	9.56	0.6985	0.0700	0.7860	4.889E-08	14.8161
B Mstream - 21:06	Stream	21:06	9.23	0.7743	0.0360	0.9430	2.787E-08	8.4467
B Mstream - 1:04	Stream	01:04	9.05	1.0240	0.0424	0.9071	4.345E-08	13.1666
B Mstream - 8:15	Stream	08:15	8.71	1.3309	0.0258	1.2045	3.427E-08	10.3857
Puit Camp B	Groundwater	12:27	7.66	4.2070	0.0098	5.1404	4.121E-08	12.4868

LIST OF REFERENCES

Arendt, Anthony A., Keith A. Echelmeyer, William D. Harrison, Craig S. Lingle et Virginia B. Valentine. 2002. « Rapid Wastage of Alaska Glaciers and Their Contribution to Rising Sea Level ». *Science,* vol. 297, nº 5580, p. 382-386.

Bagard, Marie-Laure, François Chabaux, Oleg S. Pokrovsky, Jérome Viers, Anatoly S. Prokushkin, Peter Stille, Sophie Rihs, Anne-Désirée Schmitt et Bernard Dupré. 2011. « Seasonal variability of element fluxes in two Central Siberian rivers draining high latitude permafrost dominated areas ». *Geochimica et Cosmochimica Acta,* vol. 75, nº 12, p. 3335-3357.

Baraer, M., J. M. McKenzie, B. G. Mark, J. Bury et S. Knox. 2009. « Characterizing contributions of glacier melt and groundwater during the dry season in a poorly gauged catchment of the Cordillera Blanca (Peru) ». *Adv. Geosci.,* vol. 22, p. 41-49.

Baraer, Michel, Bryan G. Mark, Jeffrey M. McKenzie, Thomas Condom, Jeffrey Bury, Kyung-In Huh, Cesar Portocarrero, Jesús Gómez et Sarah Rathay. 2012. « Glacier recession and water resources in Peru's Cordillera Blanca ». *Journal of Glaciology,* vol. 58, nº 207, p. 134-150.

Baraer, Michel, Jeffrey McKenzie, Bryan G. Mark, Ryan Gordon, Jeffrey Bury, Thomas Condom, Jesus Gomez, Sara Knox et Sarah K. Fortner. 2015. « Contribution of groundwater to the outflow from ungauged glacierized catchments: a multi-site study in the tropical Cordillera Blanca, Peru ». *Hydrological Processes,* vol. 29, nº 11, p. 2561-2581.

Barnett, T. P., J. C. Adam et D. P. Lettenmaier. 2005. « Potential impacts of a warming climate on water availability in snow-dominated regions ». *Nature,* vol. 438, nº 7066, p. 303-309.

Barr, I. D., et H. Lovell. 2014. « A review of topographic controls on moraine distribution ». *Geomorphology,* vol. 226, p. 44-64.

Barrand, N. E., et M. J. Sharp. 2010. « Sustained rapid shrinkage of Yukon glaciers since the 1957–1958 International Geophysical Year ». *Geophysical Research Letters,* vol. 37, nº 7, p. n/a-n/a.

Barthold, Frauke, Christoph Tyralla, Katrin Schneider, Kellie Vache, Hans-Georg Frede, Kellie Vaché et Lutz Breuer. 2011. « How many tracers do we need for end member mixing analysis (EMMA)? A sensitivity analysis ». *Water resources research,* vol. 47, nº 8.

Barthold, Frauke, Jinkui Wu, Kellie Vache, Katrin Schneider, Hans-Georg Frede, Kellie Vaché et Lutz Breuer. 2010. « Identification of geographic runoff sources in a data sparse region: hydrological processes and the limitations of tracer-based approaches ». *Hydrological processes,* vol. 24, nº 16, p. 2313-2327.

Benn, D., et D Evans. 1998. *Glaciers and glaciation,* . London: Arnold, London, 734 p.

Berthier, E., E. Schiefer, G. K. C. Clarke, B. Menounos et F. Remy. 2010. « Contribution of Alaskan glaciers to sea-level rise derived from satellite imagery ». *Nature Geosci,* vol. 3, nº 2, p. 92-95.

Blaen, Phillip, David Hannah, Lee Brown et Alexander Milner. 2014. « Water source dynamics of high Arctic river basins ». *Hydrological processes,* vol. 28, nº 10, p. 3521-3538.

Bonnaventure, P. P., et A. G. Lewkowicz. 2008. « Mountain permafrost probability mapping using the BTS method in two climatically dissimilar locations, northwest Canada ». *Canadian Journal of Earth Sciences,* vol. 45, nº 4, p. 443-455.

Boon, S., G. E. Flowers et D. S. Munro. 2009. « Canadian glacier hydrology, 2003-2007 ». *Canadian Water Resources Journal,* vol. 34, nº 2, p. 195-203.

Brabets, T.P. , et P. Schuster. 2008. *Transport of Water, Carbon, and Sediment Through the Yukon River Basin*. 3005. Alaska Science Center.

Bring, A., I. Fedorova, Y. Dibike, L. Hinzman, J. Mård, S. H. Mernild, T. Prowse, O. Semenova, S. L. Stuefer et M. K. Woo. 2016. « Arctic terrestrial hydrology: A synthesis of processes, regional effects, and research challenges ». . *Journal of Geophysical Research G: Biogeosciences,* vol. 121, nº 3, p. 621-649.

Bring, A., J. Jarsjö et G. Destouni. 2015. « Water information and water security in the arctic ». In *The New Arctic*. p. 225-238. In *Scopus*. < https://www.scopus.com/inward/record.uri?eid=2-s2.0-84943395412&partnerID=40&md5=d0fd376a2debdd92b0268a2c1cc6a03c >.

"groundwater". *Encyclopædia Britannica. Encyclopædia Britannica Online*. Encyclopædia Britannica Inc., 2016. Web. 07 Aug. 2016 <https://www.britannica.com/science/groundwater>.

"qualitative chemical analysis". *Encyclopædia Britannica. Encyclopædia Britannica Online.* Encyclopædia Britannica Inc., 2016. Web. 07 Aug. 2016 <https://www.britannica.com/science/qualitative-chemical-analysis>.

Brook, Martin, et Sheryl Paine. 2012. « ABLATION OF ICE-CORED MORAINE IN A HUMID, MARITIME CLIMATE: FOX GLACIER, NEW ZEALAND ». *Geografiska annaler. Series A. Physical geography,* vol. 94A, nº 3, p. 339-349.

Brown, Lee, David Hannah, Alexander Milner, Chris Soulsby, Andrew Hodson et Mark Brewer. 2006. « Water source dynamics in a glacierized alpine river basin (Taillon-Gabiétous, French Pyrénées) ». *Water resources research,* vol. 42, nº 8.

Brown, R.D., et R.O. Braaten. 1998. « Spatial and temporal variability of Canadian monthly snow depths, 1946-1995 ». *Atmosphere-Ocean,* vol. 36, p. 37-45.

Brukner, M. Z. 2016. « Measuring Dissolved and Particulate Organic Carbon (DOC and POC) ». In *Microbial Life Educational Resources*. < http://serc.carleton.edu/microbelife/research_methods/biogeochemical/organic_carbon.html >. Consulté le July 26.

Burn, C. R. 1994. « Permafrost, tectonics, and past and future regional climate change,Yukon and adjacent Northwest Territories ». *Canadian Journal of Earth Sciences,* vol. 31, p. 182-191.

Cable, Jessica, Kiona Ogle et David Williams. 2011. « Contribution of glacier meltwater to streamflow in the Wind River Range, Wyoming, inferred via a Bayesian mixing model applied to isotopic measurements ». *Hydrological processes,* vol. 25, nº 14, p. 2228-2236.

Carey, S. K., et J. W. Pomeroy. 2009. « Progress in canadian snow and frozen ground hydrology, 2003-2007 ». *Canadian Water Resources Journal,* vol. 34, nº 2, p. 127-138.

Carey, S. K., et W. L. Quinton. 2005. « Evaluating runoff generation during summer using hydrometric, stable isotope and hydrochemical methods in a discontinuous permafrost alpine catchment ». *Hydrological processes,* vol. 19, nº 1, p. 95-114.

Carey, S. K., et M. Woo. 1998. « Snowmelt Hydrology of Two Subarctic Slopes, Southern Yukon, Canada ». *Nordic Hydrology,* vol. 29, p. 331-346.

Carey, S. K., et M. Woo. 2001. « Spatial variability of hillslope water balance, Wolf Creek basin, subarctic Yukon ». *Hydrological Processes,* vol. 15, nº 16, p. 3113-3132.

Chesnokova, Anna. 2015. « Multi-Scale Assessment of Environmental Changes, Impact on Glaciarized Watersheds Hydrology ». In *Canadian Water Resources Association (CWRA)*. (Montreal, Canada).

Christophersen, Nils, et Richard P. Hooper. 1992. « Multivariate analysis of stream water chemical data: The use of principal components analysis for the end-member mixing problem ». *Water Resources Research,* vol. 28, nº 1, p. 99-107.

Comeau, S., G. Gorsky, R. Jeffree, J. L. Teyssié et J. P. Gattuso. 2009. « Impact of ocean acidification on a key Arctic pelagic mollusc (Limacina helicina) ». *Biogeosciences,* vol. 6, nº 9, p. 1877-1882.

Crompton, Jeff W., Gwenn E. Flowers, Dirk Kirste, Birgit Hagedorn et Martin J. Sharp. 2015. « Clay mineral precipitation and low silica in glacier meltwaters explored through reaction-path modelling ». *Journal of Glaciology,* vol. 61, nº 230, p. 1061-1078.

Cruz R. V., Harasawa H., Lal M., S. Wu, Y. Anokhin, B. Punsalmaa, Y. Honda, Jafari M., C. Li et N. Huu Ninh. 2007. *Asia. Climate Change 2007: Impacts, Adaptation and Vulnerability*. Coll. « Contribution of Working Group II to the Fourth Assessment Report of the Intergovernmental ». Cambridge, UK.: Cambridge University Press, 469 – 506 p.

Deb, D., J. Butcher et R. Srinivasan. 2015. « Projected Hydrologic Changes Under Mid-21st Century Climatic Conditions in a Sub-arctic Watershed ». *Water Resources Management,* vol. 29, nº 5, p. 1467-1487.

Dodds, C.J., et R.B. Campbell. 1992. *Geology of Mount St. Elias map area (115B and F[E1/2]), Yukon Territory*. Open File 2189. Geological Survey of Canada.

Drever, James I. 1988. *The geochemistry of natural waters*, 437. prentice Hall New Jersey.

Dugan, H. A., T. Gleeson, S. F. Lamoureux et K. Novakowski. 2012. « Tracing groundwater discharge in a High Arctic lake using radon-222 ». *Environmental Earth Sciences,* vol. 66, nº 5, p. 1385-1392.

Elliot, Trevor. 2014. « Environmental Tracers ». *Water,* vol. 6, nº 11, p. 3264-3269.

Fleming, S. W., et G. K. C. Clarke. 2003. « Glacial control of water resource and related environmental responses to climatic warming: Empirical analysis using historical streamflow data from Northwestern Canada ». *Canadian Water Resources Journal,* vol. 28, nº 1, p. 69-86.

Flowers, G. E., L. Copland et C. G. Schoof. 2014. « Contemporary glacier processes and global change: Recent observations from kaskawulsh glacier and the donjek range, st. elias mountains ». *Arctic,* vol. 67, nº 5 SUPPL.1, p. 22-34.

Freyer, K., H. C. Treutler, J. Dehnert et W. Nestler. 1997. « Sampling and measurement of radon-222 in water ». *Journal of Environmental Radioactivity,* vol. 37, nº 3, p. 327-337.

Fujita, Koji, Takeshi Ohta et Yutaka Ageta. 2007. « Characteristics and climatic sensitivities of runoff from a cold-type glacier on the Tibetan Plateau ». *Hydrological processes,* vol. 21, nº 21, p. 2882-2891.

Gascoin, S., C. Kinnard, R. Ponce, S. Lhermitte, S. MacDonell et A. Rabatel. 2011. « Glacier contribution to streamflow in two headwaters of the Huasco River, Dry Andes of Chile ». *The Cryosphere,* vol. 5, nº 4, p. 1099-1113.

Gat, Joel R. 2010. *Isotope Hydrology, A Study of the Water Cycle*. Coll. « Environmental Science and Management », 6. Imperial College Press.

Gonfiantini, R., M-A. Roche, J-C. Olivry, J-C. Fontes et G. M. Zuppi. 2001. « The altitude effect on the isotopic composition of tropical rains ». *Chemical Geology,* vol. 181, p. 147-167.

Grah, O., et J. Beaulieu. 2013. « The effect of climate change on glacier ablation and baseflow support in the Nooksack River basin and implications on Pacific salmonid species protection and recovery ». *Climatic Change,* vol. 120, nº 3, p. 657-670.

Harris, Daniel C. 2007. *Quantitative Chemical Analysis*, 7. New York, NY, USA: W. H. Freeman and Company.

Harris, S. 1987. « Altitude Trends in Permafrost Active Layer Thickness, Kluane Lake, YT. ». *Arctic,* vol. 40, nº 3, p. 179-183.

Hay, Lauren E., et Gregory J. McCabe. 2010. « Hydrologic effects of climate change in the Yukon River Basin ». *Climatic Change,* vol. 100, nº 3-4, p. 509-523.

Heckmann, T., S. McColl et D. Morche. 2016. « Retreating ice: Research in pro-glacial areas matters ». *Earth Surface Processes and Landforms,* vol. 41, nº 2, p. 271-276.

Hock, Regine. 2005. « Glacier melt: a review of processes and their modelling ». *Progress in Physical Geography,* vol. 29, nº 3, p. 362-391.

Hodgkins, Richard, Martyn Tranter et Julian A. Dowdeswell. 2004. « The Characteristics and Formation of A High-Arctic Proglacial Icing ». *Geografiska Annaler: Series A, Physical Geography,* vol. 86, nº 3, p. 265-275.

Hodson, Andy, Martyn Tranter, Angela Gurnell, Mike Clark et Jon Ove Hagen. 2002. « The hydrochemistry of Bayelva, a high Arctic proglacial stream in Svalbard ». *Journal of Hydrology,* vol. 257, nº 1–4, p. 91-114.

Hopmans, Jan. 2000. « Isotope Tracers in Catchment Hydrology, Carol Kendall and Jeffrey J. McDonnell (Eds.); Elsevier, Amsterdam, 1998, ISBN 0-444-81546 (hardbound) or 0-1444-50155-X (softbound) ». *Advances in water resources,* vol. 23, nº 4, p. 441-442.

Humlum, O. 1997. « Origin of Rock Glaciers: Observations from Mellemfjord, Disko Island, central West Greenland ». *Permafrost and Periglacial Processes,* vol. 7, p. 1-20.

IPCC, Intergovernmental Panel on Climate Change. 2007. *Fourth Assessment Report*. Coll. « Intergovernmental Panel on Climate Change Secretariat ». Geneva, Switzerland. < http://www.ipcc.ch/ >.

Irvine-Fynn, Tristram D. L., Andrew J. Hodson, Brian J. Moorman, Geir Vatne et Alun L. Hubbard. 2011. « POLYTHERMAL GLACIER HYDROLOGY: A REVIEW ». *Reviews of Geophysics,* vol. 49, nº 4, p. n/a-n/a.

Janowicz, J. R. 2011. « Streamflow responses and trends between permafrost and glacierized regimes in northwestern Canada ». In *IAHS-AISH Publication*. Vol. 346, p. 9-14. In *Scopus*. < https://www.scopus.com/inward/record.uri?eid=2-s2.0-84860551090&partnerID=40&md5=270a4b1d94c81cb3ae61a68fe2124d80 >.

Johnson, P. G. 1992. « Stagnant Glacier Ice, St. Elias Mountains, Yukon ». *Geografiska annaler. Series A. Physical geography,* vol. 74, nº 1, p. 13-19.

Kang, E., C. Liu, Z. Xie, L. I. Xin et Y. Shen. 2009. « Assessment of glacier water resources based on the glacier inventory of China ». *Annals of Glaciology,* vol. 50, nº 53, p. 104-110.

Kaser, G., J. G. Cogley, M. B. Dyurgerov, M. F. Meier et A. Ohmura. 2006. « Mass balance of glaciers and ice caps: Consensus estimates for 1961–2004 ». *Geophysical Research Letters,* vol. 33, nº 19, p. n/a-n/a.

Keller, K., J. D. Blum et G. W. Kling. 2010. « Stream geochemistry as an indicator of increasing permafrost thaw depth in an arctic watershed ». *Chemical Geology,* vol. 273, nº 1-2, p. 76-81.

Kinnard, C., et A. G. Lewkowicz. 2005. « Movement, moisture and thermal conditions ata turf-banked solidfuction lobe, Kluane Range, Yukon Territory, Canada ». *Permafrost and Periglacial Processes,* vol. 16, nº 3, p. 261-275.

Klaus, J. J. 2013. « Hydrograph separation using stable isotopes: Review and evaluation ». *Journal of hydrology,* vol. 505, p. 47-64.

Kokelj, S. V., C. A. S. Smith et C. R. Burn. 2002. « Physical and chemical characteristics of the active layer and permafrost, Herschel Island, western Arctic Coast, Canada ». *Permafrost and periglacial processes,* vol. 13, nº 2, p. 171-185.

Kong, Yanlong, et Zhonghe Pang. 2012. « Evaluating the sensitivity of glacier rivers to climate change based on hydrograph separation of discharge ». *Journal of Hydrology,* vol. 434–435, p. 121-129.

La Frenierre, J., et B. G. Mark. 2014. « A review of methods for estimating the contribution of glacial meltwater to total watershed discharge ». *Progress in Physical Geography,* vol. 38, nº 2, p. 173-200.

Ladouche, B., A. Ladouche, D. Probst, S. Viville, D. Idir, M. Baqué, T. Probst et T. Probst. 2001. « Hydrograph separation using isotopic, chemical and hydrological approaches (Strengbach catchment, France) ». *Journal of hydrology,* vol. 242, nº 3, p. 255-274.

Lafreniere, M. , et M. Sharp. 2005. « A comparison of solute fluxes and sources from glacial and non-glacial catchments over contrasting melt seasons ». *Hydrological Processes,* vol. 19, p. 2991-3012.

Langston, G., M. Hayashi et J. W. Roy. 2013. « Quantifying groundwater-surface water interactions in a proglacial moraine using heat and solute tracers ». *Water Resources Research,* vol. 49, nº 9, p. 5411-5426.

Laudon, Hjalmar, et Olav Laudon. 1997. « Hydrograph separation using stable isotopes, silica and electrical conductivity: an alpine example ». *Journal of hydrology,* vol. 201, nº 1, p. 82-101.

Levy, A., Z. Robinson, S. Krause, R. Waller et J. Weatherill. 2015. « Long-term variability of proglacial groundwater-fed hydrological systems in an area of glacier retreat, Skeiarársandur, Iceland ». *Earth Surface Processes and Landforms,* vol. 40, nº 7, p. 981-994.

Liu, S., Y. Zhang, Y. Zhang et et al. 2009. « Estimation of glacier runoff and future trends in the Yangtze River source region, China ». *Journal of Glaciology,* vol. 55, p. 353-362.

Lotsari, Eliisa, Noora Veijalainen, Petteri Alho et Jukka KÄYhkÖ. 2010. « IMPACT OF CLIMATE CHANGE ON FUTURE DISCHARGES AND FLOW CHARACTERISTICS OF THE TANA RIVER, SUB-ARCTIC NORTHERN FENNOSCANDIA ». *Geografiska Annaler: Series A, Physical Geography,* vol. 92, nº 2, p. 263-284.

Lukas, Sven. 2011. « Ice-Cored Moraines ». In *Encyclopedia of Snow, Ice and Glaciers*, sous la dir. de Singh, Vijay P., Pratap Singh et Umesh K. Haritashya. Lukas2011. p. 616-

619. Dordrecht: Springer Netherlands. < http://dx.doi.org/10.1007/978-90-481-2642-2_666 >.

Lukas, Sven, Lindsey I. Nicholson, Fionna H. Ross et Ole Humlum. 2005. « Formation, Meltout Processes and Landscape Alteration of High-Arctic Ice-Cored Moraines—Examples From Nordenskiold Land, Central Spitsbergen ». *Polar Geography,* vol. 29, nº 3, p. 157-187.

Luthcke, Scott B., Anthony A. Arendt, David D. Rowlands, John J. McCarthy et Christopher F. Larsen. 2008. « Recent glacier mass changes in the Gulf of Alaska region from GRACE mascon solutions ». *Journal of Glaciology,* vol. 54, nº 188, p. 767-777.

MacLean, Robert, Mark MacLean, John Oswood et William Irons. 1999. « The effect of permafrost on stream biogeochemistry: A case study of two streams in the Alaskan (U.S.A.) taiga ». *Biogeochemistry,* vol. 47, nº 3, p. 239-267.

Maloszewski, Piotr, Willibald Stichler, Andrzej Zuber et Dieter Rank. 2002. « Identifying the flow systems in a karstic-fissured-porous aquifer, the Schneealpe, Austria, by modelling of environmental 18O and 3H isotopes ». *Journal of Hydrology,* vol. 256, nº 1–2, p. 48-59.

Manabe, S., R.T. Wetherald, P.C.D. Milly, T.L. Delworth et R.J. Stouffer. 2004. « Century-scale change in water availability: CO2-quadrupling experiment ». *Climatic Change,* vol. 64, p. 59–76.

Mark, Bryan G, Jeffrey M McKenzie et Jesus Gomez. 2005. « Hydrochemical evaluation of changing glacier meltwater contribution to stream discharge: Callejon de Huaylas, Peru/Evaluation hydrochimique de la contribution évolutive de la fonte glaciaire à l'écoulement fluvial: Callejon de Huaylas, Pérou ». *Hydrological Sciences Journal,* vol. 50, nº 6.

Mark, Bryan, et Geoffrey Seltzer. 2003. « Tropical glacier meltwater contribution to stream discharge: a case study in the Cordillera Blanca, Peru ». *Journal of Glaciology,* vol. 49, nº 165, p. 271-281.

Martins, V., M. Babinski, I. Ruiz, K. Sato, S. Souza et R. Hirata. 2008. « Analytical Procedure for Determining Pb and Sr Isotopic Composition in Water Samples by ID-TIMS ». *Quim. Nova,* vol. 31, nº 7, p. 1836-1842.

Mason, P. R. D., K. Kaspers. et M. J. van Bergen. 1999. « Determination of sulfur isotope ratios and concentrations in water samples using ICP-MS incorporating hexapole ion optics ». *Journal of Analytical Atomic Spectrometry,* vol. 14, p. 1067-1074.

Menzies, John. 2002. *Modern and Past glacial Environment*, Butterworth - Heinemann. Butterworth - Heinemann.

Milner, A. M., L. E. Brown et D. M. Hannah. 2009. « Hydroecological response of river systems to shrinking glaciers ». *Hydrological Processes,* vol. 23, nº 1, p. 62-77.

Mitchell, A. C., et G. H. Brown. 2007. « Diurnal hydrological - physicochemical controls and sampling methods for minor and trace elements in an Alpine glacial hydrological system ». *Journal of Hydrology,* vol. 332, nº 1-2, p. 123-143.

Moorman, B. J., et F. A. Michel. 2000. « Glacial hydrological system characterization using ground-penetrating radar ». *Hydrological Processes,* vol. 14, nº 15, p. 2645-2667.

Moorman, Brian J. 2005. « Glacier-permafrost hydrological interconnectivity: Stagnation Glacier, Bylot Island, Canada ». *Geological Society, London, Special Publications,* vol. 242, nº 1, p. 63-74.

Nijssen, Bart, Greg M. O'Donnell, Dennis P. Lettenmaier, Dag Lohmann et Eric F. Wood. 2001. « Predicting the Discharge of Global Rivers ». *Journal of Climate,* vol. 14, nº 15, p. 3307-3323.

Nolin, Anne W, Jeff Phillippe, Anne Jefferson et Sarah L Lewis. 2010. « Present-day and future contributions of glacier runoff to summertime flows in a Pacific Northwest watershed: Implications for water resources ». *Water Resources Research,* vol. 46, nº 12.

Nuttall, Mark. 2007. « An environment at risk: Arctic indigenous peoples, local livelihoods and climate change ». In *Arctic Alpine Ecosystems and People in a Changing Environment*, sous la dir. de Ørbæk, Jon Børre, Roland Kallenborn, Ingunn Tombre, Else N. Hegseth, Stig Falk-Petersen et Alf H. Hoel. Nuttall2007. p. 19-35. Berlin, Heidelberg: Springer Berlin Heidelberg. < http://dx.doi.org/10.1007/978-3-540-48514-8_2 >.

Ørbæk, Jon Børre, Stig Falk-Petersen, Else N. Hegseth, Alf H. Hoel, Roland Kallenborn et Ingunn Tombre. 2007. *Arctic Alpine Ecosystems and People in a Changing Environment* (2007). Berlin, Heidelberg: Springer-Verlag Berlin Heidelberg.

Osterkamp, T. E., et C. R. Burn. 2003. « PERMAFROST A2 - Holton, James R ». In *Encyclopedia of Atmospheric Sciences*. p. 1717-1729. Oxford: Academic Press. < http://www.sciencedirect.com/science/article/pii/B0122270908003110 >.

Petrone, Kevin C., Jeremy B. Jones, Larry D. Hinzman et Richard D. Boone. 2006. « Seasonal export of carbon, nitrogen, and major solutes from Alaskan catchments with discontinuous permafrost ». *Journal of Geophysical Research: Biogeosciences,* vol. 111, nº G2, p. G02020.

Ricketts, Taylor H. et al. (485). 1999. *Terrestrial ecoregions of North America : a conservation assessment*. Washington, D.C: Island Press.

Rouse, W. R., M. S. V. Douglas, R. E. Hecky, A. E. Hershey, G. W. Kling, L. Lesack, P. Marsh, M. McDonald, B. J. Nicholson, N. T. Roulet et J. P. Smol. 1997. « Effects of climate change on the freshwaters of arctic and subarctic North America ». *Hydrological Processes,* vol. 11, nº 8, p. 873-902.

Schaner, Neil, Voisin Nathalie, Nijssen Bart et P. Lettenmaier Dennis. 2012. « The contribution of glacier melt to streamflow ». *Environmental Research Letters,* vol. 7, nº 3, p. 034029.

Schindler, D. W., et J. P. Smol. 2006. « Cumulative effects of climate warming and other human activities on freshwaters of Arctic and subarctic North America ». *Ambio,* vol. 35, nº 4, p. 160-198.

Schomacker, Anders, et Kurt H. Kjær. 2008. « Quantification of dead-ice melting in ice-cored moraines at the high-Arctic glacier Holmströmbreen, Svalbard ». *Boreas,* vol. 37, nº 2, p. 211-225.

Sharp, M., G. H. Brown, M. Tranter, I. C. Willis et B. Hubbard. 1995. « COMMENTS ON THE USE OF CHEMICALLY BASED MIXING MODELS IN GLACIER HYDROLOGY ». *Journal of Glaciology,* vol. 41, nº 138, p. 241-246.

Shur, Y. L., et M. T. Jorgenson. 2007. « Patterns of permafrost formation and degradation in relation to climate and ecosystems ». *Permafrost and Periglacial Processes,* vol. 18, nº 1, p. 7-19.

Sinclair, C. 2014. « Glacial and Groundwater Contribution to Dry-Season Discharge and Bofedales in Tuni, Cordillera Real (Bolivia), and Pastoruri, Cordillera Blanca (Peru) ». University of Ohio, 52 p.

Singh, P., U. K. Haritashya, Ramasastri K. S. et N. Kumar. 2005. « Diurnal variations in discharge and suspended sediment concentration, including runoff-delaying characteristics, of the Gangotri Glacier in the Garhwal Himalayas ». *Hydrological Processes,* vol. 19, nº 7, p. 1445-1457.

Singh, V. P., P. Singh et U. K. Haritashya. 2011. *Encyclopedia of Snow, Ice and Glaciers*. Coll. « Encyclopedia of Earth Sciences Series ». Netherlands: Springer, 1253 p.

Stotler, R. L., S. K. Frape et L. Labelle. 2014. « Insights gained from geochemical studies in the Waterloo Moraine: Indications and implications for anthropogenic loading ». *Canadian Water Resources Journal,* vol. 39, nº 2, p. 136-148.

Stumpp, C., P. Maloszewski, W. Stichler et J. Fank. 2009. « Environmental isotope (δ18O) and hydrological data to assess water flow in unsaturated soils planted with different crops: Case study lysimeter station "Wagna" (Austria) ». *Journal of Hydrology,* vol. 369, nº 1–2, p. 198-208.

Thayyen, R. J., et J. T. Gergan. 2010. « Role of glaciers in watershed hydrology: a preliminary study of a "Himalayan catchment" ». *The Cryosphere,* vol. 4, nº 1, p. 115-128.

Tranter, Martyn, Giles H. Brown, Andrew J. Hodson et Angela L. Gurnell. 1996. « Hydrochemistry as an indicator of subglacial drainage system structure: A comparison of alpine and sub-polar environments ». *Hydrological processes,* vol. 10, nº 4, p. 541-556.

Turnadge, Chris, et Brian D. Smerdon. 2014. « A review of methods for modelling environmental tracers in groundwater: Advantages of tracer concentration simulation ». *Journal of hydrology,* vol. 519, p. 3674-3689.

Wadham, J. L., M. Tranter et J. A. Dowdeswell. 2000. « Hydrochemistry of meltwaters draining a polythermal-based, high-Arctic glacier, south Svalbard: II. Winter and early Spring ». *Hydrological Processes,* vol. 14, nº 10, p. 1767-1786.

Wainstein, Pablo, Brian Moorman et Ken Whitehead. 2014. « Glacial conditions that contribute to the regeneration of Fountain Glacier proglacial icing, Bylot Island, Canada ». *Hydrological Processes,* vol. 28, nº 5, p. 2749-2760.

Walvoord, M. A., et R. G. Striegl. 2007. « Increased groundwater to stream discharge from permafrost thawing in the Yukon River basin: Potential impacts on lateral export of carbon and nitrogen ». *Geophysical Research Letters,* vol. 34, p. 1-6.

Whitfield, P. H. 2001. « Linked hydrologic and climate variations in British Columbia and Yukon ». *Hydrological Processes,* vol. 67, nº 1-2, p. 217-238.

Williams, M. W., M. Knauf, N. Caine, F. Liu et P. L. Verplanck. 2006. « Geochemistry and source waters of rock glacier outflow, Colorado Front Range. ». *Permafrost and Periglacial Processes,* vol. 17, nº 1, p. 13-33.

Williams, Peter J., et Michael W. Smith. 1989. *The Frozen Earth*. Cambridge University Press.

Wilson, N. J., M. T. Walter et J. Waterhouse. 2015. « Indigenous knowledge of hydrologic change in the Yukon river basin: A case study of Ruby, Alaska ». *Arctic,* vol. 68, nº 1, p. 93-106.

Yde, Jacob C., Andy J. Hodson, Irina Solovjanova, Jørgen Steffensen, P.,, Per Nørnberg, Jan Heinemeier et Jesper Olsen. 2012. « Chemical and isotopic characteristics of a glacier-devired naled in front of Austre Grønfjordbreen, Svalbard ». *Polar Research,* vol. 31.

Yuanqing, H., W. H. Theakstone, Y. Tandong et Y. F. Shi. 2001. « The isotopic record at an alpine glacier and its implications for local climatic changes and isotopic homogenization processes ». *Journal of Glaciology,* vol. 47, nº 156, p. 147-151